(2)

Supramolecular Assembly Containing α-Helical Peptide Molecules in Lipid Bilayer Membrane and at the Air/Water Interface

Katsuhiko Fujita

1994

CONTENTS

LIST OF ABBREVIATIONS

Aib	2-aminoisobutyric acid
AdmA16B	$C_{10}H_{15}CO$-(Ala-Aib)$_8$-$OCH_2C_6H_5$
AdmA16OH	$C_{10}H_{15}CO$-(Ala-Aib)$_8$-OH
Ant	anthrylmethyl group
BA16M	Boc-(Ala-Aib)$_8$-OCH_3
BA16B	Boc-(Ala-Aib)$_8$-$OCH_2C_6H_5$
BioA16M	biotinyl-NH-$(CH_2)_5$-CO-(Ala-Aib)$_8$-OCH_3
BioS3A16M	biotinyl-NH-$(CH_2)_5$-CO-Sar$_3$-(Ala-Aib)$_8$ OCH_3
BKZ16M	Boc-(Lys(Z)-Aib)$_8$-OCH_3
BL16B	Boc-(Leu-Aib)$_8$-$OCH_2C_6H_5$
BMA16B	Boc-MeAla-Pro-MeAla-Aib-(Ala-Aib)$_6$-$OCH_2C_6H_5$
Boc	*tert*-butyloxycarbonyl
BOP reagent	benzotriazol-1-yl-oxytris(dimethylamino)phosphonium hexafluorophosphate
BS3A16M	Boc-Sar$_3$-(Ala-Aib)$_8$-OCH_3
CD	circular dichroism
COOHA16M	HOOC-$(CH_2)_2$-CO-(Ala-Aib)$_8$-OCH_3
DCC	dicyclohexylcarbodiimide
DiIC$_1$	1, 1, 3, 3, 3', 3'-hexamethylindocarbocyanine iodide
DMF	dimethylformamide
DMPC	dimyristoylphosphatidylcholine
DPPC	dipalmitoylphosphatidylcholine
FITC	fluorescein-5-isothiocyanate
F-MPX-A	MPX-A with fomylated Trp
HA16B	TFA • H-(Ala-Aib)$_8$-$OCH_2C_6H_5$
HA16M	TFA • H-(Ala-Aib)$_8$-OCH_3
HKZ16M	TFA • H-[Lys(Z)-Aib]$_8$-OCH_3
HL16B	TFA • H-(Leu-Aib)$_8$-$OCH_2C_6H_5$
HOBt	1-hydroxybenzotriazole
HPLC	high performance liquid chromatography
HS3A16M	TFA • H-Sar$_3$-(Ala-Aib)$_8$-OCH_3
HS3L16B	TFA • H-Sar$_3$-(Leu-Aib)$_8$-$OCH_2C_6H_5$
MeAla	*N*-methyl L-alanine

MPX	mastoparan X
MPX-A	MPX derivative having an anthryl group at the C-terminal residue
NMR	nuclear magnetic resonance
OBzl	benzyloxy
OMe	methyloxy
π-A isotherm	surface pressure-area isotherm
RAS	reflection absorption spectroscopy
Rh-SAv	streptavidin labeled with rhodamine
SAv	streptavidin
Sar	sarcosine (*N*-methylglycine)
SPR	surface plasmon resonance
SUV	small unilamellar vesicle
TFA	trifluoroacetic acid
TFMSA	trifluoromethanesulfonic acid
TMP	trimethyl phosphate
TLC	thin layer chromatograpgy
Z	benzyloxycarbonyl

INTRODUCTION

It is evident that the creation of a new exquisite structure is indispensable for the development of novel functional materials. From the view point of the exquisite structure, the protein is the perfect example.[1] However, the molecular design of artificial proteins or peptides for the construction of specific protein-like structures is almost impossible under the current understanding of protein structures. Synthetic proteins in which peptide molecules are forced to aggregate on a matrix have been proposed as a method to realize the protein-like structure without encountering the above-mentioned difficulties.[2] In this method, proteins are considered as the self-assembly of peptide molecules taking various secondary structures such as α-helix and β-sheet structures. Also, the proteins form the supramolecular structures by the self-assembly of protein molecules of the same kind or of different kinds, and exhibit effective functionalities.[3] These facts indicate the importance of assembling in the exhibition of functionality. Therefore, it might be possible for peptide molecules or their aggregates to construct the protein-like higher-order structure to exhibit specific functionalities, if the molecular design to control the aggregation of peptide molecules is established. Furthermore, molecular assemblies exhibiting novel functionalities which are not seen in the individual peptide molecules might be produced.

There are several structural motifs common to many natural proteins.[4] Among them, the α-domain structure, which is a bundle of α-helices, is one of the most frequently occuring motifs in many kinds of proteins. It has been shown that the α-domain structure is very stable and plays an important role in the exhibition of protein functionalities.[4,5] On the other hand, specific secondary structures found in

proteins can be reproduced in oligopeptides or in polypeptides.[6] In particular, the molecular design of α-helix-forming peptides has been established.[7] In the present investigation, the construction of supramolecular assemblies of synthetic α-helical peptides was attempted in terms of the relation between the self-assembling properties with the molecular structures. To attain the goal, it was necessary to align peptide molecules regularly so that the self-assembly of peptide molecules was investigated in the lipid bilayer assembly and at the air/water interface. The intermolecular interactions between peptide molecules in the formation of molecular assembly was investigated by comparison of the behaviors in the two different states, and the guideline for the construction of supramolecular assembly of peptides was searched for.

It has been pointed out that the primary or secondary amphiphilic structure plays an important role in the interaction of amphiphilic molecule with lipid membrane.[8] The primary amphiphilic structure represents a peptide molecule in which hydrophilic amino acid residues are separated from hydrophobic residues along the primary sequence. When the primary amphiphilic peptides are taken in the lipid membrane, they are oriented having the hydrophobic segments residing in the hydrophobic core of the lipid membrane and having the hydrophilic segments residing at the polar region of the membrane surface or in the aqueous phase.[9] On the other hand, the secondary amphiphilicity refers to an unequal distribution of hydrophilic and hydrophobic amino acid residues with regard to a secondary conformation such as α-helix. In this case, the peptide molecules tend to be bound on the membrane surface.[10] In general, amphiphilic peptide molecules taken in an anisotropic medium assume a specific orientation according to their structure. In the peptide monolayer spread at the air/water interface, which is another anisotropic

circumstance, peptide molecules aggregate under a specific orientation to form supramolecular assembly with a specific structure.

A two-dimensional crystallization of proteins can be done by using the peptide monolayer prepared at the air/water interface. The two-dimensional crystallization of proteins at the air/water interface has been reported by Ringsdorf, et al. by using lipid derivatives.[11] The monolayer of lipid derivatives only serves to immobilize proteins at the air/water interface. In the case of peptide monolayers, the structure of monolayer can be varied by designing peptide molecules and furthermore the two dimensional crystalline structure of proteins can be controlled by the structure of monolayer matrix. The preparation of peptide monolayer is very significant in the viewpoint of the controlled synthesis of supramolecular assembly.

This thesis consists of two parts including six chapters. In Part 1 of this thesis, the monolayer formation of α-helical peptides at the air/water interface was investigated by the measurement of the surface pressure-area (π-A) isotherm and the fluorescence micrograph.

Chapter 1 describes the monolayer formation of helical peptides (Figure 1)

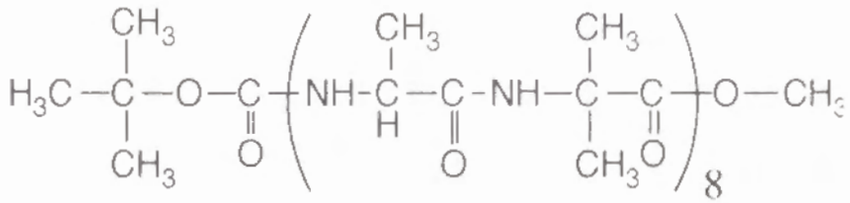

Boc-(Ala-Aib)$_8$-OMe (BA16M)

Figure 1 Molecular structure of a helical peptide investigated in Chapter 1.

spread at the air /water interface, which shows various states such as gas-analogous, liquid and solid phases, depending on the surface pressure. These phases can be analyzed on the basis of the π-A isotherm which reflects interactions between the amphiphilic molecules. In the past, polypeptide monomolecular films at the air/water interface have been investigated on their intermolecular interactions, especially molecular packing.[12] However, their π-A isotherms did not show either phase transition or collapse, possibly because of the molecular weight distribution or the unstable secondary structure against the surface pressure. In the present thesis, hydrophobic peptides having a defined chain length and secondary structure were synthesized and the intermolecular interactions at the air/water interface was investigated (Figure 2). Furthermore, the helical peptides having various terminal groups were synthesized and their monolayer properties at the air/water interface was investigated.

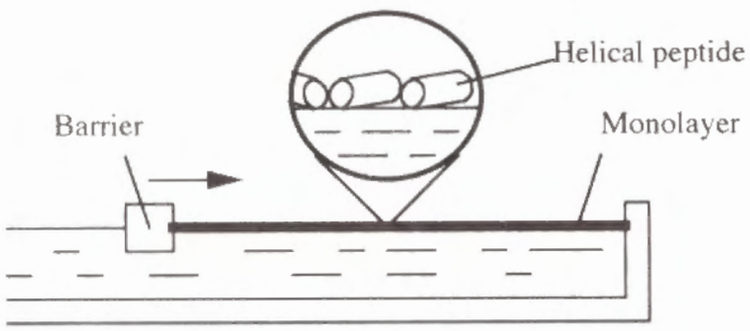

Figure 2 Schematic illustration of the formation of the peptide monolayer at the air/water interface.

In Chapter 2, the properties of the peptide monolayer was investigated by a fluorescence microscopy. It has been reported that lipid aggregates at the air/water interface can be visualized as a dark solid domain from which fluorescence-labeled

lipid is excluded.[13] However, the formation of two-dimensional domain based on the phase transition has never been observed in proteins or peptides. In the present investigation, the peptide derivatives were synthesized, in which the helix segment is identical and a fluorescence probe is introduced at a terminal, and peptide monolayers were constructed. When the molecules of a hydrophobic helical peptide and its derivatives modified at the N or C terminal were spread at the air/water interface, the phase transitions between a liquid state and a solid state were observed depending on surface pressure. Upon the phase transition from a liquid state to a solid state, a local minimum of the surface pressure based on molecular rearrangement was also observed. In order to visualize the phase transition, the peptide monolayer containing a small amount of fluorescence probe was investigated by fluorescence microscopy.

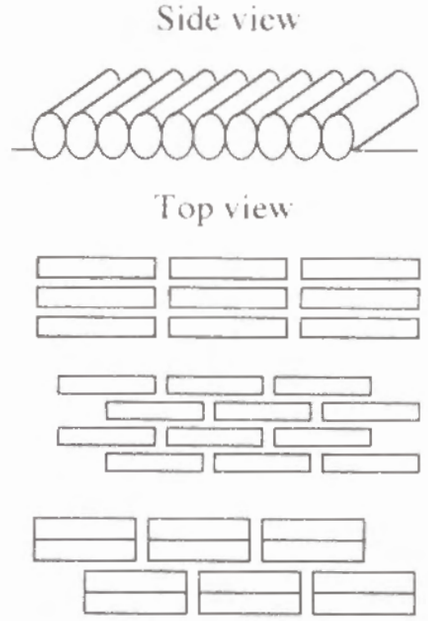

Figure 3 Schematic illustration of possible alignment of helical peptides at the air/water interface in the solid state.

In Chapter 3, various peptide monolayers, showing phase transition from a liquid state to a solid state, were transferred onto substrates and characterized by CD and IR spectroscopy. Hydrophobic helical peptides having an adamantyl group at the N terminal and other helical peptides containing Leu residues formed stable monolayers at the air/water interface. Langmuir-Blodgett membranes of the

peptides were prepared and the conformation in the membrane was investigated by CD spectroscopy. The orientation of the helical peptides on the substrate determined by IR transmission and refraction-absorption spectroscopy was compared with that at the air/water interface.

In Part II of this thesis, the two-dimensional crystallization of a protein, streptavidin (SAv), was induced by alignment of α-helical peptides spread at the air/water interface. The conformation, orientation and assembly formation of a biologically active natural peptide, mastoparan X (MPX), was investigated at the biological concentrations in phospholipid bilayer membrane.

Peptide molecules are advantageous in designing functional molecules, because a variety of side chains can be chosen and the conformations can be investigated in detail. In Chapter 4, in an attempt to synthesize functional hydrophobic helical peptides and their monolayers at the air/water interface, a biotinyl group was connected to the N terminal of the hydrophobic helical peptides, and the two-dimensional crystallization of SAv was attempted according to the

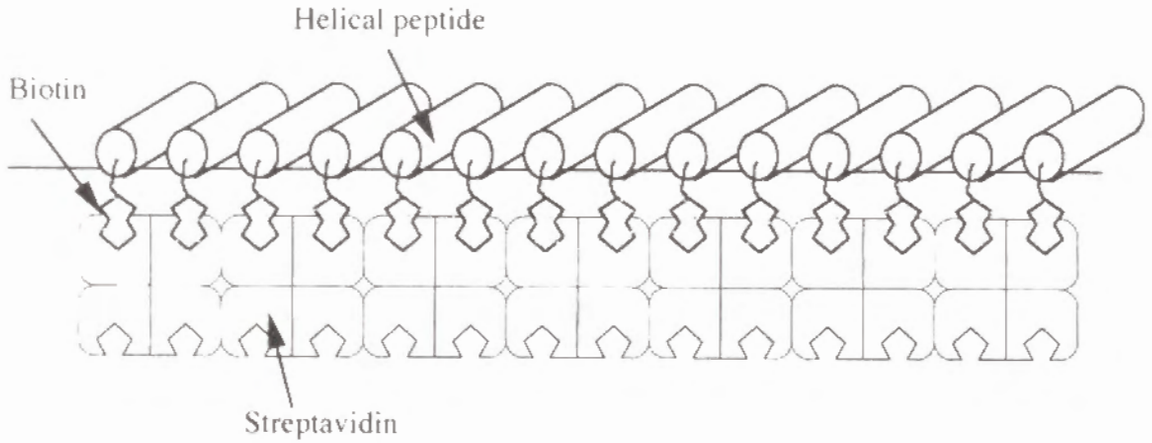

Figure 4 Possible structure of supramolecular assembly of the biotinyl peptide-streptavidin complex at the air/water interface.

specific interactions between biotin and SAv as sketched in Figure 4. A water-soluble protein, SAv, has four binding sites for biotin and the dissociation constant of the specific complex is extremely small (10^{-15} M).[14] The biotin-SAv system has been investigated as a model of the receptor-ligand pair on the cell surface.[15] In the present investigation, the monolayer of biotinyl peptides was prepared at the air/water interface, and an aqueous solution of fluorescence-labeled SAv was injected underneath the monolayer and the two-dimensional crystallization at the interface was investigated.

A thin layer of proteins could be used as a functional molecular device. The self-organization of protein molecules at the air/water interface can be a technique to construct ultra-thin film of proteins. It has been reported that the two-dimensional crystal is formed at the air/water interface by the specific interaction of SAv with biotinylated lipid spread at the interface.[11] Although two of the four binding sites of SAv are occupied by the biotin groups at the interface, the rest of them remains to be free in the aqueous subphase. The two-dimensional crystal of SAv can be a template for multilayer systems of proteins.[16] In Chapter 5, the construction of functional multilayer systems was attempted. For the construction, SAv was selected as a protein binding to the template layer to construct the second layer, because the molecular size and distance between the binding sites are identical to those of the template layer. To construct a double layer of SAv crystal, a bis-(biotinyl) linker molecule was used (Figure 5). For the molecular design, the two biotinyl groups of the linker molecule should not coordinate to two binding sites of the same SAv molecule or the neighboring SAv molecules in the same layer. Therefore, it is a supreme order that the linker molecule has an appropriate chain length and chain rigidity. A hydrophilic helical peptide was considered for the linker molecule, because it takes a rigid secondary structure and the distance between

the terminals can be regulated by the number of constituting residues. A water-soluble helical peptide containing Aib residues amounting 2/3 of the total number of residues was synthesized and two biotinyl groups were connected to the both terminals. The structure of fluorescence-labeled SAv multilayer structure bridged by the bis(biotinyl) peptide linker was investigated by fluorescence microscopy, and the thickness of the multilayer was assessed by surface plasmon resonance.

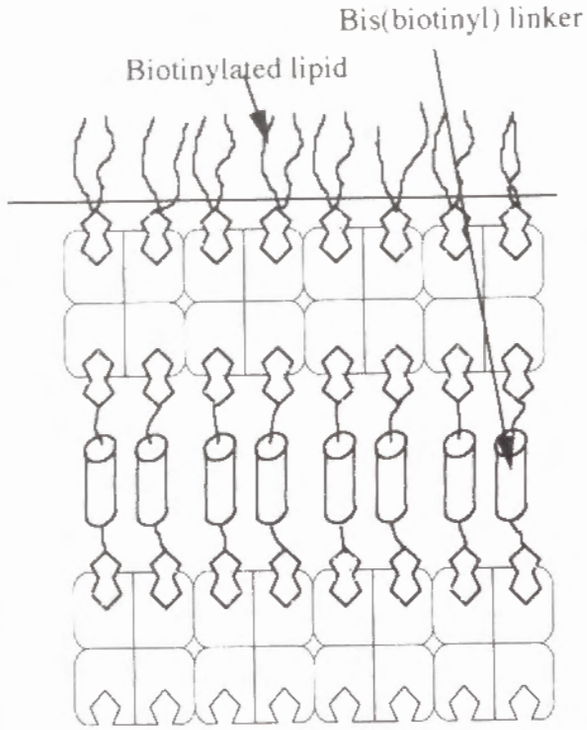

Figure 5 Schematic illustration of multilayer system of streptavidin bridged by the bis(biotinyl) peptide at the air/water interface.

Some biologically active peptides forming amphiphilic α-helical structure have been found in the nature, and their structure plays an important role in the interaction with lipid membrane.[8] In Chapter 6, the mastoparan derivatives in the lipid bilayer membrane were investigated. Mastoparan X (MPX), which is extracted from vasp venom, is a tetradecapeptide and has biological activities such as degranulation of mast cell, stimulation of G proteins, and activation of phospholipase A_2 and ion channel formation. MPX shows amphiphilicity upon forming α-helical structure, having hydrophilic residues localized on one side of the helix rod and hydrophobic residues localized on the other side.[17] This kind of

structure has been revealed to play an important role in biological activities such as erythrocyte lysis.[18] An MPX derivative, MPX-A, having an anthryl group introduced in the side chain of the C-terminal residue, was synthesized. On the basis of the excited energy transfer from the Trp^3 residue to the anthryl group, the conformation, orientation and aggregation of MPX-A in lipid membrane were investigated. Throughout the experiments, the possibility of a vertical orientation of an amphiphilic helical peptide, such as MPX, to the lipid bilayer membrane was the focus of interest. It is notable that these experiments were carried out at micromolar concentrations, where MPX is biologically active.[19]

The present investigation was carried out to obtain fundamental knowledge concerning supramolecular assembly of peptides. It is believed that the knowledge is useful for the design and synthesis of molecular device, which might be realized by a novel supersecondary structure of nonnatural peptide assembly. The experimental results will be described in the following chapters.

References

(1) Branden, C.; Tooze, J. *Introduction to Protein Structure*; Garland Publishing: New York & London, 1991; Chapter 2.

(2) Mutter, M. Vuilleumier, S. *Angew. Chem. Int. Ed. Engl.* **1989**, *28*, 535.

(3) Alberts, B.; Bray, D.; Lewis, J.; Raff, M.; Roberts, K.; Watson, J. D. *Molecular Biology of the Cell, 2nd ed.*, Garland Publishing: New York & London, 1989; Chapter 3.

(4) Fermi, G.; Perutz, M. F. *Atlas of Molecular Structures in Biology. 2. Haemoglobin and Myoglobin;* Clarendon Press: Oxford, 1981.

(5) Hargrave, P. A.; McDowell, J. H.; Curtis, D. R.; Wang, J. K.; Juszczak, E.;

Fong, S. -L.; Rao, J. K. M.; Argos, P. *Biopys. Struct. Mech.* **1983**, *9*, 235.
(6) Richardson, J. S.; Richardson, D. C. *Trends in Biochem. Sci.* **1989**, *14*, 304.
(7) (a) Burgess, A. W.; Leach, S. J. *Biopolymers* **1973**, *12*, 2599. (b) Karle, I. L.; Balaram, P. *Biochemistry* **1990**, *29*, 6747. (c) Davis, J. H.; Clare, D. M.; Hodges, R. S.; Bloom, M. *Biochemistry* **1983**, *22*, 5298.
(8) Gennis, R. *Biomembranes; Molecular Structure and Function*: Springer-Verlag: New York, 1989; Chapter 3.
(9) Schwyzer, R. *Helv. Chim. Acta* **1986**, *69*, 1685.
(10) Terwillinger, T. C.; Weissman, L.; Eisenberg, D. *Biopys. J.* **1982**, *37*, 353.
(11) Blankenburg, R.; Meller, P.; Ringsdorf, H.; Salesse, C. *Biochemistry* **1989**, *28*, 8214.
(12) Birdi, K. S. *Lipid and biopolymer monolayers at liquid interfaces*, Plenum Press: New York, 1989; Chapter 5.
(13) Lösche, M.; Sackmann, E; Möhwald, H. *Ber. Bunsenges. Phys. Chem.* **1983**, *87*, 848.
(14) Green, N. M. *Adv. Protein Chem.* **1975**, *29*, 85.
(15) Kitano, H.; Kato, N.; Ise, N. *J. Am. Chem. Soc.* **1989**, *111*, 6809.
(16) Knoll, W.; Liley, M.; Muller, W.; Ringsdorf, H.; Rump, E.; Spinke, J.; Wildburg, G.; Zhang, X. *Science* **1993**, *262*, 1706.
(17) Higashijima, T.; Wakamatsu, K.; Takemitsu, M.; Fujino, M.; Nakajima, T.; Miyazawa, T. *FEBS Lett.* **1983**, *152*, 227.
(18) DeGrado, W. F.; Kézdy, F. J.; Kaiser, E. T. *J. Am. Chem. Soc.* **1981**, *103*, 679.
(19) Hirai, Y.; Yasuhara, T.; Yoshida, H.; Nakajima, T.; Fujino, M.; Kitada, C. *Chem. Pharm. Bull.* **1979**, *27*, 1942.

Part I Monolayer Formation of α-Helical Peptides Spread at Air/Water Interface

Chapter 1

Monolayer Properties of Hydrophobic α-Helical Peptides Having Various End Groups at Air/Water Interface

Introduction

Hydrophobic helical peptides are often found in water-soluble globular proteins (e.g. hemoglobin)[1] and the transmembrane region of membrane proteins (e.g. bacteriorhodopsin).[2] Several helices associate together in the protein, forming a so-called helix bundle, which is one of the major structural motifs of naturally-occurring proteins. It is, therefore, important to study interactions between helices in terms of the formation of a tertiary structure or the stability of the protein.[3-5]

The monolayer technique is a unique means to investigate intermolecular interactions, because it detects intermolecular forces acting in a low dimensional array of molecules.[6] When amphiphilic molecules are spread at the air/water interface, they show various states such as gas-analogous, fluid-expanded, fluid-condensed, and solid-condensed phases, depending on the surface pressure.[7] These phases can be analyzed on the basis of π-A isotherm which reflects electrostatic interactions or molecular packing between amphiphilic molecules in each phase.[6,8] The relationship between the structure of amphiphiles, especially the polar head group, and the surface properties of

monolayers have been investigated.[8,9] Synthetic poly(α -amino acid)s have been shown to form monomolecular films at the air/water interface.[10-16] However, their π-A isotherms did not show phase transitions or sharp collapses. A possible reason is the distribution of molecular weight, which causes irregularities of molecular packing. Another possible reason is instability of the secondary structure against the surface pressure. In the present chapter, hydrophobic helical peptides having a defined chain length and various terminal groups were synthesized and their behavior at the air/water interface was investigated.

The monolayer formation of a mixture of different types of peptides was also analyzed to know the nature of the interhelix interactions. Since the primary sequence of one helix in the helix bundle is not necessarily the same as the other, there should be several factors which contribute to the stability of the helix-bundle structure depending on the composing amino acids. This knowledge will be important for construction of a helix monolayer with a novel function, where a few helices with different functional groups associate together.

Peptides containing α -aminoisobutyric acid (Aib) tend to form a helical structure because of the steric hindrance around the α -carbon atom of Aib residues in other conformations.[17] For example, a hexadecapeptide, Boc-(Ala-Aib)$_8$-OMe (BA16M), has been revealed to take an α -helical structure in the crystalline state by X-ray diffraction.[18] The dimension of the unit cell was 9.3×9.3×25.7 Å, which is in good agreement with the calculated value for a complete α -helical structure.[15,19] This peptide and the derivatives having

various end groups were synthesized and their monolayer properties at the air/water interface were investigated.

Materials and Methods

Peptide Preparation

The structures of synthetic peptides with their abbreviations are shown in Figure 1. All the peptides were synthesized by a conventional liquid-phase method and identified by ^{1}H NMR, and the purity was checked by TLC using two different solvent systems. TLC was performed on silica-gel plate 60 F254, 0.2-mm thick (Merk) with the solvent system (A) chloroform / methanol / acetic acid (90 : 10 : 3 v/v/v) or (B) ethyl acetate / methanol (85 : 15

Boc-(Ala-Aib)$_8$-O-CH_3 — BA16M

TFA·H-(Ala-Aib)$_8$-O-CH_3 — HA16M

Boc-(Ala-Aib)$_8$-O-(benzyl) — BA16B

TFA·H-(Ala-Aib)$_8$-O-(benzyl) — HA16B

COOH-CH_2-CH_2-CO-(Ala-Aib)$_8$-O-CH_3 — COOHA16M

Boc-(Ala-Aib)$_8$-O-H — BA16OH

Boc-Sar$_3$-(Ala-Aib)$_8$-O-CH_3 — BS3A16M

TFA·H-Sar$_3$-(Ala-Aib)$_8$-O-CH_3 — HS3A16M

Figure 1 Molecular structure and abbreviation of the helical peptides used in this chapter.

v/v). Peptides on the plate were visualized by spraying ninhydrin or *o*-tolidine.[20]

Aib-OBzl

Benzyl ester of Aib was prepared from Aib (Tokyo Chemical Industry Co. Ltd., Tokyo) and p-toluenesulfonic acid (Tos-OH) monohydrate suspended in a benzyl alcohol / toluene (1 : 3 v/v) mixture. Tos-OH•Aib-$OCH_2C_6H_5$ (Tos•Aib-OBzl) was obtained as a white crystal after the conventional synthetic procedure.[21]

Aib-OMe

$SOCl_2$ was added dropwise into methanol cooled with an ice bath and Aib was dispersed in the solution. The reaction mixture was stirred for 15 h at room temperature, followed by evaporation. The crude product was precipitated by addition of diethyl ether. The obtained powder was recrystallized from isopropyl alcohol/isopropyl ether.

BA16M, BA16B, HA16M and HA16B

BA16M and BA16B were synthesized from Boc-Ala and Aib-OMe or Aib-OBzl, respectively, by the previous procedure[22] with some modifications. The Boc group of BA16M and BA16B was removed with TFA to obtain HA16M and HA16B, respectively. TLC: BA16M; R_f(A) 0.70, R_f(B) 0.65. BA16M; R_f(A) 0.65, R_f(B) 0.61. HA16M; R_f(A) 0.25, R_f(B) 0.18. HA16B; R_f(A) 0.28, R_f(B) 0.20.

BA16OH

The benzyl ester in BA16B was removed by the catalytic hydrogenation

in DMF solution with palladium carbon, followed by gel filtration with a Sephadex LH-20 (Pharmacia, Uppsala, Sweden) column by using methanol as the elution solvent.. The major fraction was collected and concentrated, followed by recrystallization from methanol, to obtain BA16OH. TLC: R_f(A) 0.35, R_f(B) 0.30.

COOHA16M

HA16M was reacted with 5-fold molar succinic anhydride in pyridine at 40 °C for 14 h, followed by gel filtration as described above, to obtain COOHA16M. TLC: R_f(A) 0.50, R_f(B) 0.45.

BS3A16M and HS3A16M

Boc-Sar_3-OH was synthesized by stepwise elongation as reported elsewhere.[23] HA16M was connected to Boc-Sar_3-OH using a coupling reagent, DCC / HOBt,[24] in DMF, followed by purification with gel filtration as described above to obtain BS3A16M. HS3A16M was prepared from BS3A16M in the same way as the synthesis of HA16M from BA16M. TLC: BS3A16M; R_f(A) 0.65, R_f(B) 0.60. HS3A16M: R_f(A) 0.40, R_f(B) 0.25.

Method

The peptide samples were dissolved in chloroform / methanol (9 : 1 v/v)(Merck analytical grade) at concentrations of $(1.5 - 3) \times 10^{-4}$ M. The π-*A* isotherm was recorded at a constant rate of reducing area of 0.37 cm^2/s with a home-made Langmuir trough.[25] The peptide solution was spread on the aqueous phase by using a microsyringe, and equilibrated for 15 min before

compression. The Millipore water, 50 mM citrate buffer (pH 3.5-5.0), and 50 mM phosphate buffer (pH 5.5-11.0) were used for the aqueous subphase. Each experiment was repeated several times to check the reproducibility.

Circular dichroism (CD) of the peptides was measured in ethanol / water (95 : 5 v/v) at room temperature on a JASCO J-600 CD spectropolarimeter using an optical cell of 1 cm path length.

Results

Conformation

The CD spectra of all the synthesized peptides showed a double-minimum profile, which is characteristic of an α-helical structure.[26] The helix content of BA16M was estimated to be *ca.* 60 % from the molar ellipticity at 222 nm,[27,28] while it forms a perfect α-helical structure in the solid state.[17] It is known that the helical structure of peptides is destabilized in highly dielectric environment.[29] The low helix content in solution should represent a conformational destabilization in the polar solvent. The Cotton effects of HA16M, BA16OH and COOHA16M at 222 nm were scarcely affected by the addition of hydrochloric acid or aqueous sodium hydroxide under different ionization states of the end groups (Table I). It is, therefore, concluded that each peptide takes an α-helical conformation in ethanol containing 5% water and that the conformation is stable irrespective of the charge state of the helix terminal. This observation is in sharp contrast to the previous reports[30,31] that the helix conformation is affected by the interaction of the terminal charge with the macrodipole of the helix.

Table I. The molar ellipticity $[\theta]$ of the helical peptides at 222 nm in ethanol/water (95/5, v/v).

Compound	$[\theta]$(deg•cm²/dmol)
BA16M	-3.28×10^5
HA16M	-2.47×10^5
	-2.63×10^5 [a]
BA16OH	-2.36×10^5
	-2.68×10^5 [b]
COOHA16M	-3.18×10^5
	-3.22×10^5 [b]

[a] addition of equimolar NaOH.
[b] addition of equimolar HCl .

Fully Protected Helical Peptide, BA16M, at the Interface

π-*A* isotherms of BA16M on the water subphase at 10, 20, and 30 °C are shown in Figure 2. The inflection point appearing in the π-*A* isotherm, which corresponds to the maximum value of the area elastic modulus, $-A(d\pi/dA)$, was independent of the temperature (Table II). The irregular bumping was observed in smaller areas than the inflection point, indicating collapse of the monolayer.[32] The area at the inflection point coincides with the sectional area of this helical peptide along the helix axis (239 Å²), which has been determined by X-ray analysis.[17] The π-*A* isotherm, therefore, indicates that the peptides take an α-helical structure at the air/water interface and orient the helix axis parallel to the interface. In the region between the inflection point

and the starting point of the irregular bumping, interdigitation should occur such that the side chain of the α-helix is allowed to penetrate to the neighbor.[15] Further compression collapsed the monolayer.

In the π-A isotherm, a mound was observed at around 300 Å^2. The local maximum appeared at higher pressure as the temperature was raised. The same sort of temperature dependence has been observed with the phase transition from the fluid-expanded state to the fluid-condensed state of lipid or fatty acid monolayers.[33] The mound was observed either in the compression experiment after aging equilibration (160 min) or in both compression stages

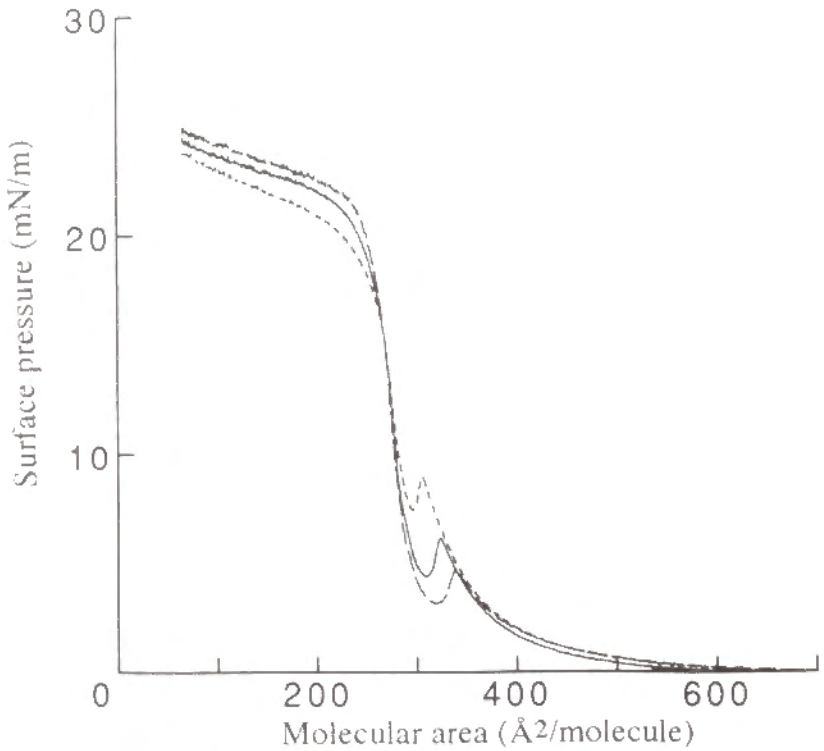

Figure 2 π-A isotherms of BA16M on water subphase at 10 (– – –), 20 (——) and 30 (-----) °C.

during a compression to 13 mN/m, depression and compression process. It was found to become smaller with decreasing compression speed, indicating that the mound is due to kinetic effects as reported on the monolayer of azacrown derivatives.[34] The mound nearly vanished and a plateau level appeared in the π-A isotherm at extremely slow compression. Therefore, the mound should not result from destruction of monolayers but from rearrangement of the molecules in the monolayer. The depression from the top of the mound to the bottom represents the phase transition from a liquid to a solid state. It is well-known that the phase transition of an insoluble monolayer can be observed with a fluorescence microscope by using a fluorescence probe added to the monolayer.[35,36] The domain formation of the monolayer containing a fluorescence-labeled helix at a concentration of 1 or 2 mol % was observed under a fluorescence microscope when the compression was held at the mound.[37] In addition, fluorescence anisotropy was observed. These observations support the phase transition from a liquid to a solid state around

Table II. Inflection point and phase transition point in the pressure-area isotherms of the completely protected peptide, BA16M.

Subphase	Temp. (°C)	Inflection point		Top of mound	
		area (Å^2)	pressure (mN/m)	area (Å^2)	pressure (mN/m)
Water	10	254.2	11.6	312.8	4.7
Water	20	255.6	11.5	299.5	6.1
Water	30	256.3	11.8	282.0	8.9
0.5 M NaCl	20	257.8	15.6	292.8	9.0

the mound region in the π-A curve. In the solid state, the helix rods should be arranged regularly, while they might be dispersed irregularly or form small crystalline domains in the liquid state.[38]

The surface pressure at the inflection point and at the top of the mound was higher on the 0.5 M NaCl aqueous subphase than on the water subphase at the same temperature, 20 °C (Table II). It is hard to explain the higher collapse pressure or phase transition pressure in terms of the interaction of ions with BA16M, which is a nonionizable peptide molecule. It is considered that the collapse pressure was increased by the "salting out" effect [39,40] under high

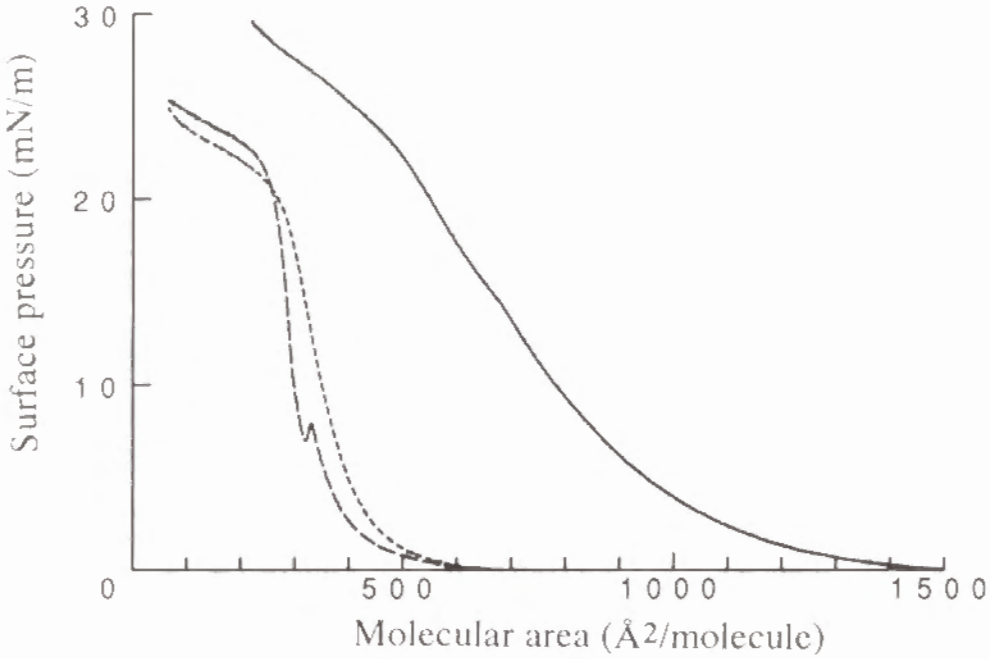

Figure 3 π-A isotherms of BA16M on 50 mM phosphate buffer (pH 11) (– – –), 25 mM (-----) and 100 mM (——) sodium diphosphate solution (pH 11) at 20 °C.

ionic strength in the subphase.

Sodium diphosphate has been shown to affect the protein structure strongly.[41] The surface pressure in the π-A isotherm began to increase at a large surface area in the presence of 100 mM sodium diphosphate in the aqueous subphase (Figure 3), suggesting that the peptide underwent the transition from an α-helix to a random-coil conformation.

Amphiphilic Helical Peptides with a Terminal Amino Group, HA16M and HA16B

In the π-A isotherms of HA16M and HA16B on a water subphase or on

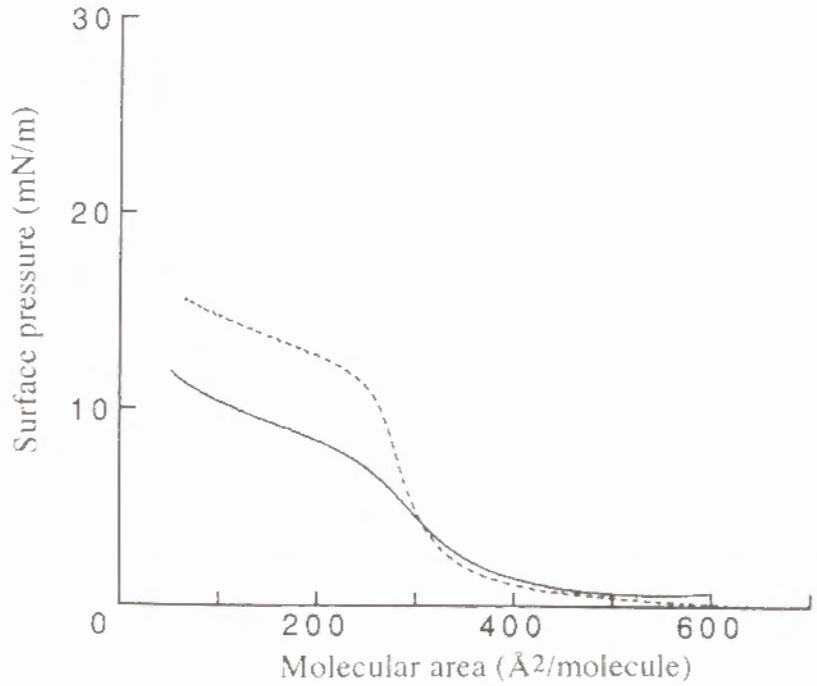

Figure 4 π-A isotherms of HA16M (——) and HA16B (-----) on water subphase at 20 °C.

a buffered subphase (Figure 4), the phase transition from a liquid to a solid state was not observed. The surface area at the inflection point was similar to

Table III. Inflection point and phase transition point in the pressure-area isotherms of the amphiphilic peptides with amino group at 20 °C.

Compound	Subphase	Inflection point	
		area (Å²)	pressure (mN/m)
HA16M	Water	253.7	5.5
HA16M	pH 9.3[a]	255.2	8.8
HA16M	pH 4.0[b]	258.5	6.0
HA16B	Water	253.5	8.5
HA16B	pH 9.3[a]	255.6	10.9
HA16B	pH 5.5[a]	250.0	9.5
HA16B	pH 4.0[b]	256.4	10.0
HA16B	pH 9.3[c]	252.0	14.5
HA16B	pH 7.7[c]	255.6	11.0
HA16B	pH 5.5[c]	255.6	9.0
HA16B	pH 4.0[d]	254.2	9.3

[a]50 mM sodium phosphate buffer.
[b]50 mM sodium citrate buffer.
[c]50 mM sodium phosphate-0.5 M NaCl buffer.
[d]50 mM sodium citrate-0.5 M NaCl buffer.

that of BA16M. Therefore, HA16M and HA16B also take an α-helical conformation and orient the helix axis parallel to the interface.

The collapse pressure at higher pH than 7.7 was higher than that at low pH at the same NaCl concentration (Table III, bottom four lines). This is probably due to disappearance of electrostatic repulsion between ammonium groups at high pH. The terminal amino groups of both peptides might be deprotonated at pH 9.3, which is much higher than the pKa value of an α-amino group of amino acids. Under any conditions HA16B collapsed at higher surface pressure than HA16M.

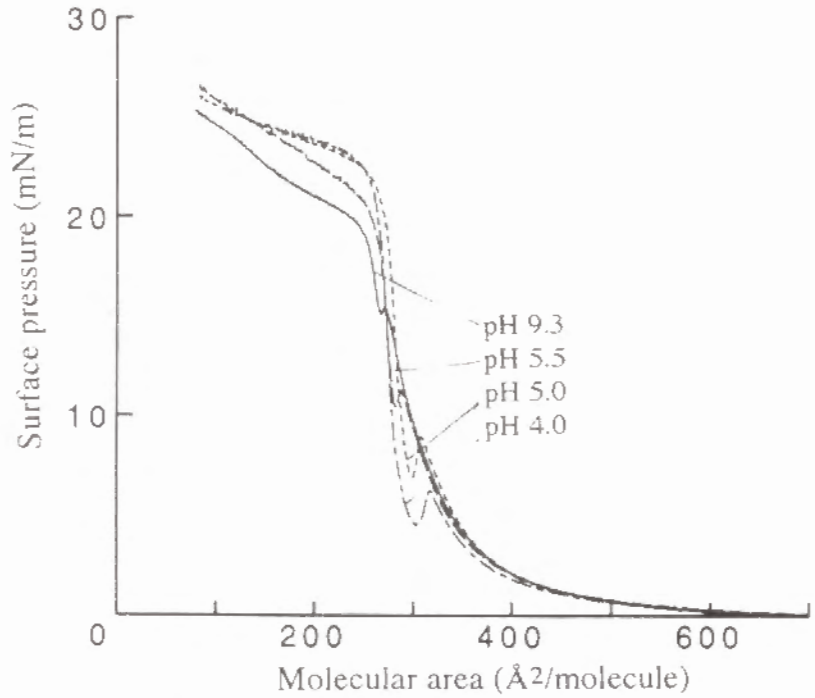

Figure 5 π-A isotherms of BA16OH on various pH subphase containing 0.5 M NaCl at 20 °C. pH 4.0 (– – – –), pH 5.0 (-----), pH 5.5 (– – –) and pH 9.3 (——)

Amphiphilic Helical Peptides with a Terminal Carboxyl Group, BA16OH and COOHA16M

The inflection point in the π-A isotherms of the above peptides (Figures 5 and 6 and Tables IV and V) was observed at the area comparable to that of BA16M (Table II). These peptides should take an α-helical conformation at the air/water interface and orient the helix axis parallel to the interface. The phase transition from a liquid to a solid state was observed always in the isotherm of BA16OH and sometimes in that of COOHA16M.

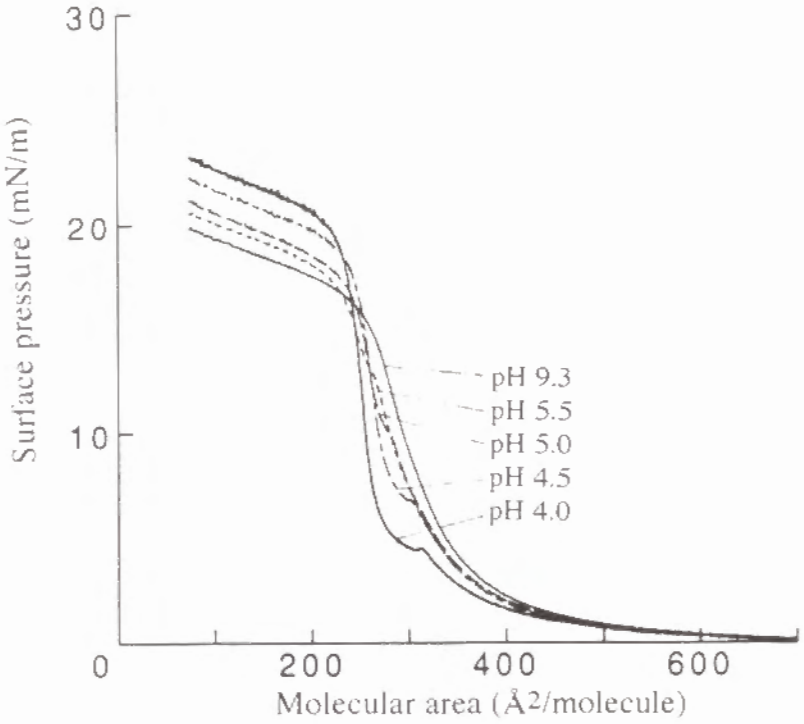

Figure 6 π-A isotherms of COOHA16M on various pH subphase containing 0.5 M NaCl at 20 °C. pH 4.0 (——), pH 4.5 (– – – -), pH 5.0 (-----), pH 5.5 (– – –) and pH 9.3 (——).

In the case of BA16OH, the local maximum pressure of the mound increased with increasing pH of the aqueous subphase in the presence of 0.5 M NaCl (Table IV). The increasing surface pressure at the phase transition should be explained by repulsion between likely charged end groups. The terminal carboxyl group of the peptide may be ionized around pH 5.5, though the pKa value of the carboxyl group at the C terminus of peptides is 3.4. Since the pKa value of polyelectrolytes deviates from the standard value due to dense distribution of dissociative group along the molecule,[42] the pKa value of

Table IV. Inflection point and phase transition point in the pressure-area isotherms of BA16OH at 20 °C.

Subphase	Inflection point		Top of mound	
	area (Å^2)	pressure (mN/m)	area (Å^2)	pressure (mN/m)
Water	262.5	12.5	320.5	4.3
pH 9.3[a]	253.9	12.2	273.7	10.8
pH 5.5[a]	262.5	11.1	276.5	8.8
pH 4.0[b]	264.5	12.2	324.5	3.4
pH 9.3[c]	243.8	17.2	253.9	15.5
pH 5.5[c]	256.3	15.2	271.1	11.3
pH 5.0[d]	262.5	16.1	290.9	8.9
pH 4.0[d]	264.8	14.6	306.8	6.2
pH 3.5[d]	268.7	15.6	310.7	6.3

[a]50 mM sodium phosphate buffer. [b]50 mM sodium citrate buffer.
[c]50 mM sodium phosphate-0.5 M NaCl buffer.
[d]50 mM sodium citrate-0.5 M NaCl buffer.

the terminal group of peptides should shift to higher value in monolayer. The inflection point, however, was not influenced significantly by changing the pH of the subphase.

On the other hand, the π-A isotherm of COOHA16M changed dramatically with the change of pH (Table V). The phase transition occurred at low pH, but did not occur at pH 9.3. This observation suggests that the monolayer of COOHA16M undergoes phase transition only when it is unionized.

Table V. Inflection point and phase transition point in the pressure-area isotherms of COOHA16M at 20°C.

Subphase	Inflection point		Top of mound	
	area (Å^2)	pressure (mN/m)	area (Å^2)	pressure (mN/m)
Water	236.2	8.6	319.5	2.3
pH 9.3[a]	265.7	8.4	-	-
pH 5.5[a]	238.7	11.7	253.2	8.7
pH 4.0[b]	249.1	11.7	325.1	3.6
pH 9.3[c]	256.5	13.3	-	-
pH 5.5[c]	230.4	14.8	260.6	10.2
pH 5.0[d]	239.3	14.0	263.0	10.0
pH 4.5[d]	243.4	12.8	282.3	6.8
pH 3.5[d]	236.9	12.5	306.3	3.5

[a]50 mM sodium phosphate buffer. [b]50 mM sodium citrate buffer.
[c]50 mM sodium phosphate-0.5 M NaCl buffer.
[d]50 mM sodium citrate-0.5 M NaCl buffer.

Amphiphilic Helical Peptide with Sar Residues, BS3A16M

The π-A isotherm of BS3A16M (Figure 7) did not show any evidence for phase transition, and it was similar to that of HA16M or COOHA16M at high pH. In the case of the deprotected compound, HS3A16M, the surface pressure scarcely increased with compression.

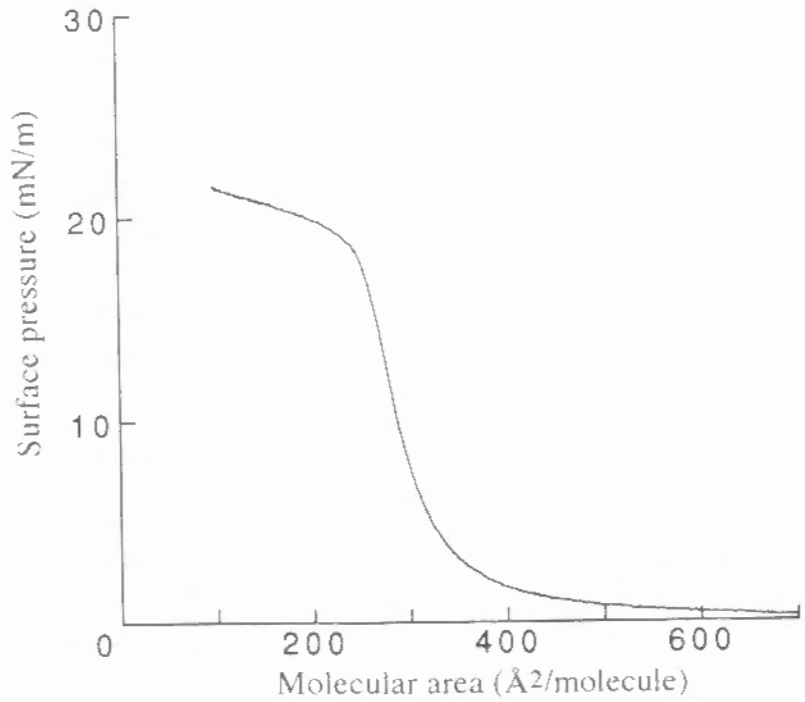

Figure 7 π-A isotherm of BS3A16M on water subphase at 20 °C.

Mixture of Peptides

Although the monolayer of HA16M did not undergo phase transition from a liquid to a solid state in the π-A isotherms, the monolayer of an equimolar mixture of HA16M and BA16OH underwent phase transition on a

pure water subphase (Figure 8). However, the phase transition was detected neither at pH 4.0 nor in the presence of 100 mM NaCl. These results suggest that the electrostatic interaction between the ammonium group of HA16M and the carboxylate group of BA16OH stabilizes the molecular packing in the monolayer. At pH 4.0 the slope of the π-A isotherm began to increase at the molecular area of 130 Å^2, which is half the molecular area at the inflection point in the π-A isotherm of pure BA16OH. Therefore, the monolayer of the mixture is fully phase-separated under this condition.

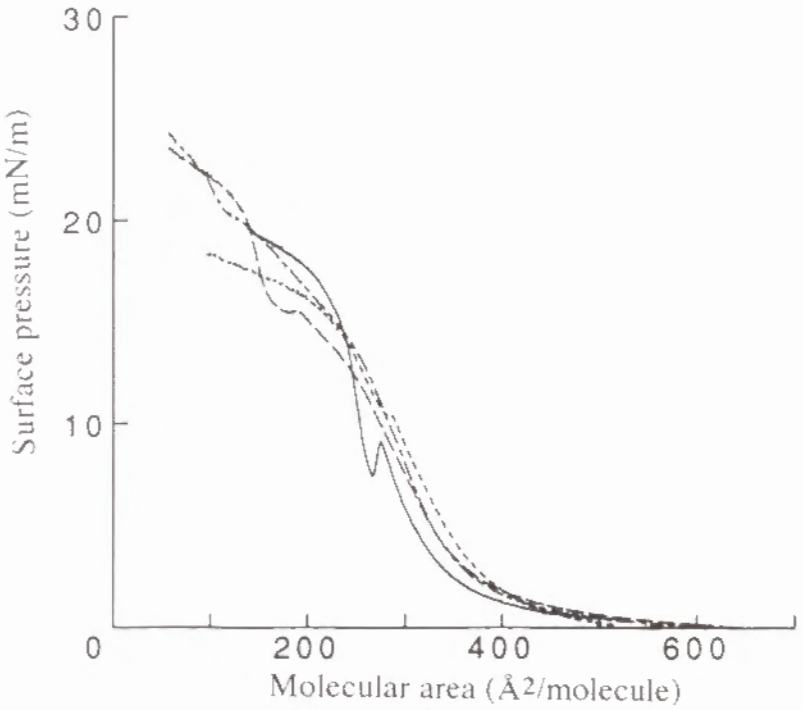

Figure 8 π-A isotherms of the equimolar mixture of HA16M and BA16OH on water (——), 100 mM NaCl (– – –), 50 mM phosphate buffer of pH 9.3 (-----) and 50 mM citrate buffer of pH 4.0 (– – –) at 20 °C.

In the case of the mixture of HA16M and COOHA16M (1/1), the phase transition was not observed under any conditions (Figure 9), in contrast to the mixture of HA16M and BA16OH, though the same kind of interaction might occur in both mixture systems. Since the monolayer of HA16M or ionized COOHA16M did not undergo phase transition, the electrostatic interaction alone is not enough for the phase transition of the monolayer. At pH 4.0, the area at the inflection point is approximately half that in the pure COOHA16M monolayer, suggesting that the phase separation of the monolayer as observed in the mixture of HA16M and BA16OH took place.

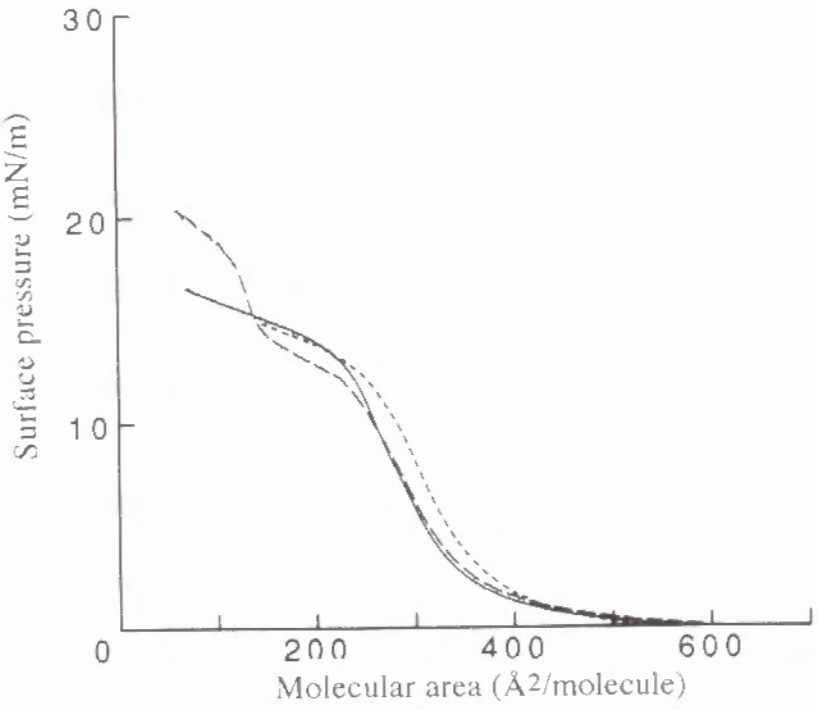

Figure 9 π-A isotherms of the equimolar mixture of HA16M and COOHA16M on water (——), 50 mM phosphate buffer of pH 9.3 (-----) and 50 mM citrate buffer of pH 4.0 (– – –) at 20 °C.

The monolayer of an equimolar mixture of BA16OH and COOHA16M underwent phase transition on a pure water subphase and an aqueous solution buffered at pH 4.0 (Figure 10). The monolayer of each component peptide underwent the phase transition under these conditions. On the other hand, at pH 9.3, the monolayer of the mixture did not show phase transition. This is probably because the molecular packing of COOHA16M in the monolayer is not so stable as to undergo phase transition at pH 9.3.

The monolayer of an equimolar mixture of BA16M with BA16OH on a water subphase gave a π-A isotherm having the phase transition (Figure 11)

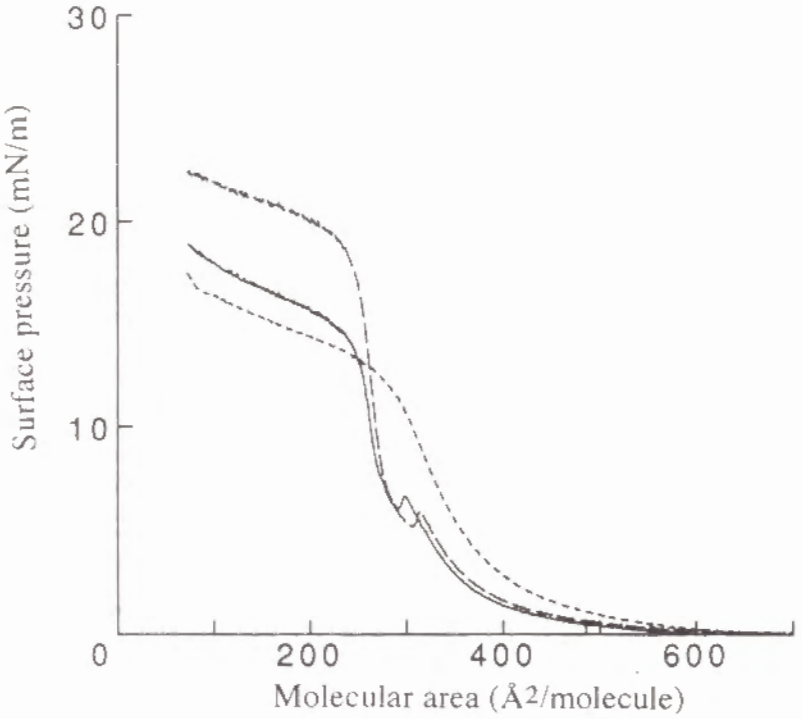

Figure 10 π-A isotherms of the equimolar mixture of BA16OH and COOHA16M on water (——), 50 mM phosphate buffer of pH 9.3 (-----) and 50 mM citrate buffer of pH 4.0 (– – –) at 20 °C.

similar to that of the BA16M or BA16OH monolayer. However, the mixture of BA16M and COOHA16M shows a different behavior. Apparently, the interaction of BA16OH with a fully protected peptide, BA16M, is different from that of COOHA16M with BA16M, although both BA16OH and COOHA16M have a terminal carboxyl group. In the case of the mixture of BA16M and HA16M, the π-A isotherm has an inflection point at a molecular area of around 130 Å^2, which is half the molecular area at the inflection point of the pure BA16M monolayer, indicating a complete phase separation in the

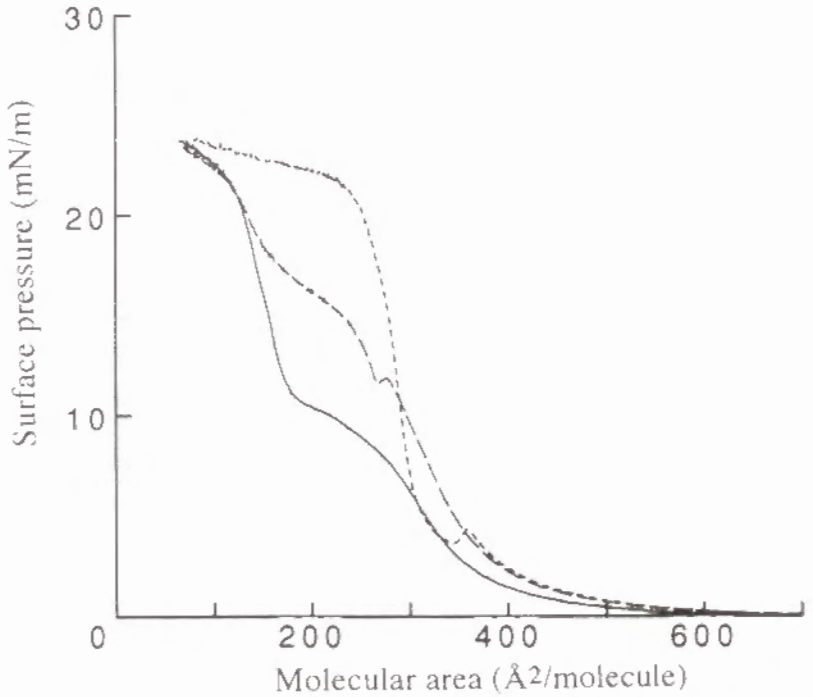

Figure 11 π-A isotherms of the equimolar mixture of BA16M and COOHA16M (– – –), BA16M and BA16OH (-----), and BA16M and HA16M (——) on water at 20 °C.

monolayer. To compare Figure 10 with Figure 7, the electrostatic interaction between the end groups of HA16M and BA16OH should promote the molecular packing in the monolayer.

Discussion

The peptides synthesized in the present investigation were shown to take a perfect α-helical conformation at the air/water interface, although the helix content was around 60 % in ethanol/water (95/5 v/v). Since the helical structure is stabilized in the environment of low dielectric constant, the major part of the peptide should be exposed to air when the peptide molecules are spread at the air/water interface. It is worth noting that the peptides oriented the helix axis parallel to the air/water interface. The helical structure is stabilized by intramolecular hydrogen bonds. However, three amide protons and carbonyl groups, respectively, at the N- and C-terminal ends of the helix are free from intramolecular hydrogen bonds.[43] These amide groups should be hydrated at the air/water interface. This should be the reason for the helices to take an orientation parallel to the interface. The extent of hydration at both ends of a peptide chain should be different according to their hydrophilicity, and should also affect the molecular packing of the monolayer. The strong hydration at the chain ends should be the reason for the absence of phase transition in the monolayers of HA16M, HA16B, BS3A16M, HS3A16M, and COOHA16M (at high pH), although these peptides take an α-helical conformation (Table II). In general, the negative charge at the N terminus and the positive charge at the C terminus is considered to stabilize the helical structure as a result of the interaction with the macrodipole of the helices.[30,31]

The monolayer of COOHA16M formed only expanded aggregates at higher pH (Table V), but condensed aggregates at a lower pH, even though the negative charge on the N terminus might stabilize the helical structure at high pH. Therefore, the deformation of the helical structure due to the terminal charge cannot explain the expansion of the monolayer. On the other hand, the monolayer of HA16B carrying a terminal benzyl group, which is bulky and hydrophobic to inhibit hydration of the terminal amide bonds, showed much higher surface pressure at the inflection point than HA16M. This observation gives support for the explanation considering destabilization of the monolayer by the hydration of the peptide terminus. In the case of HS3A16M, a strong hydration of the N-terminal region prohibited monolayer formation of the peptide molecule.

The π-A isotherm of the BA16M monolayer showed a mound at the molecular area of around 300 Å^2. The isotherm was reversible at larger areas than that at the mound. Therefore, the mound is not caused by the formation of a multilayer as previously reported for homopolymers of α-amino acids.[12,13] The mound should have resulted from the molecular rearrangement from a liquid to a solid state. The peptides might be dispersed irregularly in the liquid state. However, it is considered that the peptide forms smaller aggregates in the liquid state, which grow to a larger crystal in the solid state. This explanation is based on the high tendency of the peptide to associate together, which was shown by the previous report that the hexadecapeptide and the longer peptides associate together in an ordered form when incorporated in a lipid bilayer membrane.[44]

The behavior of the binary peptide system is complex. When the

monolayers of individual peptides show a mound in the π-A isotherm, the two components mix homogeneously at the air/water interface. Examples are the combinations of BA16M and BA16OH, and BA16OH and COOHA16M at low pH. However, phase separation occurs, when one component shows a mound in the π-A isotherm and the other does not. Examples are the combinations of BA16M and HA16M, BA16OH and HA16M at low pH or high ionic strength, BA16OH and COOHA16M at high pH, and COOHA16M and HA16M at low pH. However, the combination of BA16OH and HA16M is an exception of this category. Although the monolayer of BA16OH shows a mound in the π-A isotherm and the monolayer of HA16M does not, these peptides are mixed homogeneously due to electrostatic attraction acting between the two components. This is the first interesting example showing that the nature of the terminal group of a helix peptide has a strong influence on the interhelix interaction, and hence the packing of helices. Proteins forming an ion channel such as a Na^+ channel have been shown to be composed of several strands of helices.[45] Since these helices are embedded in the phospholipid bilayer membrane, each helix should suffer on internal pressure of *ca.* 30 mN/m.[46] However, each helix does not necessarily have to be resistant to this pressure by itself, if interhelix interactions take place favorably as exemplified by the monolayer of a mixture of BA16OH and HA16M on the pure water subphase.

References

(1) Fermi, G.; Perutz, M. F. *Atlas of Molecular Structures in Biology. 2. Haemoglobin and Myoglobin;* Clarendon Press: Oxford, 1981.

(2) Michel, H. *J. Mol. Biol.* **1982**, *158*, 567.

(3) Alberts, B.; Bray, D.; Lewis, J.; Raff, M.; Roberts, K.; Watson, J. D. *Molecular Biology of the Cell, 2nd ed.*, Garland Publishing: New York & London, 1989; Chapter 3.

(4) Rao, S. T.; Rossmann, M. G. *J. Mol. Biol.* **1973**, *76*, 241.

(5) Ho, S. P.; DeGrado, W. F. *J. Am. Chem. Soc.* **1987**, *109*, 6751.

(6) Gaines, G. L., Jr. *Insoluble Monolayers at liquid interface*; Interscience: New York, 1966; Chapter 5.

(7) Birdi, K. S. *Lipid and biopolymer monolayers at liquid interfaces*, Plenum Press: New York, 1989; Chapter 3.

(8) Heath, J. G.; Arnett, E. M. *J. Am. Chem. Soc.* **1992**, *114*, 4500.

(9) Ikeura, Y.; Kurihara, K.; Kunitake, T. *J. Am. Chem. Soc.* **1991**, *113*, 7342.

(10) Malcolm, B. R. *Proc. R. Soc. London Ser. A* **1968**, *305*, 363.

(11) Loeb, G. I.; Baier, R. E. *J. Colloid Interface Sci.* **1968**, *27*, 38.

(12) Takeda, T.; Matsumoto, M; Takenaka, Y.; Fujiyoshi, Y.; Uyeda, N. *J. Colloid Interface Sci.* **1983**, *91*, 267.

(13) Malcolm, B. R. *Biochem. J.* **1968**, *110*, 733.

(14) Birdi, K. S. *Lipid and biopolymer monolayers at liquid interfaces*, Plenum Press: New York, 1989; Chapter 5.

(15) Lavigne, P.; Tancrede, P.; Lamarche, F.; Max, J.-J. *Langmuir* **1992**, *8*, 1988.

(16) Weisenhorn, A. L.; Romer, D. U.; Lorenzi, G. P. *Langmuir* **1992**, *8*, 3145.

(17)(a) Burgess, A. W.; Leach, S. J. *Biopolymers* **1973**, *12*, 2599. (b)

Karle, I. L.; Balaram, P. *Biochemistry* **1990**, *29*, 6747.

(18) Otoda, K; Kitagawa, Y.; Kimura, S.; Imanishi, Y. *Biopolymers* **1993**, *33*, 1337.

(19) Branden, C.; Tooze, J. *Introduction to Protein Structure*; Garland Publishing: New York & London, 1991.

(20) Pataki, G. *J. Chromatogr.* **1963**, *12*, 541.

(21) Izumiya, N.; Makisumi, S. *Nippon Kagaku Zasshi* **1957**, *78*, 662.

(22) Otoda, K; Kimura, S.; Imanishi, Y. *Biochim. Biophys. Acta* **1993**, *1145*, 33.

(23) Sugihara, T.; Imanishi, Y.; Higashimura, T. *Biopolymers* **1975**, *14*, 723.

(24) Konig, W.; Geiger, R. *Chem. Ber.* **1970**, *103*, 788.

(25) Albrecht, O. *Thin Solid Films* **1983**, *99*, 227.

(26) Holzwarth, G.; Doty, P. *J. Am. Chem. Soc.* **1965**, *87*, 218.

(27) Greenfield, N.; Fasman, G. D. *Biochemistry* **1969**, *8*, 4108.

(28) Chen, Y. -H.; Yang, J. T.; Chau, K. H. *Biochemistry* **1974**, *13*, 3350.

(29) Balaram, H.; Sukumar, M.; Balaram, P. *Biopolymers* **1986**, *25*, 2209.

(30) Wada, A. *Adv. Biophys.* **1976**, *9*, 1.

(31) Shoemaker, K. R.; York, E. J.; Stewart, J. M.; Baldwin, B. L. *Nature (London)* **1987**, *326*, 563.

(32) Gaines, G. L., Jr. *Insoluble Monolayers at liquid interface*; Interscience: New York, 1966; Chapter 4, Section 3.

(33) For example: Chi, L. F.; Johnston, R. R.; Ringsdorf, H. *Langmuir* **1991**, *7*, 2323.

(34) Mertesdorf, C.; Ringsdorf, H. *Liq. Cryst.***1989**, *5*, 1757.

(35) Meller, P.; Peters, R.; Ringsdorf, H. *Colloid Polym. Sci.* **1989**, *267*, 97.

(36)(a) Lösche, M.; Rabe, J.; Fischer, A.; Rucha, U.; Knoll, W.; Möhwald, H. *Thin Solid Films* **1984**, *117*, 269. (b) McConnell, H. M.; Tamm, L. K.; Weis, R. M. *Proc. Natl. Acad. Sci. U. S. A.* **1984**, *81*, 3249.

(37) Fujita, K.; Kimura, S.; Imanishi, Y.; Rump, E.; Ringsdorf, H. *Langmuir* accepted.

(38) Kajiyama, T.; Oishi, Y.;Uchida, M.; Morotomi, N.; Ishikawa, J.; Tanimoto, Y. *Bull. Chem. Soc. Jpn.* **1992**, *65*, 864.

(39) Hofmeister, F. *Archi. Expe. Pathol. Pharmakol.* **1888**, *24*, 247.

(40) Ciferri, A.; Orofino, T. A. *J. Phys. Chem.* **1966**, *70*, 3277.

(41) Goto, Y.; Aimoto, S. *J. Mol. Biol.* **1991**, *218*, 378.

(42) For example: Nagasawa, M.; Holtzer, A. *J. Am. Chem. Soc.* **1964**, *86*, 538.

(43) Branden, C.; Tooze, J. *Introduction to Protein Structure*; Garland Publishing: New York & London, 1991; Chapter 2.

(44) Otoda, K; Kimura, S.; Imanishi, Y. *Biochim. Biophys. Acta* **1993**, *1150*, 1.

(45) Catterall, W. A. *Science* **1988**, *242*, 50.

(46) Pink, D. A. *Can. J. Biochem. Cell Biol.* **1984**, *63*, 767.

Chapter 2

Two Dimensional Assembly Formation of Hydrophobic Helical Peptides at the Air/Water Interface: Fluorescence Microscopic Study

Introduction

Two-dimensional crystallization of biological macromolecules, especially proteins, has attracted much attention with respect to the molecular mechanism of assembly formation[1] and the development of functional thin layers.[2] It has been reported that two dimensional protein crystals formed by adsorption onto a mercury surface[3] or lipid monolayer surfaces.[4,5] However, in other cases, for example, at the air/water interface, proteins are denatured easily.[6]

The author has synthesized various hexadecapeptides that take α-helical conformation,[9] and studied their properties at the air/water interface.[10,11] The peptides stayed at the interface having the helix axis oriented parallel to the surface. Interestingly, some peptides undergo a phase transition from a liquid state to a solid state, whereas polypeptides of inhomogeneous molecular weight do not.

Several amphiphiles such as lipids and fatty acids having long alkyl chains form monolayers at the air/water interface and undergo phase transition depending on temperature and the molecular density at the surface.[12] The

phase separation in the monolayers can be visualized via fluorescence microscopy by incorporation of a small amount of fluorescence probe into the monolayer.[13-17] The solid domains are dark in the fluorescence micrograph due to exclusion of the fluorescent probe, while the fluid domains are bright. The shape of the solid domains is mostly elliptical, needle-like or spiral according to the molecular structure of the amphiphiles and the composition of the subphase. The dark domains have been identified to be two-dimensional crystals by electron microscopical analysis.[18] In the present chapter, the phase-transition behavior of α-helical peptides at the air/water interface was studied by fluorescence microscopy. The formation of two-dimensional crystal of the helical peptides was discussed in terms of molecular properties of the peptides.

Materials and Methods

Materials

The molecular structure of the peptides synthesized are shown in Figure 1. BA16M, BA16B, HA16M, HA16B, BS3A16M, HS3A16M, BA16OH and COOHA16M were prepared as described in Chapter 1. BioS3A16M and BioA16M were synthesized by the reaction of the amino end group of HA16M and HS3A16M with biotin aminocapronate N-hydroxysuccinimide (Sigma, St. Louis, USA), respectively. The fluorescein-5-isothiocyanate (FITC)-labeled peptide was prepared by the reaction of FITC (Molecular Probes, Eugene, USA) with HA16M in ethanol. The obtained crude peptides were purified by gel filtration through a Sephadex LH20 (Pharmacia) column using methanol as the elution solvent. The major fraction was collected and

concentrated, followed by recrystallization from methanol to obtain BioS3A16M, BioA16M and FITC-A16M, respectively. A cationic dye, 1, 1, 3, 3, 3', 3'-hexamethylindocarbocyanine iodide ($DiIC_1$) was purchased from Molecular Probes, Eugene, USA.

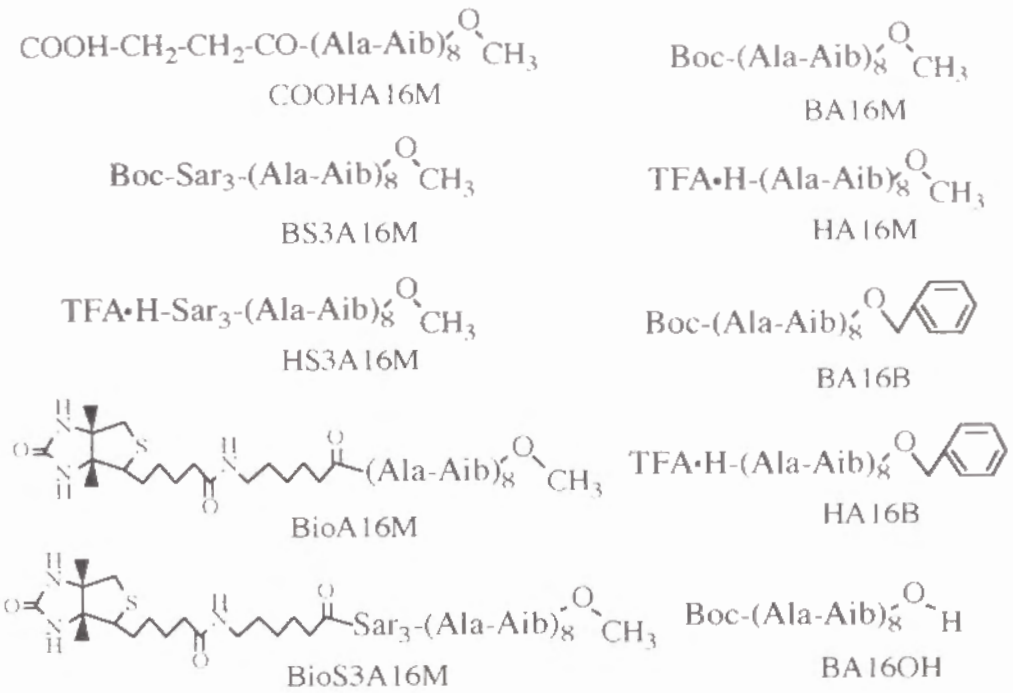

Figure 1 Molecular structure of hydrophobic helical peptides.

Methods

π-A isotherms were measured with a home-made Langmuir trough[19] with the surface area of 490 cm^2 at 20 °C. The experimental procedures are described in Chapter 1.

The fluorescence microscopy was combined with a Langmuir trough with a surface area of 250 cm^2, whose set-up has been reported previously.[20]

A one-cm diameter teflon ring with a small slit was used to provide a separated area in the plane of monolayer surface to eliminate the flow of the monolayer. The small slit allows the surface pressure in the small compartment equilibrated with that of the whole trough.[20] In order to observe the monolayers by fluorescence microscopy, FITC-A16M (1 or 2 mol%) was added in the spreading peptide solutions. In the cases of negatively charged peptides, BA16OH or COOHA16M, 2 μl of an aqueous $DiIC_1$ solution (2.8×10^{-7} M) was injected into the compartment (800 μl) of the subphase underneath the monolayer in a gas-analogous state, followed by 10-min incubation for equilibrium.[21] The monolayers, which were spread at the air/water interface at a surface density of 900 Å^2/molecule, were compressed at the rate of 0.14 - 0.5 cm^2/s and observed by fluorescence microscope with a cut-off filter for sulforhodamine.[21,22]

The Langmuir-Blodgett transfer of the monolayer[23] onto mica plates (1 × 3 cm) was carried out at a dipping rate of 1.0 cm/min at the surface pressure where phase transition occurs.

Results

Protected Helical Peptide, BA16B

The π-A isotherm of BA16B on water at 20 °C is shown in Figure 2. A mound was observed at 300 Å^2 in the isotherm similarly to that of BA16M.[10] The mound is ascribed to the phase transition from a liquid state to a solid state of the monolayer. The mound in the isotherm became smaller with decreasing compression speed, indicating that the mound is due to kinetic

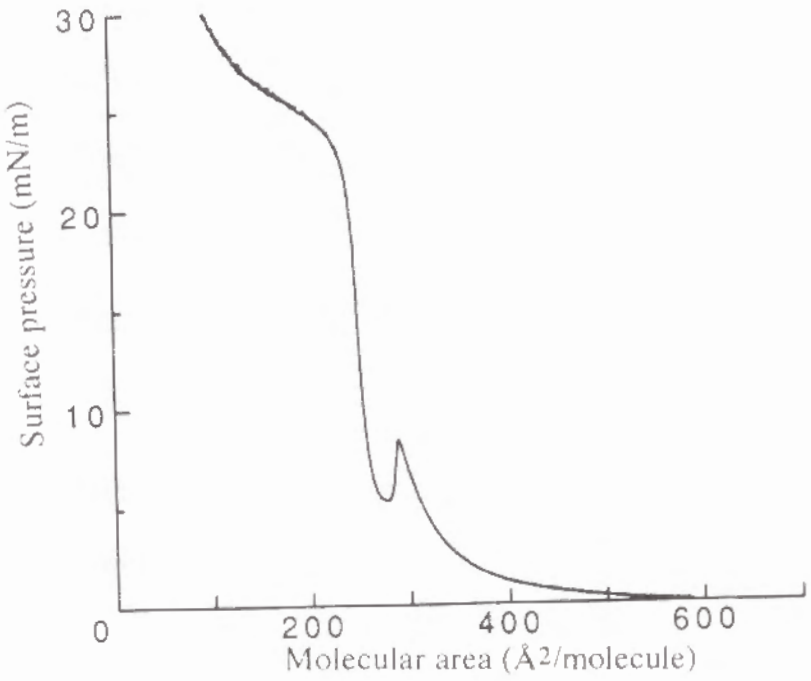

Figure 2 π-A isotherm of BA16B monolayer on the surface of water at 20 °C.

effects. The shape of the isotherm and the molecular area of the mound were identical in the larger (490 cm^2) trough and the small (250 cm^2) fluorescence trough. Therefore, the size effect of the trough is negligible. The observation by fluorescence microscopy revealed the presence of dark leafy domains, when the monolayer containing FITC-A16M (1 mol%) was held at the surface pressure corresponding to the top of the mound (Figure 3). The domains were enlarged as compression proceeded, and finally the field of view became nearly dark. The identical domain formation was observed in an experiment without the teflon ring separating the small compartment. The monolayer of

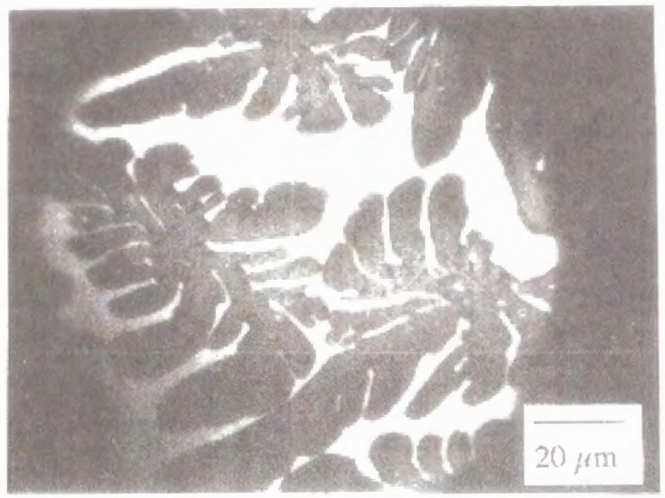

Figure 3 Fluorescence micrograph of BA16B monolayer containing FITC-A16M (1 mol%) deposited on the surface of water. The monolayer was held at the surface pressure corresponding to the top of the mound in the π-A isotherm.

BA16M behaved similarly to that of BA16B under fluorescence microscope. The dark domains should have been caused by exclusion of FITC-A16M from the domains composed of BA16B. It is notable that faintly bright regions were observed in the dark domains, which looked like veins in a leaf or small patches. The bright regions showed fluorescence anisotropy, indicating that the arrangement of the fluorescence probe is regular in the domain. The monolayer of BA16B in a condensed state is, therefore, considered to be composed of large crystalline domains.

Helical Peptides With a Terminal Carboxyl Group, BA16OH and COOHA16M

The π-A isotherms of BA16OH (Figure 4a) and COOHA16M (Figure

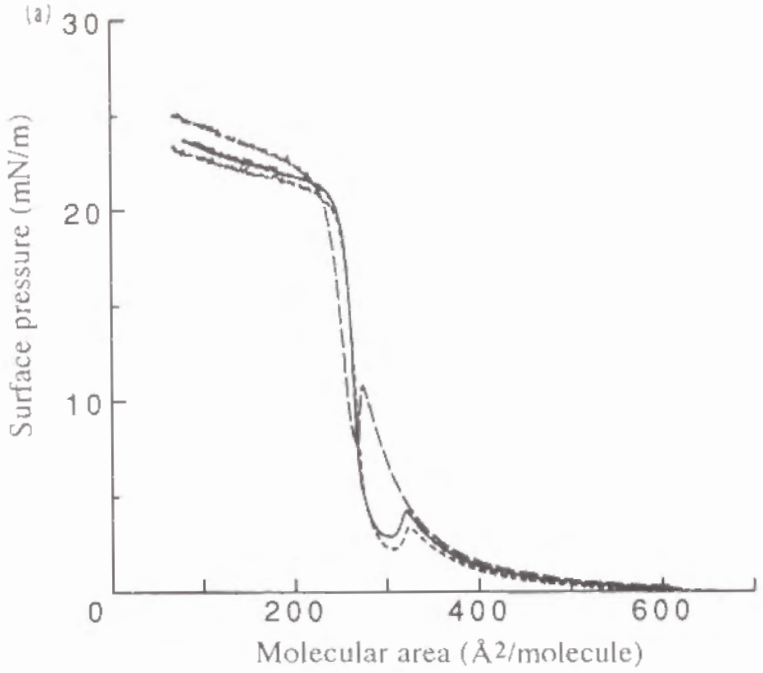

Figure 4 π-A isotherms of (a) BA16OH and (b) COOHA16M monolayer recorded on water (——), a 50 mM phosphate buffer solution (pH 9.3) (- - -) and a 50 mM citrate buffer solution (pH 4.0) (---) at 20 °C.

4b) spread on water showed a mound or a plateau region at the molecular area of *ca.* 300 Å^2, respectively. The isotherm was measured on water, a 50 mM phosphate buffer solution (pH 9.3) and a 50 mM citrate buffer solution (pH 4.0) as subphase. A mound related to phase transition was observed in the isotherm of BA16OH under any conditions. On the other hand, a plateau region appeared in the isotherm of COOHA16M when an acidic subphase was used, but it disappeared on the alkaline subphase.

In the case of BA16OH, dark leafy domains which are quite similar to those of BA16B were detected when the monolayer containing FITC-A16M (1 mol%) was held at the surface pressure corresponding to the top of the mound on the surface of water, a phosphate buffer or a citrate buffer solution (Figure 5a, b and c). The bright regions appearing in dark domains, which looked like veins, showed fluorescence anisotropy.

The leafy domains of BA16OH observed by the fluorescence microscopy are also seen on a mica plate, when the monolayer containing FITC-A16M (2 mol%) was transferred onto the mica plate by the vertical dipping method after holding at the surface pressure of the local minimum that is found aside the mound (Figure 5d). It indicates that the domains are stable enough for the transfer process despite the relatively low surface pressure of the monolayer.

The monolayer of COOHA16M containing FITC-A16M (2 mol%) held at the phase-transition pressure on water (Figure 6a) and an acidic buffer solution (Figure 6b) also showed dark domains under fluorescence microscope. However, domains were not detected on an alkaline buffer solution, which corresponds to the disappearance of phase transition from the isotherm. The shape of domains of COOHA16M deposited on water was needle-like. The same pattern of fluorescence microscope as BA16OH was observed when

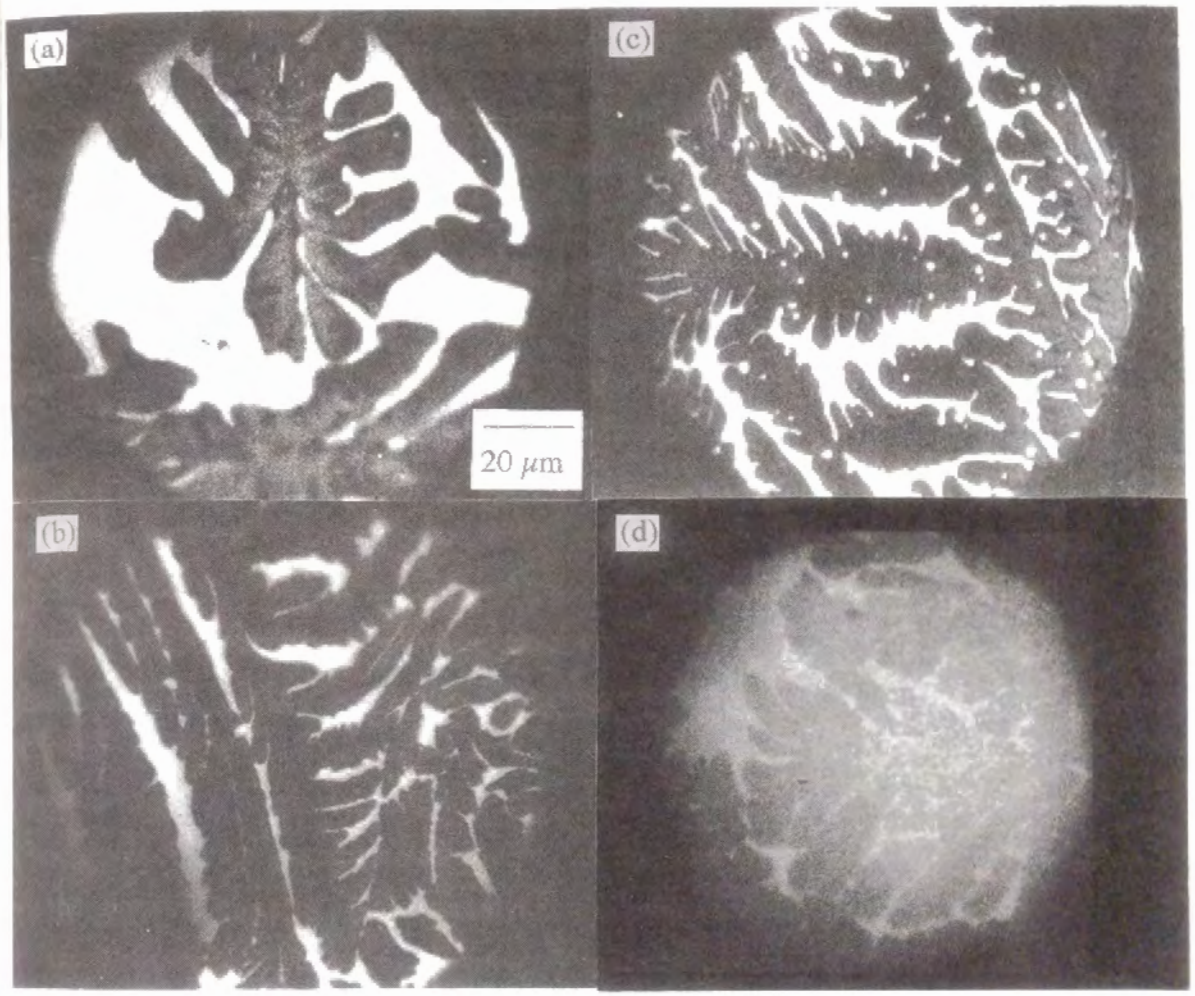

Figure 5 Fluorescence micrographs of BA16OH containing FITC-A16M (2 mol%) on the surface of (a) water, (b) an acidic subphase and (c) an alkaline subphase. The monolayers were held at the surface pressure corresponding to the phase-transition pressure.
(d) Fluorescence micrograph of BA16OH monolayer transferred onto the surface of a mica plate by holding the monolayer on water at the phase-transition pressure.

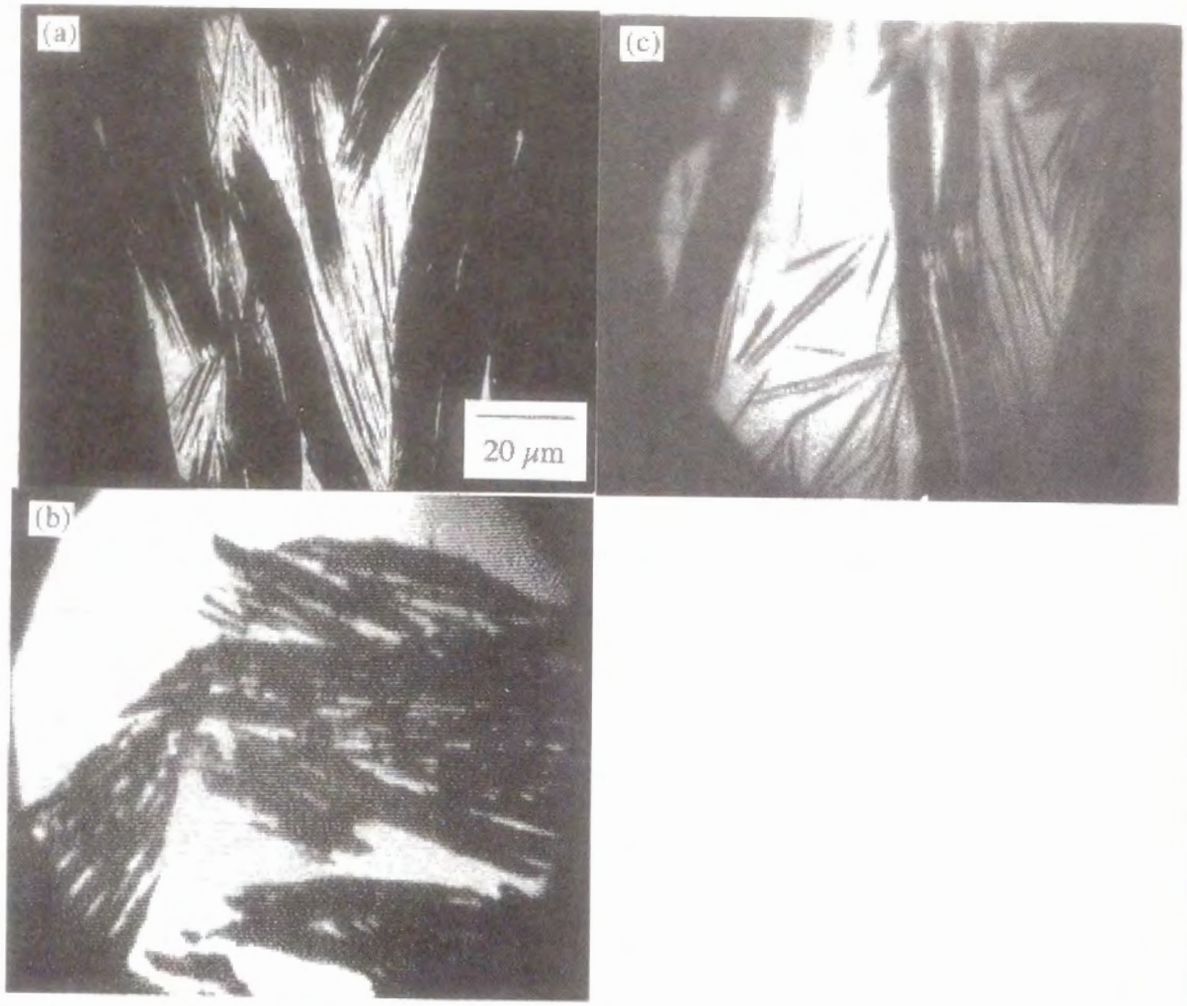

Figure 6 Fluorescence micrographs of COOHA16M monolayer containing FITC-A16M (2 mol%) on the surface of (a) water and (b) an acidic subphase. The monolayers were held at the surface pressure corresponding to the phase-transition pressure. (c) Fluorescence micrograph of COOHA16M monolayer transferred onto the surface of a mica plate by holding the monolayer on water at the phase-transition pressure.

transferred onto a mica plate (Figure 6c).

The monolayers were stained by other fluorescent probe, $DiIC_1$, which is bound strongly by a negatively charged surface due to electrostatic interactions.[24] A dye solution was injected into the subphase of the monolayers in a gas-analogous state. The dye diffused immediately in the subphase and bound to the monolayer. The monolayer fluoresced uniformly, indicating that dye molecules bound to the negatively charged end-groups of peptides, which were spread at the air/water interface. When the monolayer was compressed to induce phase transition, dark domains of leafy shape (BA16OH, Figure 7a) and of needle-like shape (COOHA16M, Figure 7b) appeared. The domains were enlarged as the compression proceeded, and finally occupied the entire surface area.

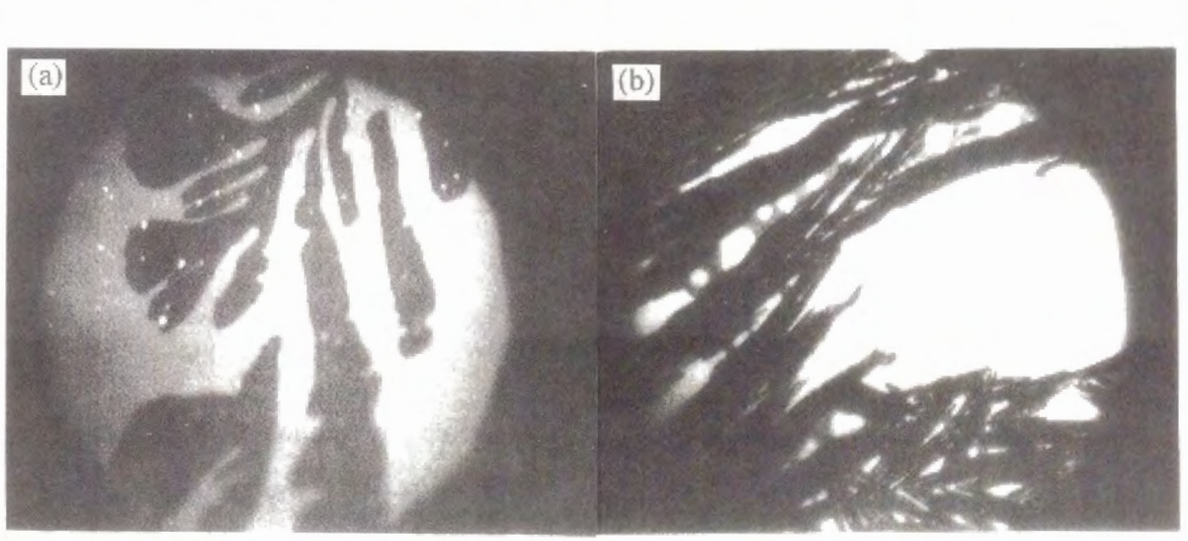

Figure 7 Fluorescence micrographs of (a) BA16OH and (b) COOHA16M monolayers on the surface of water. $DiIC_1$ was injected into the aqueous subphase. The monolayer was held at the surface pressure corresponding to phase-transition pressure.

Biotinylated Helical Peptides, BioA16M and BioS3A16M

The π-A isotherms of BioA16M and BioS3A16M monolayers on the surface of water are shown in Figure 8. The BioA16M monolayer on water or on a 0.5 M aqueous NaCl solution[11] showed a mound related to the phase transition. On the other hand, the BioS3A16M monolayer on water did not show the mound in the isotherm, although it appeared when spread on a 0.5 M aqueous NaCl solution.[11] The BioA16M monolayer containing FITC-A16M (2 mol%) exhibited dark elliptical domains on the surface of water or a 0.5 M aqueous NaCl solution when it was held at the surface pressure corresponding to the top of the mound (Figure 9a and b). On the other hand, the BioS3A16M monolayer containing FITC-A16M (2 mol%) produced bright domains of a spindle shape on water (Figure 9c) and dark rectangular domains on a 0.5 M aqueous NaCl solution. (Figure 9d).

The monolayer of other peptides, HA16M, HA16B and BS3A16M, which did not show phase transition in the π-A isotherms,[10] did not form any domains on water, alkaline and acidic solution.

Discussion

It is described in Chapter I that some hydrophobic α-helical hexadecapeptides show a mound at the molecular area of *ca.* 300 Å^2 in the π-A isotherm. The appearance of the mound was ascribed to the molecular re-arrangement due to phase transition from an expanded state to a condensed state. This is confirmed by the fluorescence microscopic observation of the monolayers as described above. Monolayers of the peptides containing

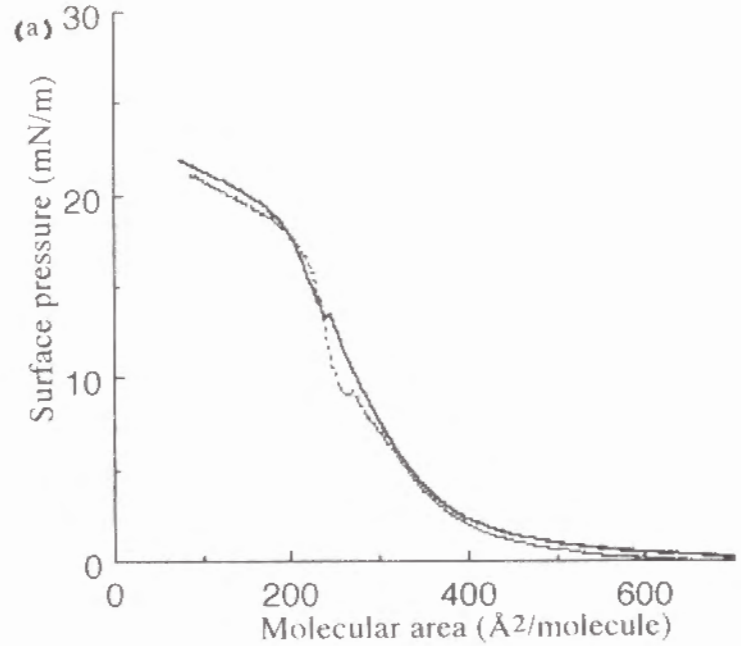

Figure 8 π-A isotherms of (a) BioA16M and (b) BioS3A16M monolayers on the surface of water (---) or 0.5 M NaCl solution (—) at 20 °C.

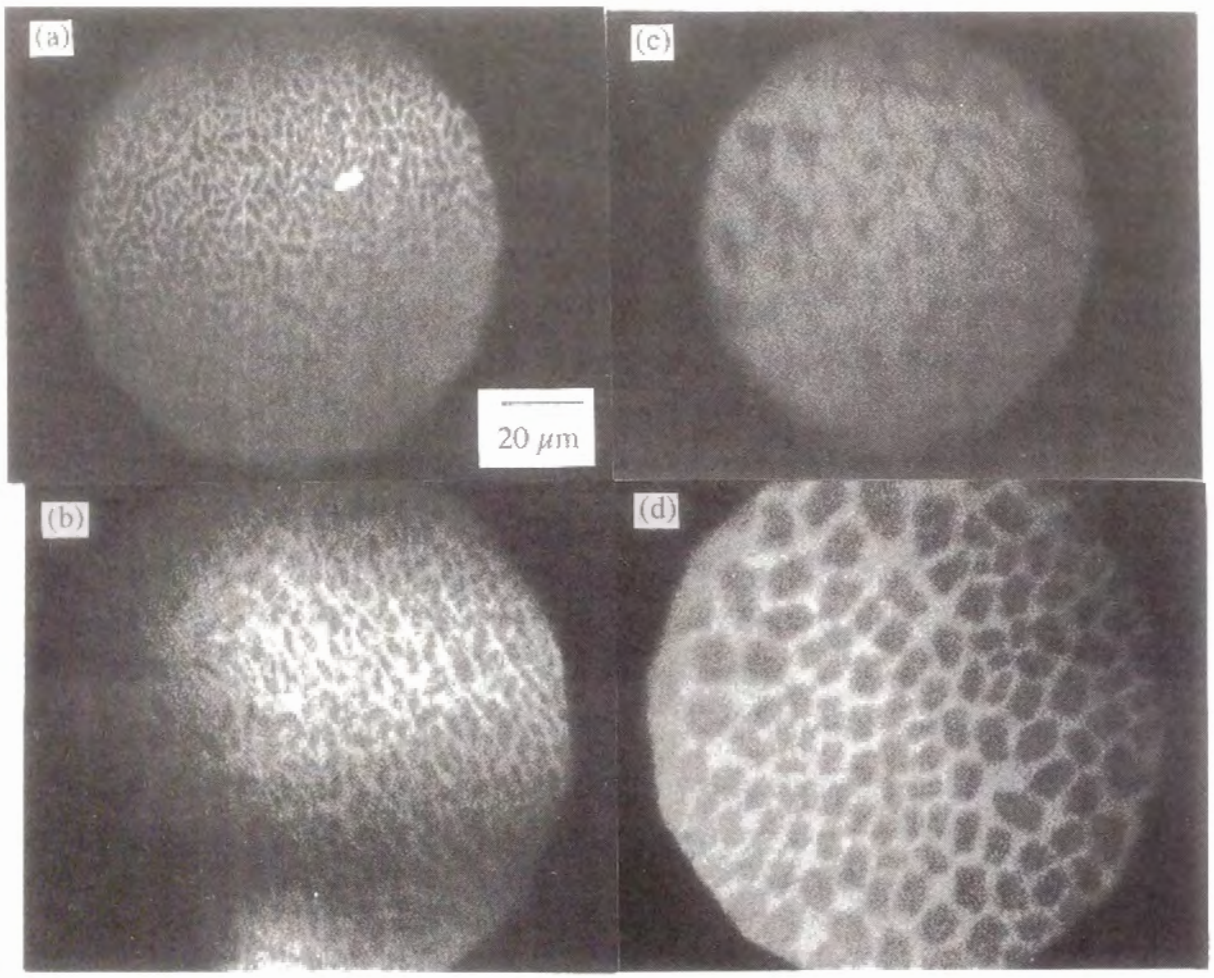

Figure 9 Fluorescence micrographs of BioA16M monolayer containing FITC-A16M (2 mol%) on the surface of (a) water and (b) a 0.5 M aqueous NaCl solution, and BioS3A16M monolayer containing FITC-A16M (2 mol%) on (c) water and (d) a 0.5 M aqueous NaCl solution. The monolayers were held at the surface pressure corresponding to the phase-transition pressure.

FITC-A16M formed dark domains when held at the surface pressure corresponding to the top of the mound or the largest end of the plateau region in the π-A isotherm. On the other hand, other peptides, which did not show phase transition, did not produce any domains detectable *via* fluorescence microscopy. The domain formation may be related with the two-dimensional crystallization of peptide monolayers because bright regions in the dark domains, due to small amount of incorporated labeled peptide, showed fluorescence anisotropy.

The HA16M, HA16B, and BS3A16M, which showed neither phase transition nor domain formation, possess the more hydrophilic N-terminal region than the other peptides. Probably, the hydrophilic part of these peptides is pulled into the subphase due to strong hydration, resulting in disturbance of the crystallization of the monolayers. This explanation is consistent with the observation that the BioS3A16M monolayer formed domains on a 0.5 M aqueous NaCl solution but not on water. In the saline water, the peptide should be expelled from the aqueous phase due to salting-out effect, leading to tight packing of peptide molecules in the monolayer.

The dark domains in the presence of $DiIC_1$ appeared upon compression of monolayers of COOHA16M and BA16OH (Figure 7). This observation is explained by desorption of dye molecules from the monolayer, but not by concentration quenching of $DiIC_1$ on the basis of the following considerations. $DiIC_1$ is reported to bind to an outer leaflet of the vesicles composed of negatively charged phospholipids at *ca.* three lipids/one dye ratio. Although the fluorescence was quenched at the lipid/dye ratio, it recovered the intensity upon dilution to the ratio of six lipids/one dye.[24] The molecular area occupied by a phospholipid at the vesicle surface is 74 Å^2.[25] It is, therefore,

calculated that the molecular density where the dye undergoes self-quenching is less than 222 Å²/dye, and the self-quenching is negligible at areas larger than 444 Å²/dye. The dye has two positive charges, and COOHA16M and BA16OH bear a carboxylate ion at the gas phase. Since the binding of $DiIC_1$ to the monolayer is determined mainly by electrostatic interaction,[24] the amount of the dye bound to the monolayer of COOHA16M or BA16OH should be less than half of the peptide. The molecular density of the dye is, therefore, 500 Å²/molecule at most, which is calculated from the molecular area occupied by the helical peptides of 250 Å². Consequently, the dark domain should not be caused by self-quenching of the dye in the tightly packed state. This observation indicates that the peptides in the domain have no longer negative charges, because of protonation of the carboxylate ions upon crystallization of the monolayer.

Interestingly, the shape of the monolayer domains changed according to the nature of the peptides. The shape of domains, however, might be affected by impurities in the monolayer,[26] which influence the formation of nuclei for the crystallization as reported for lipid monolayers. This possibility can be excluded in the present case, because the addition of a small amount of FITC-A16M and a cationic dye $DiIC_1$ yield similar domain shapes of the two types. In addition, the domain structure was so stable that the shape was kept unchanged during transfer onto a mica plate. It is, therefore, considered that different shapes of domains in the monolayers should be attributed to different molecular structures of the peptides.

Helical peptides possess a macrodipole moment along the helix axis.[27] Since the peptides studied here have the helix axis oriented parallel to the

interface,[10] the dipole moment also takes a horizontal orientation. Theoretical considerations have shown that the molecules having a dipole moment oriented horizontally yield a needle-like solid domain at the air/water interface, when the contribution of dipolar interactions to the anisotropic line energy between an ordered and a disordered domain is more significant than that of short-range nonpolar interactions.[28] Therefore, COOHA16M, which formed needle-like domains on the water subphase, is considered to possess a stronger dipole moment than other peptides, BA16M, BA16B, and BA16OH, forming the leafy elliptical domains. This consideration leads to the following speculation on the molecular arrangement of COOHA16M in the monolayer. COOHA16M should form a side-by-side dimer in a parallel arrangement with intermolecular hydrogen bondings between the carboxylic groups, thus strengthening the dipole moment of the helix peptide. On the other hand, BA16M, BA16B, and BA16OH should lie side by side in the monolayer with an antiparallel orientation. This speculation is consistent with the molecular properties of COOHA16M for the following reasons. COOHA16M does not form solid domains on the surface of an alkaline solution, indicating that the crystallization of the peptide is disturbed by hydration of the N-terminal region as described before.[15] However, COOHA16M deposited on the surface of water and an acidic solution formed solid domains, probably because of dehydration of the N-terminal region due to intermolecular hydrogen bondings. In the case of BA16OH, the N-terminal region has a hydrophobic Boc group, and the dissociation of the C-terminal carboxylic acid is suppressed by the interaction with the negative pole of the helix macrodipole. Therefore, BA16OH should be hydrophobic enough to produce solid domains without intermolecular hydrogen bondings on the surface of an alkaline

solution.

These peptides are the first examples to form two-dimensional solid monolayers at the air/water interface without the help of long alkyl chains in the molecule. Domains were detected in the monolayer upon phase transition, and the shape of the domain was related with the molecular structure and the packing of the peptides in the monolayer. Various types of two-dimensional crystals of the peptides with a defined secondary structure were found to be formed simply by the Langmuir technique, which should be useful for developing a supramolecular assembly.

References

(1) Darst, S. A.; Ahlers, M.; Meller, P. H.; Kubalek, E. W.; Blankenburg, R.; Ribi, H. O.; Ringsdorf, H.; Kornberg, R. D. *Biopys. J.* **1991**, *59*, 387.

(2) (a) Uzgiris, E. E.; Kornberg, R. D. *Nature* **1983**, *301*, 125. (b) Ahlers, M; Blankenburg, R.; Haas, H.; Möbius, D.; Möhwald, H.; Müller, W.; Ringsdorf, H.; Siegmund, H. -S. *Adv. Mater.* **1991**, *3*, 39.

(3) Yoshimura, H.; Matsumoto, M.; Endo, S; Nagayama, K. *Ultramicrosopy* **1990**, *32*, 265.

(4) Fromherz, P *Biochim. Biophys. Acta* **1971**, *225*, 382.

(5) Blankenburg, R.; Meller, P.; Ringsdorf, H.; Salesse, C. *Biochemistry* **1989**, *28*, 8214.

(6) Owaku, K; Shinohara, H.; Ikariyama, Y.; Aizawa, M. *Thin Solid Films* **1989**, *180*, 61.

(7) Reviewed in Birdi, K. S. *Lipid and biopolymer monolayers at liquid interfaces*, Plenum Press: New York, 1989; Chapter 5.

(8) Lavigne, P.; Tancrede, P.; Lamarche, F.; Max, J.-J. *Langmuir* **1992**, *8*, 1988.

(9) Otoda, K; Kitagawa, Y.; Kimura, S.; Imanishi, Y. *Biopolymers* **1993**, *33*, 1337.

(10) Fujita, K.; Kimura, S.; Imanishi, Y.; Rump, E.; Ringsdorf, H. *Langmuir* **1994**, *10*, 2731.

(11) Fujita, K.; Kimura, S.; Imanishi, Y.; Rump, E.; Ringsdorf, H. *J. Am. Chem. Soc.* **1994**, *116*, 2185.

(12) Gaines, G. L.,Jr. *Insoluble Monolayers at liquid interface*, Interscience: New York, 1966.

(13) Lösche, M.; Sackmann, E; Möhwald, H. *Ber. Bunsenges. Phys. Chem.* **1983**, *87*, 848.

(14) Peters, R.; Beck, K. *Proc. Natl. Acad. Sci. USA* **1983**, *80*, 7183.

(15) McConnell, H. M.; Tamm, L. K.; Weis, R. M. *Proc. Natl. Acad. Sci. USA* **1984**, *81*, 3249.

(16) Shimomura, M; Fujii, K.; Shimamura, T.; Oguchi, M.; Shinohara, E.; Nagata, Y.; Matsubara, M.; Koshiishi, K. *Thin Solid Films* **1992**, *210/211*, 98.

(17) Chi, L. F.; Johnston, R. R.; Ringsdorf, H. *Langmuir* **1991**, *7*, 2323.

(18) Fischer, A.; Lösche, M.; Möhwald, H.; Sackmann, E. *J. Phys. Lett.* **1984**, *45*, L785.

(19) Albrecht, O. *Thin Solid Films* **1983**, *99*, 227.

(20) Meller, P. *Rev. Sci. Instrum.* **1988**, *59*, 2225.

(21) Reichert, A.; Ringsdorf, H.; Wagenknecht, A. *Biochim. Biophys. Acta* **1992**, *1160*, 178.

(22) Dasheiff, R. M. *J. Neurosci. Methods* **1985**, *13*, 199.

(23) Blodgett, K. B. *J. Am. Chem. Soc.* **1935**, *56*, 1007.
(24) Yu, B. -Z.; Jain, M. K. *Biochim. Biophys. Acta* **1989**, *980*, 15.
(25) Huang, C.; Mason, J. T *Proc. Natl. Acad. Sci. USA* **1978**, *75*, 308.
(26) (a) Weis, R. M.; McConnell, H. M. *J. Phys. Chem.* **1985**, *89*, 4453.
(b) Miller, A.; Möhwald, H. *J. Chem. Phys.* **1987**, *86*, 4258.
(27) Wada, A. *Adv. Biopys.* **1976**, *9*, 1.
(28) Muller, P.; Gallet, F. *J. Phys. Chem.* **1991**, *95*, 3257.

Chapter 3

Monolayer Formation and Molecular Orientation of Various Helical Peptides at the Air/Water Interface

Introduction

Hydrophobic helical peptides are one of the secondary units constructing the core region of globular or membrane proteins.[1,2] Assembly of helices frequently occurs in natural proteins.[3,4] Studies on interaction between helices and factors governing the molecular packing of helices are important in understanding the formation of tertiary structure and/or the stability of protein structure.[5,6] The monolayer technique is a useful means for the studies, because it detects intermolecular forces operating in a two-dimensional array of molecules and the π-A isotherm provides information on the molecular packing.[7,8]

The helical hexadecapeptide, BA16M, forms a monolayer at the interface with a parallel orientation of the helix axis to the interface,[9] which is revealed by the comparison of the π-A isotherm with the molecular structure determined by the X-ray analysis.[10] The monolayers of BA16M and some of its derivatives with different terminal groups showed a phase transition from a liquid state to a solid state as the surface pressure increased.[9,11] The

fluorescence microscopic investigation revealed that these molecules form a two-dimensional crystal at the air/water interface and the morphology of the monolayers is different according to the end group of the helical peptide.[12]

In the present chapter, ten kinds of helical peptides (Figure 1) were newly synthesized to study interactions between helices in the peptide monolayer formed at the air/water interface. All of the peptides have Aib residue. This residue is effective to induce the helical conformation, because the steric hindrance around the α-carbon atom of Aib residues makes other

AdmA16B

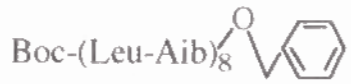

BL16B

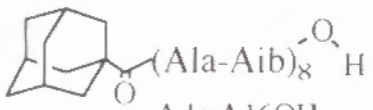

AdmA16OH

HL16B

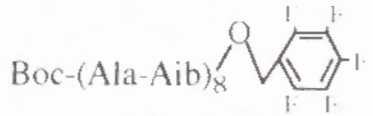

BA16FB

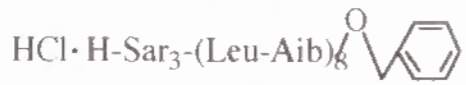

HS3L16B

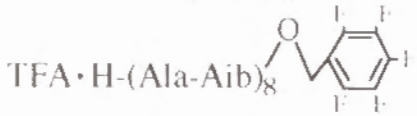

HA16FB

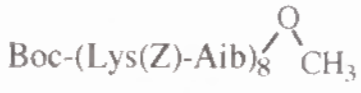

BKZ16M

BMA16B

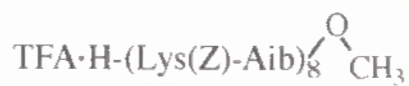

HKZ16M

Figure 1 Molecular structures of helical peptides synthesized in the present chapter.

conformations difficult to occur.[13,14] Five of those peptides have a common repeating sequence of Ala-Aib and various end groups having different hydrophobicities, other two a repeating sequence of Lys(Z)-Aib, and the rest a repeating sequence of Leu-Aib. The modification of terminal groups was designed to provide a primary amphiphilicity for the helix. Some biologically active peptide hormones possess a primary amphiphilicity to promote distribution to phospholipid bilayer membrane with a parallel orientation to the bilayer normal.[15,16] The orientation of hydrophobic peptides spread at the air/water interface may be changed by the primary amphiphilicity. In this respect, the ammonium groups in HA16FB, HKZ16M and HL16B and the trisarcosine sequence in HS3L16B at the N-terminal should be effective to give a primary amphiphilicity. These peptides were spread at the air/water interface to measure their π-A isotherms and transferred onto suitable substrates for spectroscopic analysis.

Materials and Methods

Peptide Preparation

Boc amino acids were purchased from Kokusan Chemical Works, Ltd. (Tokyo, Japan). HOBt , DCC and TFA were purchased from Peptide Institute, Inc. (Osaka, Japan). Aib-OBzl was synthesized as described in Chapter 1. All the peptides used in this chapter were prepared by the conventional liquid-phase synthesis using as coupling reagents DCC and HOBt.[17] TLC was performed on a silica-gel plate 60 F254, 0.2-mm thick (Merk) with the solvent system (A) chloroform / methanol / acetic acid (90 : 10 : 3 v/v/v) or (B) ethyl acetate / methanol (85 : 15 v/v). Peptides on the plate

were visualized by spraying ninhydrin[18] or *o*-tolidine.[19]

AdmA16B and AdmA16OH

Boc-(Ala-Aib)$_8$-OBzl was synthesized as described in Chapter 1. The benzyl ester was removed by the catalytic hydrogenation in a 2-methyl-1-propanol solution with palladium carbon. The Boc group was removed by treatment with TFA. TFA•H-(Ala-Aib)$_8$-OBzl or TFA•H-(Ala-Aib)$_8$-OH was dissolved in pyridine and reacted with 5-fold mole of 1-adamantancarbonyl chloride (Tokyo Chemical Industry, Tokyo, Japan) at room temperature for 24 h, followed by gel filtration with a Sephadex LH-20 (Pharmacia, Sweden) column by using methanol as the elution solvent. The major fraction was collected and concentrated, followed by recrystallization from methanol to obtain AdmA16B or AdmA16OH, respectively. TLC: AdmA16B; R_f(A) 0.60, R_f(B) 0.81. AdmA16OH; R_f(A) 0.43, R_f(B) 0.58.

BMA16B

A *tert*-butyloxycarbonyl-*N*-methyl-L-alanine (Boc-MeAla) was synthesized from Boc-Ala and CH_3I.[20] Boc-MeAla and Aib-OBzl were coupled in a DMF solution, followed by purification with a silica-gel column. The product dipeptide was treated with 4 N HCl in a 1,4-dioxane solution to remove the Boc group. Boc-Pro was connected to the free N terminal of the dipeptide to obtain a tripeptide. After purifying by the LH-20 column and removing the Boc group, Boc-MeAla was connected to the N terminal of the tripeptide. The tetrapeptide was purified by the LH-20 column. The tetrapeptide was hydrogenated as described above to obtain Boc-MeAla-Pro-MeAla-Aib-OH (BM4OH). BM4OH was coupled with TFA•H-(Ala-Aib)$_6$-

OBzl with DCC and HOBt. After purifying by the LH-20 column, BMA16B was recrystallized from a methanol / isopropyl ether (3:1 v/v) mixture. TLC: R_f(A) 0.65, R_f(B) 0.85.

BA16FB and HA16FB

Aib-$OCH_2C_6F_5$ (Aib-FB) was synthesized from Aib and pentafluorobenzyl alcohol (PFB) (Tokyo Chemical Industry, Tokyo, Japan) using *p*-toluenesulfonic acid as a catalyst. Boc-Ala was coupled with Aib-FB to obtain a dipeptide. The dipeptide was treated with 4 N HCl in a 1,4-dioxane solution and connected to the C terminal of Boc-(Ala-Aib)$_7$-OH with DCC and HOBt, followed by the LH-20 column and recrystallization from methanol to obtain BA16FB. HA16FB was prepared by removing Boc group from BA16FB with TFA, followed by recrystallization from methanol. TLC: BA16FB: R_f(A) 0.46, R_f(B) 0.50. HA16FB: R_f(A) 0.11, R_f(B) 0.10.

BKZ16M and HKZ16M

BKZ16M was prepared by the same procedure as BA16M from Boc-Lys(Z) and Aib-OMe.[10] The recrystallization was carried out in a methanol / isopropyl ether (1:1 v/v) mixture. BKZ16M was treated with TFA to obtain HKZ16M. TLC: BKZ16M; R_f(A) 0.59, R_f(B) 0.91. HKZ16M; R_f(A) 0.38, R_f(B) 0.42.

BL16B, HL16B and HS3L16B

BL16B was prepared by the same procedure as Boc-(Ala-Aib)$_8$-OBzl with minor modifications. BL16B was treated with TFA to remove Boc group to obtain HL16B. Boc-Sar$_3$-OH was synthesized by a stepwise

elongation as reported before.[21] HL16B was connected to Boc-Sar_3-OH, followed by purification by the LH-20 column to obtain BS3L16B. BS3L16B was treated with TFA to obtain HS3L16B. TLC: BL16B; R_f(A) 0.50, R_f(B) 0.89. HL16B; R_f(A) 0.30, R_f(B) 0.62. HS3L16B; R_f(A) 0.38, R_f(B) 0.65.

Methods

BL16B, HL16B and HS3L16B were dissolved in chloroform and other peptide samples were dissolved in chloroform / methanol (9/1 v/v) mixture at the concentrations of $(1.5 - 3) \times 10^{-4}$ M. The π-A isotherm was recorded at a constant rate of reducing area with a Langmuir trough having the surface area of 900 cm^2. The peptide solution was spread on the aqueous phase by using a microsyringe, and equilibrated for 15 min before compression. Double-distilled water was used for the subphase.

For IR transmission and reflection absorption spectra (RAS),[22,23] the monolayer was transferred onto a CaF_2 plate (2.5-cm diameter) or a slide glass coated with silver (2 × 5 cm) at a constant surface pressure. The transfer rates were nearly unity. The IR spectra were recorded by a Nicolet Model 710 Fourier transform infrared spectrophotometer equipped with an MCT detector with the resolution of 4 cm^{-1}. For RAS measurments, a Harrick Model RMA-1DG/VRA reflection attachment was used at an incident angle of 85°, with a Hitachi wire-grid polarizer.

CD spectra of peptides in ethanol / water (95/5 v/v) and of the films transferred onto quartz plates (1.2 × 2.5 cm) were measured at room temperature on a JASCO J-600 CD spectropolarimeter. An optical cell of 0.2-

cm path length was used for the peptide solution at the concentration of 1.5×10^{-5} M, and six pieces of the plates were fixed in a cell holder in series with an interval of 1-mm thick spacer. The intensity of the Cotton effect was normalized for the mole number of peptides in an unit area.

Results

The CD spectra of AdmA16B, BMA16B, BKZ16M and BL16B in an ethanol / water (95/5 v/v) mixture are shown in Figure 2. All the peptides possess a double-minimum pattern of spectrum that is characteristic of an α-helical structure.[24] The helix content of the peptides was about 70 %, and the helical structure was not seriously influenced by modification of the N or C terminal.

The π-A isotherms of AdmA16B, AdmA16OH and BMA16B at 20 °C are shown in Figure 3, and those of BA16FB and HA16FB in Figure 4. The inflection point appeared in the π-A isotherms around 260 $Å^2$/molecule (Figures 3 and 4). The irregular bumping and decrease of the surface pressure at a constant surface area were observed at smaller areas than that at the inflection point, indicating a collapse of the monolayer. The area at the inflection point of the π-A isotherms is very close to the sectional area of BA16M along the helix axis (239 $Å^2$), according to X-ray analysis.[10] This observation indicates that the peptides take the α-helical structure at the air/water interface with a parallel orientation to the interface.

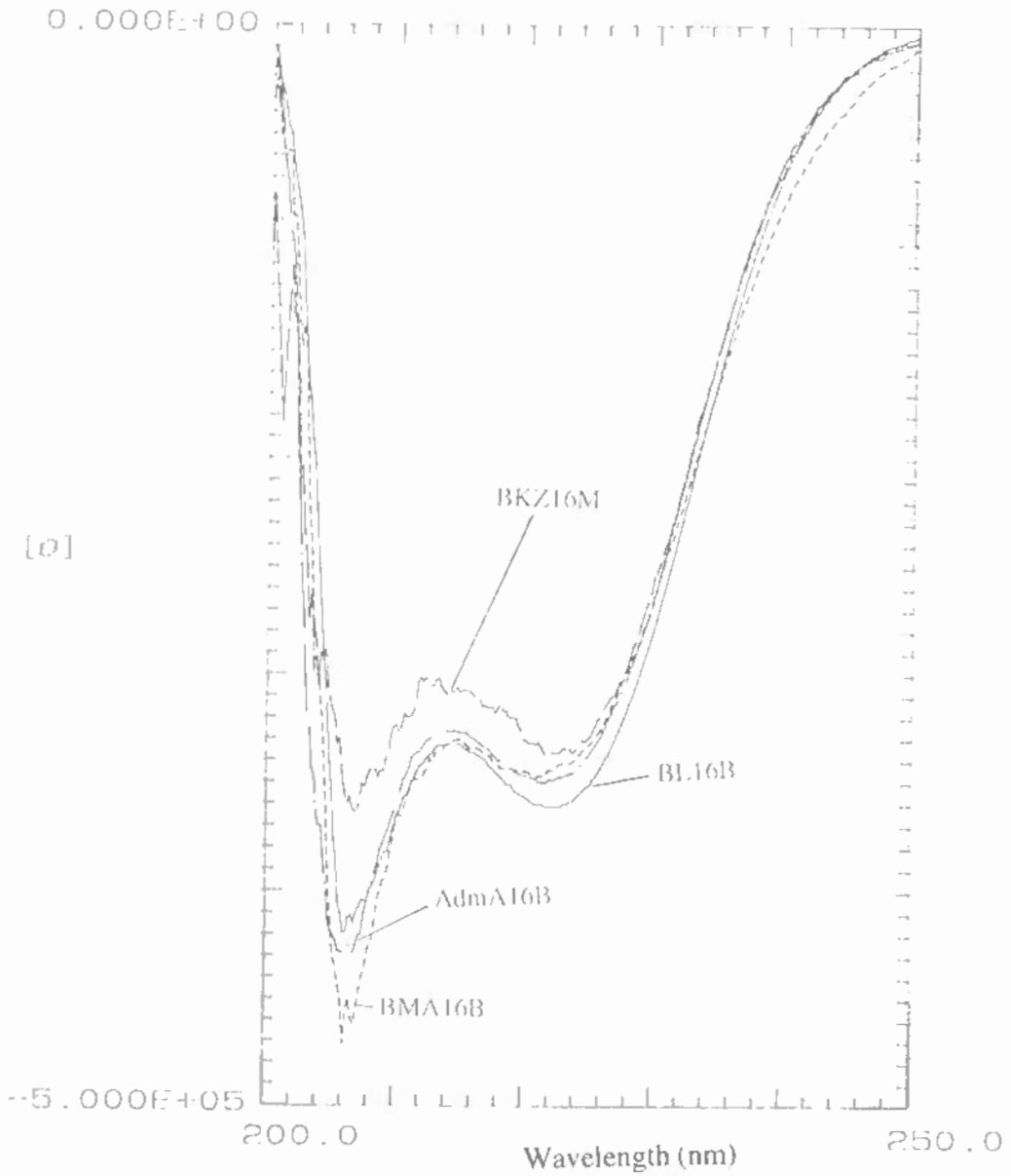

Figure 2 CD spectra of AdmA16B (– –), BMA16B (---), BKZ16M (–•–) and (—) BL16B in an ethanol / water (95/5 v/v) mixture at the concentration of 1.2×10^{-5} M at room temperature.

The π-A isotherms of BA16FB and HA16FB (Figure 4) are quite similar to those of BA16B and HA16B, respectively (see Chapter 1). Substitution of the benzyl group with the pentafluorobenzyl group did not affect the molecular orientation and packing of the monolayer.

The π-A isotherms of BKZ16M and HKZ16M (Figure 5) show a quite clear inflection around 430 Å^2/molecule. This inflection represents a collapse of the monolayer, because the surface pressure bumps irregularly and decreases when the surface area is kept at a constant value which is smaller

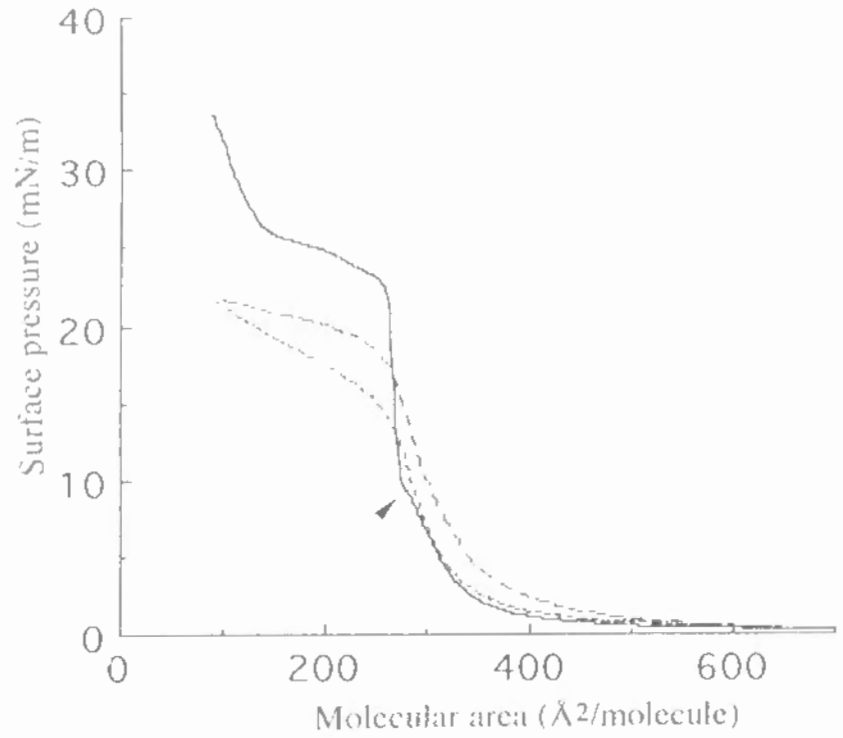

Figure 3 π-A isotherms of AdmA16B (—), AdmA16OH (---) and BMA16B (– –) on double-distilled water at 20 °C. A mound is indicated with an arrow.

than that at the inflection point. The inflection point of BL16B, HL16B and HS3L16B appears around 310 - 320 Å^2/molecule in the isotherm (Figure 6), which is also ascribed to collapse of the monolayer. These values of the surface area represent the sectional area of each helix, indicating that the peptides take a parallel orientation to the interface irrespective of the nature of end groups and amino acid residues.

A mound is observed in the π-A isotherms of AdmA16B, BA16FB, HL16B, and HS3L16B at the initial part of the sharp increase of the surface pressure (indicated by an arrow in Figures 3, 4 and 6). The mound is explained in terms of phase transition of the monolayer from a liquid state to a solid state as observed in the case of BA16M.[9,12] Although any mound was not observed in the isotherm of BL16B, the steep slope indicates the occurrence of a solid state of the monolayer. On the other hand, monolayers of AdmA16OH, BMA16B, HA16FB, BKZ16M and HKZ16M are considered to stay in a liquid state, because the slope of the isotherm is gentle and the collapse pressure is relatively low.

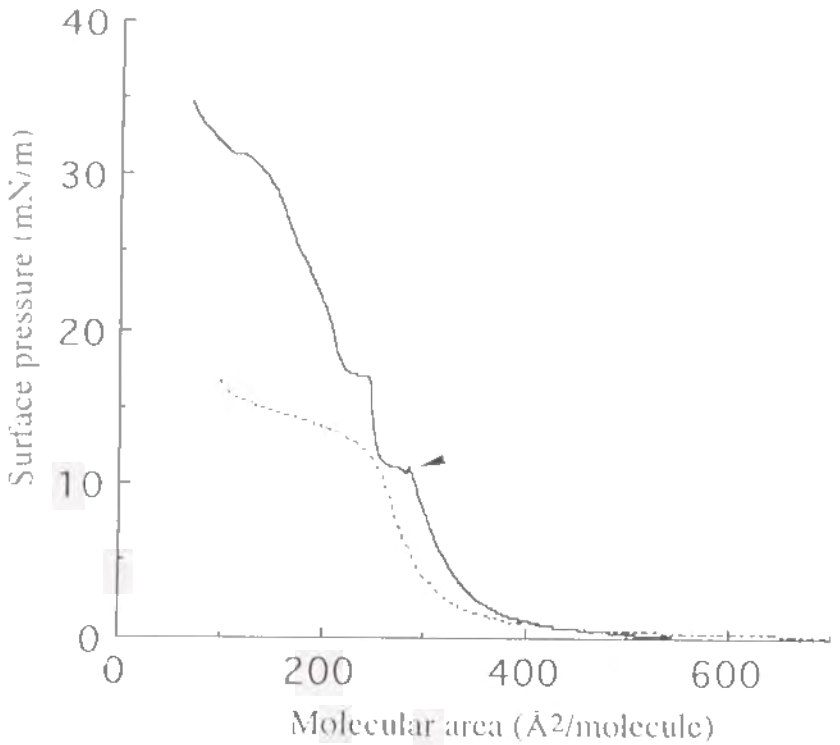

Figure 4 π-A isotherms of BA16FB (—) and HA16FB(---) on double-distilled water at 20 °C. A mound is indicated with an arrow.

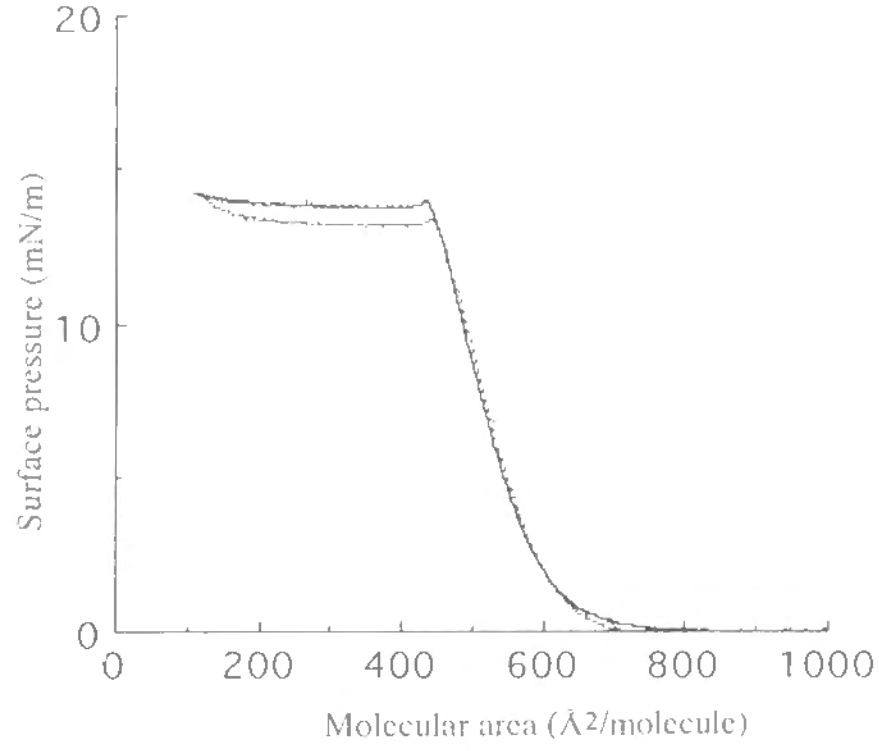

Figure 5 π-A isotherms of BKZ16M (—) and HKZ16M (---) on double-distilled water at 20 °C.

The monolayers were transferred onto quartz plates at a constant surface pressure which is smaller by 2 mN/m than that at the inflection point, and CD spectra of the monolayers were measured (Figure 7). The intensity of the Cotton effect at 222 nm changed by 15 % upon rotation of the quartz plates, probably due to linear dichroism.[25] CD spectra are the same among the peptides, AdmA16B, AdmA16OH, BKZ16M and BL16B, showing α-helical conformation.[25] No significant difference was observed in the CD spectra

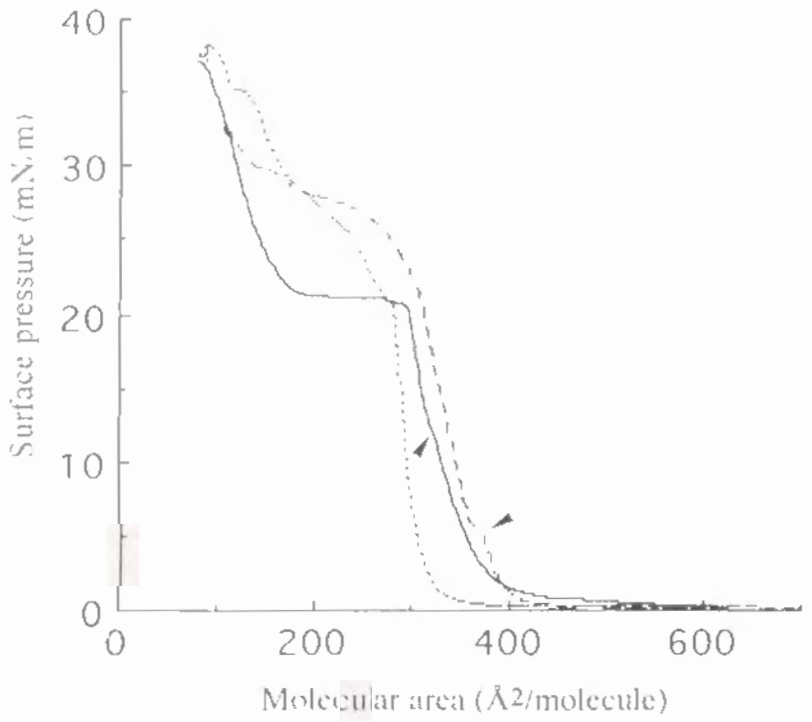

Figure 6 π-A isotherms of BL16B (---), HL16B (—) and HS3L16B (– –) on double-distilled water at 20 °C. A mound is indicated with an arrow.

between AdmA16B in a solid state and AdmA16OH in a liquid state, indicating that the different monolayer states between AdmA16B and AdmA16OH is not due to conformational difference.

RAS and IR transmission spectra of AdmA16B are shown in Figure 8. The monolayers were transferred onto Ag and CaF_2 plate, respectively, at 17

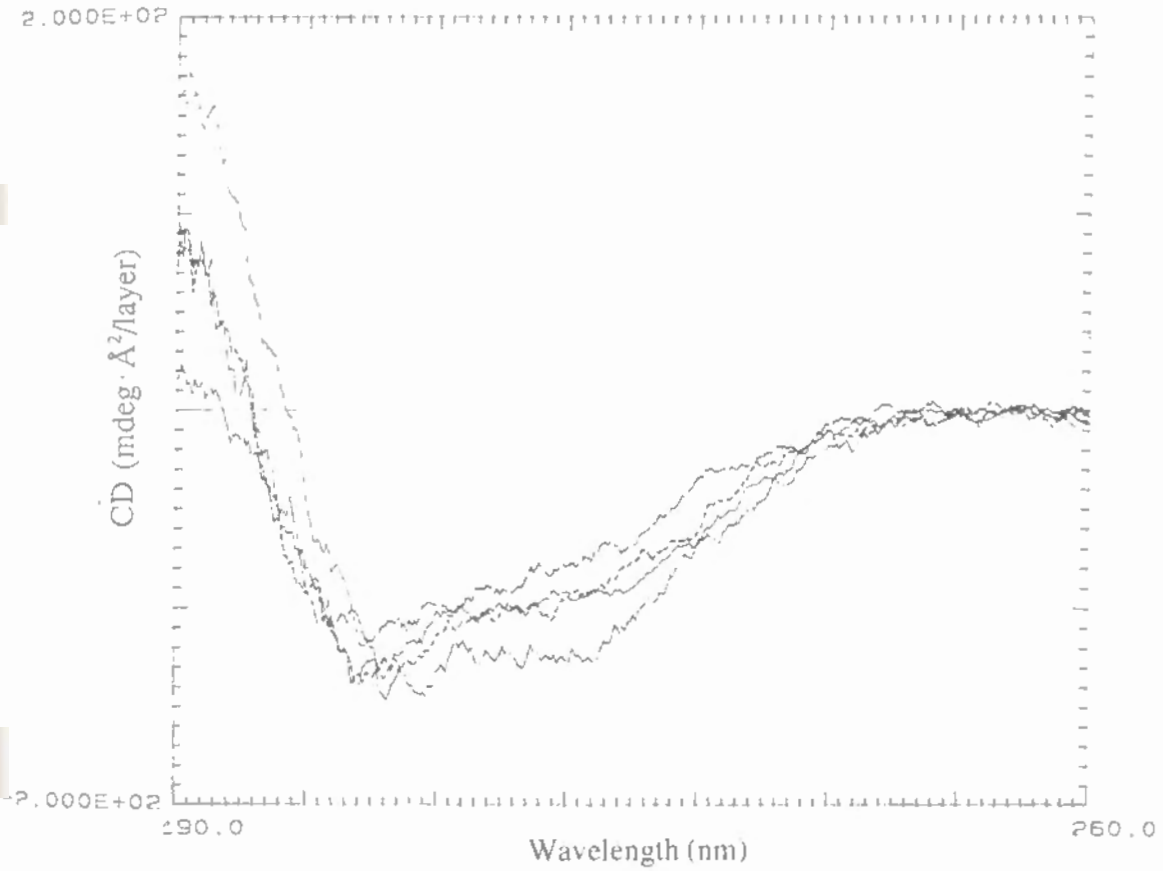

Figure 7 CD spectra of AdmA16B (---), AdmA16OH (– –), BKZ16M (– • –) and BL16B (—) monolayer transferred onto a quartz plate at the surface pressures smaller by 2 mN/m than those at inflection points.

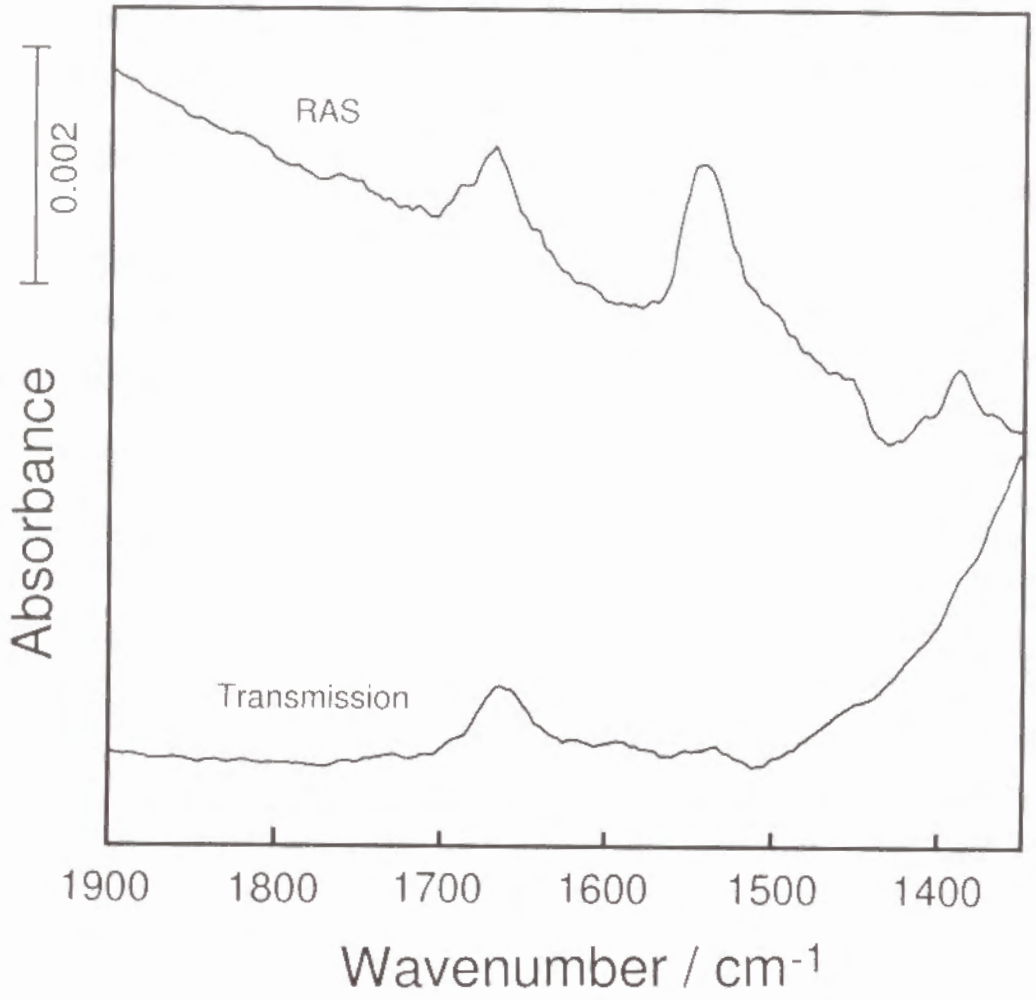

Figure 8 RAS and IR transmission spectra of AdmA16B monolayer transferred onto a slide glass coated with silver and a CaF_2 plate, respectively, at a surface pressure of 17 mN/m. Incident angle of RAS was 85°.

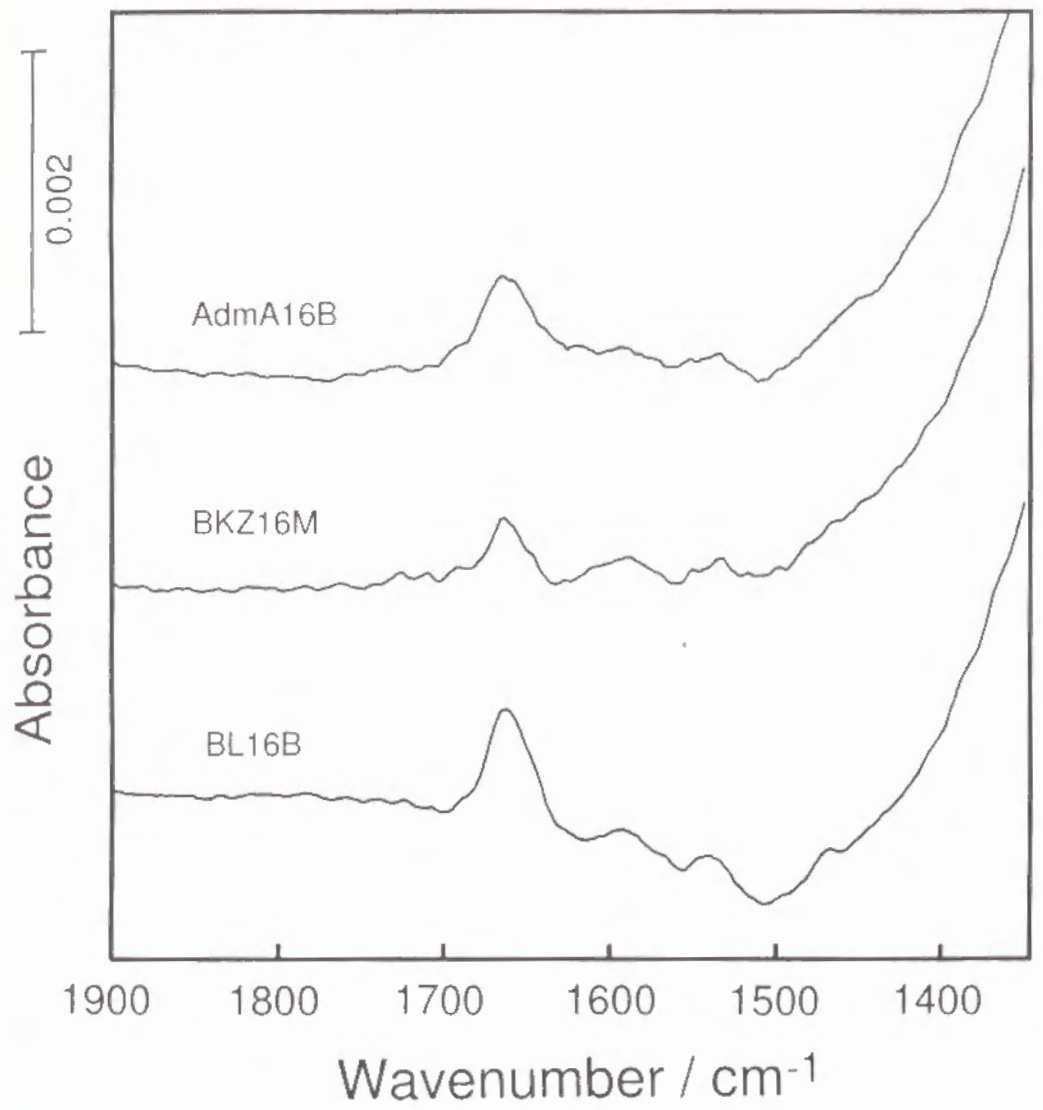

Figure 9 IR transmission spectra of AdmA16B, BKZ16M and BL16B monolayer transferred onto a CaF_2 plate at the surface pressures smaller by 2 mN/m than those at inflection points.

mN/m. The absorbance ratio of amide I band at 1660 cm^{-1} and amide II band at 1550 cm^{-1} was significantly different in the two spectra. Notably, the amide II band at 1550 cm^{-1} was stronger than the amide I band at 1660 cm^{-1} in the RAS. This result is explained in terms of orientation of peptide molecules on the substrates. The absorption having a transition moment perpendicular to the optical path axis, which is parallel to the substrate surface, appears strongly in the transmission spectrum. On the other hand, the absorption having a transition moment perpendicular to the substrate surface absorbs the p-polarized light, which produces an electric field parallel to the incidence plane, intensively in the RAS.[23] The transition moment of amide I absorption lies appreciably in parallel to the helix axis and that of amide II absorption in perpendicular to the helix axis.[26] Consequently, the helical peptide is concluded to have the helix axis oriented perpendicularly to the normal of the substrate, and therefore, in parallel to the air/water interface.

The monolayers of BKZ16M and BL16B were also transferred onto a CaF_2 plate at 11 and 18 mN/m, respectively, which are smaller by 2 mN/m than those at the inflection point, and IR transmission spectra were measured (Figure 9). The absorption of amide I band is strong, and the absorption wavenumber is the same as that of AdmA16B and is characteristic of helical structure.[27] Therefore, BKZ16M and BL16B are also concluded to take the α-helical structure at the interface having their helix axis oriented parallel to the interface.

Discussion

The π-A isotherms of the peptides spread on water are classified into following three groups: i) a steep slope; BL16B, ii) a steep slope with inflection (or a mound) at the initial part of the sharp increase of surface pressure; AdmA16B, BA16FB, HL16B, and HS3L16B, iii) a gentle slope with a relatively low collapse pressure; AdmA16OH, BMA16B, HA16FB, BKZ16M, and HKZ16M. The monolayers of class i) and iii) are in a solid and a liquid state, respectively, and in the class ii) monolayers the phase transition from a liquid state to a solid state is observed upon compression. Since all the peptides take α-helical structure in the monolayer, the different behaviors of the isotherm are due to different molecular structures of the peptides.

The isotherm of BL16B is similar to that of stearic acid,[28] indicating that BL16B is easily packed into a two-dimensional crystal. The cross-section of the peptide at the inflection point was compared with that of molecular model.[29] According to the theoretical model under the assumption that the side chains take a fully extended conformation, the longest distance from the center of the helix to the edge of the δ-methyl group of Leu residue and that from the center to the edge of the β-methyl group of Aib residue is estimated to be 7.5 and 5.8 Å, respectively. The length of the helix along the helix axis should be equivalent to that of BA16M (25.7 Å), because both have the same secondary structure. The molecular area at the inflection point is in good agreement with the product of the helix length by the sum of the external radii (13.3 Å). It is indicated that the side chains of Leu residue of a helix penetrate

into a groove of other helix, so that an interdigitation state appears. The molecular packing of BL16B should be so tight due to interdigitation that a solid monolayer of BL16B is formed.

An ammonium group at the N terminal of HL16B and HS3L16B might disturb the molecular packing of the peptide. However, this effect is overcome by the interdigitation effect upon compression, and the phase transition of the monolayer takes place.

On the other hand, the cross-section at the inflection point of BKZ16M and HKZ16M (430 Å^2/molecule), which was estimated from the CPK model, indicates that the side chains of Lys(Z) residue lie on the surface of the helix rod without interdigitation. The bulky side chains of Lys(Z) residue might sterically hinder the molecular packing, resulting in a liquid monolayer.

AdmA16OH and BMA16B did not form a solid monolayer, although BA16OH and BA16B formed it with accompanying phase transition. AdmA16OH has a hydrophobic adamantyl group at the N terminal and a hydrophilic carboxyl group at the C terminal. This structure is regarded as a primary amphiphilicity. The peptides with a primary amphiphilicity tend to orient themselves parallel to the normal of the lipid bilayer.[30] As a consequence, the helix axis of AdmA16OH take an oblique orientation to the air/water interface, resulting in a liquid monolayer. In the case of BMA16B monolayer, three residues succeeding the N-terminal group should extend to the air phase, because they do not have amide proton. The amide proton and carbonyl group at the N or C terminal, respectively, of a helix are free from intramolecular hydrogen bonding and tend to be hydrated. Therefore, the helix axis of BMA16B should be more oblique against the interface than that of BA16B, resulting in a liquid monolayer. It is expected that peptides having a

high degree of primary amphiphilicity will orient themselves perpendicularly to the interface.

References

(1) Fermi, G.; Perutz, M. F. *Atlas of Molecular Structures in Biology. 2. Haemoglobin and Myoglobin;* Clarendon Press: Oxford, 1981.

(2) Michel, H. *J. Mol. Biol.* **1982**, *158*, 567.

(3) Branden, C.; Tooze, J. *Introduction to Protein Structure*; Garland Publishing: New York & London, 1991.

(4) Alberts, B.; Bray, D.; Lewis, J.; Raff, M.; Roberts, K.; Watson, J. D. *Molecular Biology of the Cell, 2nd ed.*, Garland Publishing: New York & London, 1989; Chapter 3.

(5) Rao, S. T.; Rossmann, M. G. *J. Mol. Biol.* **1973**, *76*, 241.

(6) Ho, S. P.; DeGrado, W. F. *J. Am. Chem. Soc.* **1987**, *109*, 6751.

(7) Gaines, G. L., Jr. *Insoluble Monolayers at liquid interface*; Interscience: New York, 1966.

(8) Birdi, K. S. *Lipid and biopolymer monolayers at liquid interfaces*, Plenum Press: New York, 1989.

(9) Fujita, K.; Kimura, S.; Imanishi, Y.; Rump, E.; Ringsdorf, H. *Langmuir* **1994**, *10*, 2731.

(10) Otoda, K; Kitagawa, Y.; Kimura, S.; Imanishi, Y. *Biopolymers* **1993**, *33*, 1337.

(11) Fujita, K.; Kimura, S.; Imanishi, Y.; Rump, E.; Ringsdorf, H. *J. Am. Chem. Soc.* **1994**, *116*, 2185.

(12) Fujita, K.; Kimura, S.; Imanishi, Y.; Rump, E.; Ringsdorf, H. *Langmuir*

accepted.

(13) Burgess, A. W.; Leach, S. J. *Biopolymers* **1973**, *12*, 2599.

(14) Karle, I. L.; Balaram, P. *Biochemistry* **1990**, *29*, 6747.

(15) Schwyzer, R.; Erne, D.; Rolka, K. *Helv. Chim. Acta* **1986**, *69*, 1789.

(16) Erne, D.; Sargent, F.; Schwyzer, R.*Biochemistry* **1985**, *24*, 4261.

(17) Konig, W.; Geiger, R. *Chem. Ber.* **1970**, *103*, 788.

(18) Pataki, G *Techniques of Thin-Layer Chromatography in Amino Acid and Peptide Chemistry*, Ann Arbor Sci. Inc.: Michigan, 1968.

(19) Pataki, G. *J. Chromatogr.* **1963**, *12*, 541.

(20) Olsen, R. K. *J. Org. Chem.* **1970**, *35*, 1912.

(21) Sugihara, T.; Imanishi, Y.; Higashimura, T. *Biopolymers* **1975**, *14*, 723.

(22) Greenler, R. G. *J. Chem. Phys.* **1966**, *44*, 310.

(23) Okamura, E.; Umemura, J.; Takenaka, T. *Can. J. Chem.* **1991**, *69*, 1691.

(24) Holzwarth, G.; Doty, P. *J. Am. Chem. Soc.* **1965**, *87*, 218.

(25) Shindo, Y.; Ohmi, Y. *J. Am. Chem. Soc.* **1985**, *107*, 91.

(26) Krimm, S.; Bandeker, J. *Adv. Potein Chem.* **1986**, *38*, 181.

(27) Kennedy, D. F.; Chrisma, M.; Toniolo, C.; Chapman, D. *Biochemistry* **1991**, *30*, 6541.

(28) Kajiyama, T.; Umemura, K.; Uchida, M.; Oishi, Y.; Takei, R. *Bull. Chem. Soc. Jpn.* **1989**, *62*, 3004.

(29) (a) Momany, F.; McGuire, R. F.; Burgess, A. W.; Sheraga, H. A. *J. Phys. Chem.***1975**, *79*, 2361. (b) Sisido, M. private communication.

(30) Otoda, K; Kimura, S.; Imanishi, Y. *Biochim. Biophys. Acta* **1993**, *1150*, 1.

Part II Regular Assembly of Proteins at the Air/Water Interface and in Lipid Bilayer Membrane

Chapter 4

The Molecular Recognition of Biotinyl Hydrophobic Helical Peptides with Streptavidin at the Air/Water Interface

Introduction

Peptides are regarded as the ideal unit for construction of biologically functional molecular systems, because they take a definite conformation[1] and can be functionalized by chemical modifications at side chains[2] or chain terminals.[3] It has previously been reported that a hydrophobic peptide, Boc-(Ala-Aib)$_8$-OMe, took an α-helical conformation as evidenced by X-ray diffraction analysis of the crystalline structure.[4] In Chapter 1, the analogues modified at the chain terminus are shown to form a stable monolayer at the air/water interface. The monolayer technique is the basis of the Langmuir-Blodgett method, which might be useful for the preparation of functional thin layers.

The biotin and streptavidin (SAv) system is a well-known biological receptor/ligand pair,[6] having a specific and strong interaction ($K_d = 10^{-15}$ mol/l).[7] Many lipid derivatives having a biotin group were spread at the air/water interface, and upon adding SAv to the subphase, two-dimensional crystal of SAv was formed at the interface, due to binding of SAv to the lipid.[8]

In the present chapter, the monolayers of hydrophobic helical peptides carrying a biotinyl group at the N terminal were prepared at the air/water interface. Using the monolayers as the matrices, the two-dimensional crystallization of SAv was

attempted.

Materials and Methods

Materials

Two kinds of peptides having a biotin group, BioS3A16M and BioA16M (Figure 1) were synthesized as described in Chapter 2. A hydrophilic peptide spacer, trisarcosine, is inserted between the amino terminus of the helical peptide and the biotin group in BioS3A16M, but the spacer peptide was not used in BioA16M.

The inactive SAv was prepared by treatment of SAv with 5-fold M of biotin in water to block its binding sites followed by the gel filtration through a G-25 column. Streptavidin was labeled with FITC (FITC-SAv)[10] or rhodamine (Rh-SAv)[11] by the method described in Chapter 2.

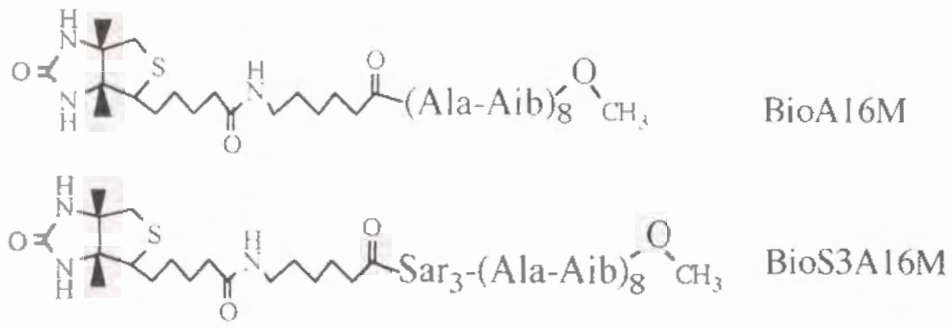

Figure 1 Molecular structure of the biotinyl peptides, BioA16M and BioS3A16M.

Methods

CD

CD of the two peptides was measured in ethanol / water (95 : 5 v/v) at room temperature using an optical cell of 1-cm path length. The other conditions were the same as employed in Chapter 1.

π-A isotherm measurements

π-A isotherm was measured by a homemade Langmuir trough with 490 cm^2 of the surface area.[12] The experimental procedures are described in Chapter 2.

The interaction of BioS3A16M or BioA16M with SAv was investigated on the trough in the following procedure. After the biotinyl peptides were spread on 0.5 M NaCl solution to the surface molecular area of 1800 Å^2/molecule, an aqueous solution containing 1 mg of SAv or inactive SAv was injected into the subphase (500 ml) and the mixture was incubated for an hour at 30 °C, followed by cooling down to 20 °C. A compression was begun at the rate of 0.17 cm^2/s. The hysteresis experiment was carried out in the following order: (1) compression to 8 mN/m; (2) immediate relaxation of pressure to attain the largest surface area; (3) incubation for 20 min at 20 °C; (4) compression at the rate of 0.17 cm^2/s to the smallest surface area.

Fluorescence microscopy

The solution of BioS3A16M or BioA16M as varying concentrations was spread at the air/water interface in a small trough (10 cm^2) to the range of 1500-500 Å^2/molecule (a gas-analogous state). FITC-SAv was injected into the aqueous subphase (0.5 M NaCl), followed by incubation for 1-18 hours. The domain formation of the labeled SAv was observed by the fluorescence microscope.[16]

Results and Discussion

The CD spectra of both peptides (Figure 2) showed the typical double-minimum pattern in ethanol / water (95 : 5 v/v), indicating that both peptides take an α-helical conformation.[9] The isotherms of both peptides show an inflection point at 250 A^2 in the absence of the protein in the subphase, which should be collapsion

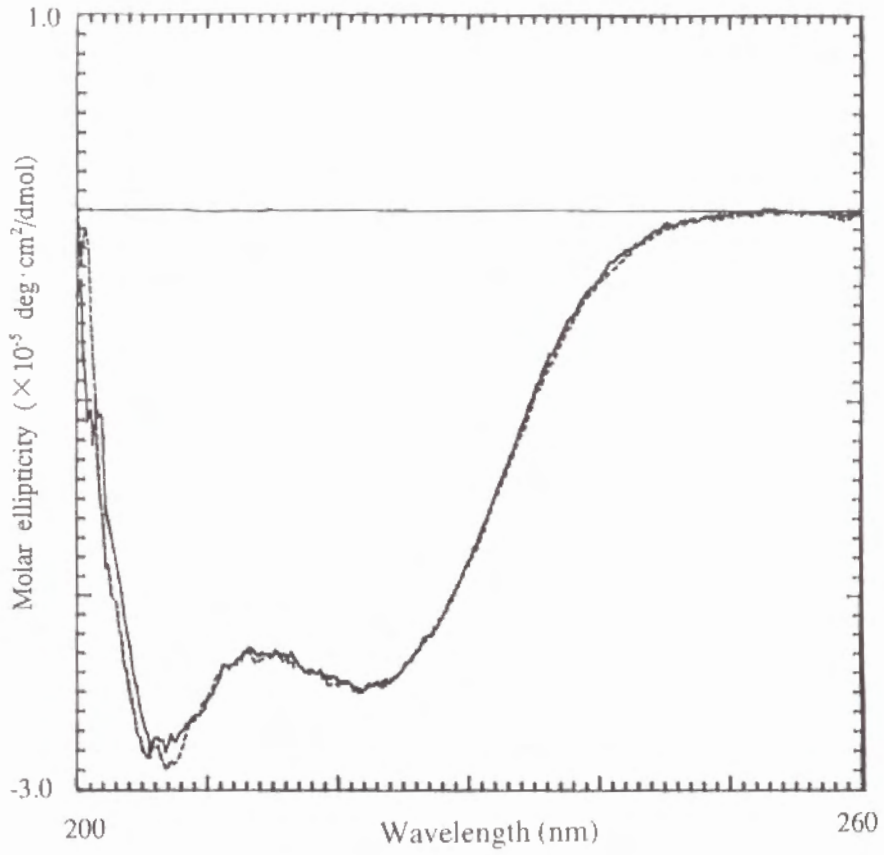

Figure 2 CD spectra of BioS3A16M (——) and BioA16M (---) in ethanol / water (95 : 5 v/v) at the concentration of 1.1 × 10^{-5} M by using a CD cell with 1-cm path length.

point of the monolayer (Figure 3, without protein).[5] The molecular area of the inflection was in agreement with the cross section along the helical axis of the helical part, which was determined by X-ray analysis.[4] The observation strongly suggests that the helical part of both BioS3A16M and BioA16M oriented the helical axis parallel to the interface.[5]

It is notable that a small mound was observed around 300 A^2 in the isotherms of both peptides under the compression process (see Figure 8 in Chapter 2). Since peptides having a definite chain length tend to associate together in an orderly form,[13] BioS3A16M and BioA16M are considered to form regular clusters even in the liquid phase. When the small clusters are forced to contact tightly with each other at the transition pressure from the liquid to solid phase by compression, the clusters might be merged into a large domain accompanying reorientation of the peptides. This is considered for the explanation of the mound observation in the isotherm in contrast to the biotinylated lipids. π-A isotherms of BioS3A16M (Figure 3a) and BioA16M (Figure 3b) with active or inactive SAv were measured. Nonspecific interaction of SAv with the interfacial film can be estimated from the effect of the inactive SAv on the isotherm.[8] The addition of inactive SAv caused a shift of the isotherm curve to the larger area, indicating nonspecific adsorption to the monolayer. It seems that higher amount of the inactive SAv was adsorbed to the biotinyl peptide monolayer than to the biotinyl lipid monolayer,[8] probably because the biotinyl peptide is more similar to SAv than the biotinylated lipid in chemical properties. The N terminus of the helix part in BioS3A16M should be pulled into the water subphase due to the hydrophilic spacer, trisarcosine, more strongly than that in BioA16M. This should explain why BioS3A16M showed slightly larger shift than BioA16M in the π-A isotherm upon interaction with inactive SAv, which

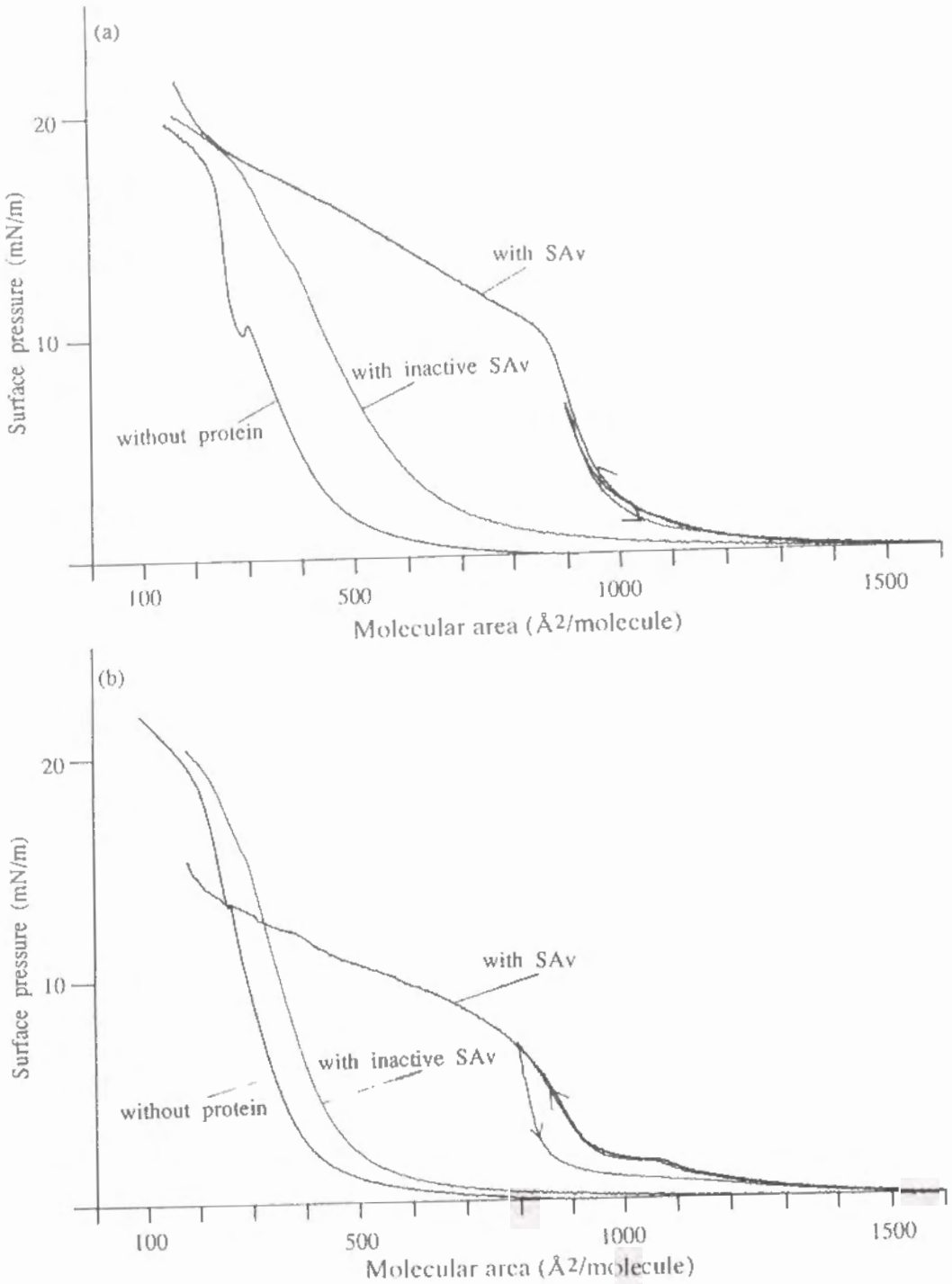

Figure 3 π-A isotherms of (a) BioS3A16M and (b) BioA16M interacting with SAv or inactive SAv or in the absence of SAv. The curves of compression, expansion and recompression in this order are shown together with arrows in the presence of active SAv.

reflects the degree of nonspecific interaction. BioS3A16M exposes a larger molecular surface to the water subphase, which promotes access of streptavidin in the subphase to the peptide. The specific interaction was estimated by the difference between the isotherms in the presence of active SAv and inactive SAv. Obviously, the presence of active SAv increased the molecular area more strikingly than the presence of inactive SAv, indicating the specific binding of SAv to both peptides, BioS3A16M and BioA16M, at the interface. The π-A isotherms were measured upon compression, expansion, and recompression in the presence of active SAv, but no hysteresis was detected in the complex formation (Figure 3). The agreement of the recompression curve with the first compression one in Figure 3a and b means that the protein-peptide complex monolayer is stable. Approximately 2/3 of the biotinyl peptides in the monolayer should have been bound to SAv, taking the following points into considerations: (1) One molecule of streptavidin occupies the area of about 3500 Å^2 at the interface in the two-dimensional crystal.[13] (2) Two of the four binding sites of SAv should contribute to the interfacial binding.[8,14,15] (3) The surface pressure begins to increase by the interaction with the active SAv at the area of 1000 Å^2/molecule or a little higher value (Figure 3, with SAv). The amount of SAv bound to the monolayer of BioS3A16M was nearly the same as that bound to the monolayer of BioA16M. The biotin moiety of BioS3A16M should stay at the aqueous phase due to the presence of hydrophilic spacer, resulting in an easy access to SAv in the aqueous phase.

In the case of BioS3A16M, domains of the FITC-SAv were observed (Figure 4), which displayed distinct fluorescence anisotropy on irradiation of polarized excitation light. The anisotropy is caused by the microscopic orientation of the fluorescence probe attached to the SAv molecule and strongly suggests that the SAv molecules are highly ordered in the domain. Therefore, the domain should be

(a)

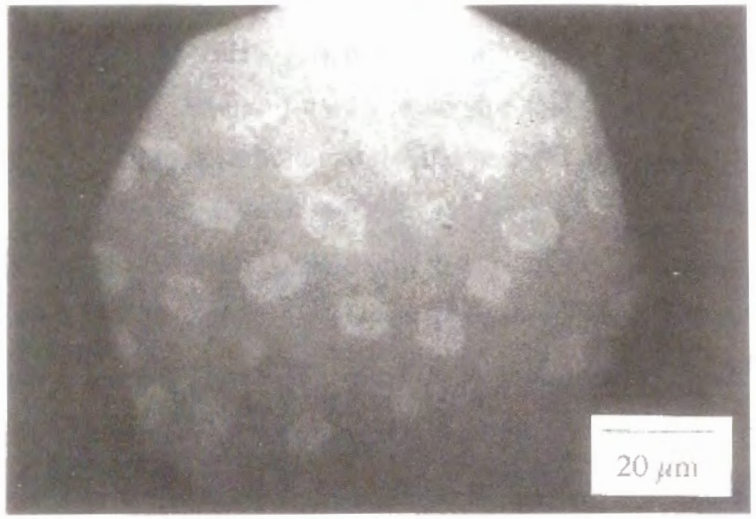

(b)

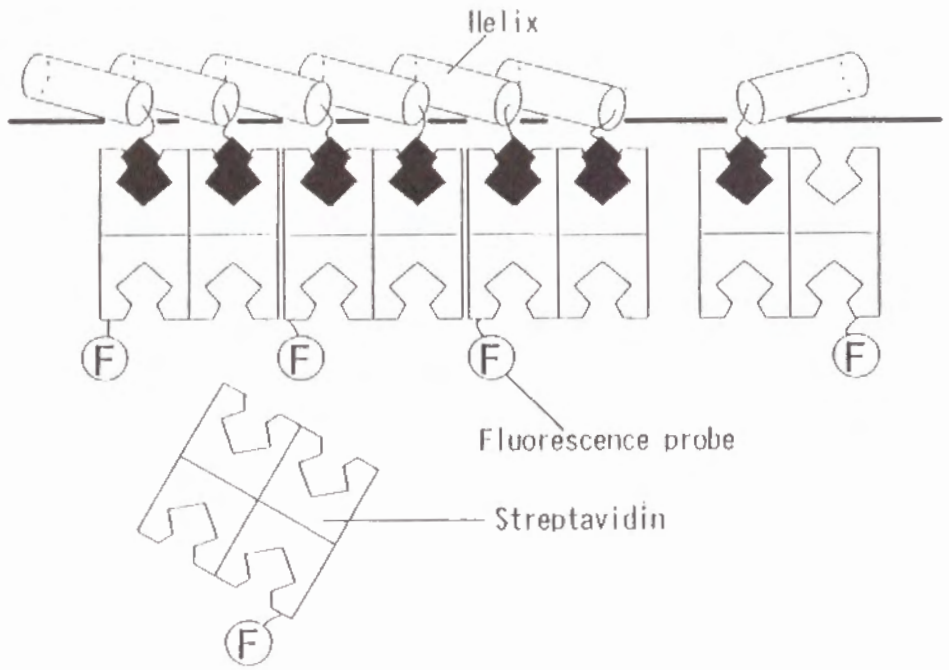

Figure 4 (a) Fluorescence micrograph and (b) schematic representation of the complex of BioS3A16M and FITC-SAv at the air/water interface.

constituted by the two-dimensional crystal of SAv.[8] When the Rh-SAv was used, a similar anisotropic domain formation was observed. However, in the case of BioA16M, which has a shorter spacer chain between the helix peptide and the biotin moiety, the domain formation was not observed, and only the homogeneous fluorescence was done with either FITC-SAv or Rh-SAv. The π-A isotherm of BioA16M was similar to that of BioS3A16M, reflecting similar binding behaviors with SAv (Figure 3). Therefore, two-dimensional crystal of SAv was not formed from BioA16M, because the short spacer chain in BioA16M did not allow the crystalline arrangement of SAv. This result is different from the case of the biotinylated lipid monolayer performed before.[8] The biotinylated lipid without a proper spacer did not induce formation of two-dimensional crystal of SAv, because SAv could not bind to the biotin group of the lipid spread at the air/water interface.[8] In the case of the peptide monolayer, however, the peptide BioA16M did not induce formation of two-dimensional crystal of SAv, although SAv binds to the peptide similarly to BioS3A16M, as evidenced by the isotherms shown in Figure 3 . The different result on two-dimensional crystal formation between the biotinylated lipid and peptides is ascribed mostly to the different molecular area occupied at the air/water interface. The molecular area of SAv facing to the interface, which contains two binding sites for biotin at the distance of 20 A, is estimated to be 55× 45 A^2.[17] The helical peptide was spread at the air/water interface with a parallel orientation of the helical axis to the interface.[5] The length of the helix is 25.7 A,[4] which is longer than the half of the shorter side of SAv cross section facing to the interface. Therefore, the peptide bound to SAv might cause steric hindrance, preventing another peptide from binding to a nearby SAv. This should be the case for BioA16M and inhibit the crystallization of SAv. On the other hand, the

molecule of BioS3A16M with a longer flexible spacer chain may reserve the molecular flexibility even after binding to SAv, which enables it to accommodate the aligned helices which are bound by SAvs accompanying the crystallization of SAv.

The hydrophobic helical peptide with a biotin group behaved as the molecular recognition unit at the air/water interface. The spacer between the biotin group and the amino end of the peptide chain is necessary for the biotinyl peptide monolayer to function like lipid-based amphiphiles. The difference between BioS3A16M and BioA16M in the formation of the protein two-dimensional crystal should be ascribed to the spacer length. However, we cannot exclude other effects of the spacer insertion into the biotin-peptide on the two-dimensional crystal formation. For example, the molecular polarity, the affinity for the water phase, and the packing properties of the peptide might be changed by the hydrophilic spacer and therefore might result in the different packing state of SAv.

References

(1) For example; Imanishi, Y. *Adv. Polym. Sci.* **1976**, *20*, 1.

(2)(a) Yagi, Y.; Kimura, S.; Imanishi, Y. *Int. J. Peptide Protein Res.* **1990**, *36*, 18.(b) Sisido, M.; Tanaka, R.; Inai, Y.; Imanishi, Y. *J. Am. Chem. Soc.* **1989**, *111*, 6790.

(3) Otoda, K; Kimura, S.; Imanishi, Y. *Bull. Chem. Soc. Jpn.* **1990**, *63*, 489.

(4) Otoda, K; Kitagawa, Y.; Kimura, S.; Imanishi, Y. *Biopolymers* **1993**, *33*, 1337.

(5) Fujita, K.; Kimura, S.; Imanishi, Y.; Rump, E.; Ringsdorf, H. *Langmuir* **1994**, *10*, 2731.

(6) Buckland, R. M. *Nature* **1986**, *320*, 557.

(7) Green, N. M. *Adv. Protein Chem.* **1975**, *29*, 85.

(8) Blankenburg, R.; Meller, P.; Ringsdorf, H.; Salesse, C. *Biochemistry* **1989**, *28*, 8214.

(9) Holzwarth, G.; Doty, P. *J. Am. Chem. Soc.* **1965**, *87*, 218.

(10) Nargessi, R. D.; Smith, D. S. *Methods Enzymol.* **1986**, *108*, 487.

(11) SAv was labeled with rhodamine according to the method similar to that reported in ref. 10 by using rhodamine X isothiocyanate (Molecular Probes, Eugene, USA) in place of fluorescein isothiocyanate.

(12) Albrecht, O. *Thin Solid Films* **1983**, *99*, 227.

(13) Otoda, K.; Kimura, S; Imanishi, Y. *Biochim. Biophys. Acta* **1993**, *1150*, 1.

(14) Darst, S. A.; Ahlers, M.; Meller, P. H.; Kubalek, E. W.; Blankenburg, R.; Ribi, H. O.; Ringsdorf, H.; Kornberg, R. D. *Biopys. J.* **1991**, *59*, 387.

(15) Herron, J. N.; Müller, W.; Paudler, M.; Riegler, H.; Ringsdorf, H.; Susi, P. A. *Langmuir* **1992**, *8*, 1413.

(16) Meller, P. *Rev. Sci. Instrum.* **1988**, *59*, 2225.

(17) Hendrickson, W. A.; Pahler, A.; Smith, J. L.; Satow, Y.; Merritt, E. A.; Phizackerley, R. P. *Proc. Natl. Acad. Sci. USA* **1989**, *86*, 2190.

Chapter 5

Bilayer Formation of Streptavidin Bridged by Bis(biotinyl) Peptide at the Air/Water Interface

Introduction

An ultrathin protein layer is an attractive system to develop a molecular device based on the function of protein.[1] A convenient method to obtain these protein layers is their preparation as monolayers at the air/liquid interface. For instance, it has been reported that SAv formed two-dimensional crystal underneath the monolayer of biotinyl lipids spread at the air/water interface.[2] In the two-dimensional crystal, two of the four binding sites for biotin in the SAv molecule are occupied by biotin groups of the lipids, the two remaining ones are free for further binding and exposed to the aqueous subphase.[3] Therefore, the SAv layer can be regarded as the template of a highly ordered binding matrix for biotinylated materials. The formation of a monolayer of a biotinylated Fab fragment of a monoclonal antibody underneath the template SAv layer has been reported recently.[4] Concanavalin A which is a water-soluble protein with specific binding sites for a sugar was bound to the template with an intervening linker molecule having a biotin group on one end and a sugar moiety on the other, resulting in a protein multilayer.[5] With regard to these results the monolayer technique seems suitable for the assembly of functional protein multilayers. The ordered structure of the first layer has an template effect on the second protein layer, inducing an ordered structure of the

latter. In this regard, a bilayer system of SAv (Figure 1) should be interesting, because the distance between the binding sites of SAv in the second layer is the same as that in the first template layer. Here, it should be noted that a linker molecule to connect the first and the second SAv layers should possess a suitable chain length with an appropriate rigidity to avoid coordination of two terminal biotinyl groups with neighboring binding sites of SAv in the first template layer.

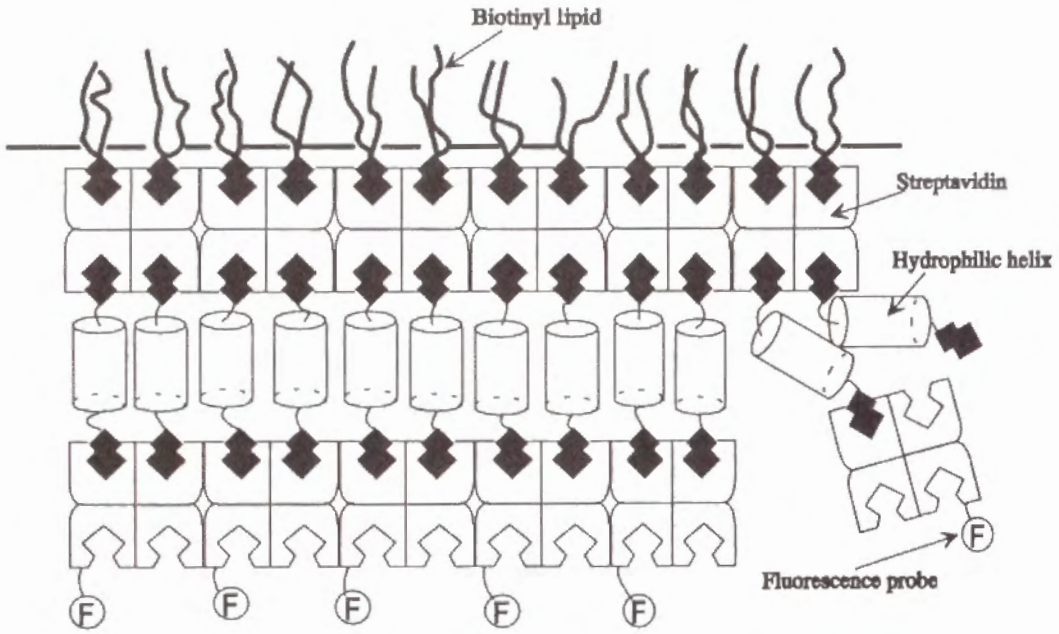

Figure 1 Schematic representation of the SAv bilayer system.

Hydrophilic helical peptides take a rigid secondary structure, and the end-to-end distance is variable by changing the number of amino acid residues. Therefore, the helical peptides are suitable for the linker molecule. In the present chapter, a bisbiotinyl helical peptide was used as the linker peptide. It is well known that the peptide containing Aib residue has a strong tendency to form a helical structure, because the dihedral angles of Aib are constrained in the helical region due to the steric hindrance around α-carbon atom of Aib.[6] Therefore, the linker peptide, **1**, containing Aib residues in the amount of 2/3 of the total residues was designed and synthesized (Figure 2). The formation of the protein bilayer connected by the linker peptide was investigated by the surface plasmon resonance (SPR) and the fluorescence microscopy.

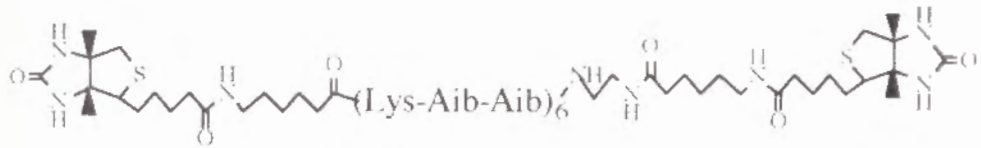

Peptide **1**

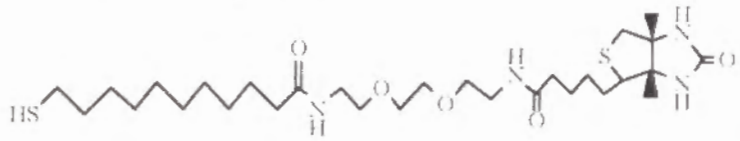

Biotinyl thiol **2**

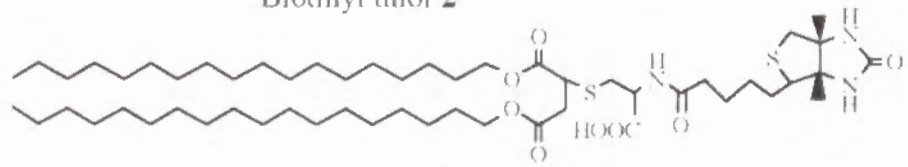

Biotinyl lipid **3**

Figure 2 Molecular structure of the compounds, bis(biotinyl) helical peptide **1**, biotinyl thiol **2** and biotinyl lipid **3**.

Materials and Methods

Materials

Boc amino acids, DCC, HOBt and Boc_2O were purchased from Kokusan Chemical Works (Tokyo, Japan). Biotin aminocapronate *N*-hydroxysuccinimide was purchased from Sigma (St. Louis, USA). Synthesis of the biotin thiol **2** and the biotinyl lipid **3** has been described elsewhere.[2, 7] FITC-SAv and inactive SAv were prepared by the method described in Chapter 4.

Peptide prepatation

Boc-Aib was prepared by the reaction of Aib with Boc_2O in DMF. Aib-OMe was synthesized by the method described in Chapter 1. The peptide linker, **1**, was synthesized by a conventional liquid-phase synthesis using DCC and HOBt as coupling reagents (Scheme1). The crude peptide was purified by the partition chromatography using a Sephadex G50 column, which was equilibrated with the upper phase of 1-butanol / acetic acid / water (4 : 1 : 5) and eluted with the lower phase. Fractions of the main peak were collected and concentrated by evaporation. TLC was performed on a silica-gel plate 60 F254, 0.2-mm thick (Merk, Darmstadt, Germany) in the solvent system (A) butanol / acetic acid /warer (10 : 1 : 3 v/v/v) or (B) ethyl acetate / pyridine / formic acid / water (63 : 21 : 10 : 6 v/v/v/v) with visualization by spraying ninhydrin. TLC: Peptide **1**; R_f(A) 0.43, R_f(B) 0.55.

Methods

CD

CD spectra of the peptides were measured in distilled water, 500 mM aqueous NaCl solution or 50 mM phosphate buffer solution (pH 4.5, 11.0 and 7.0) at room

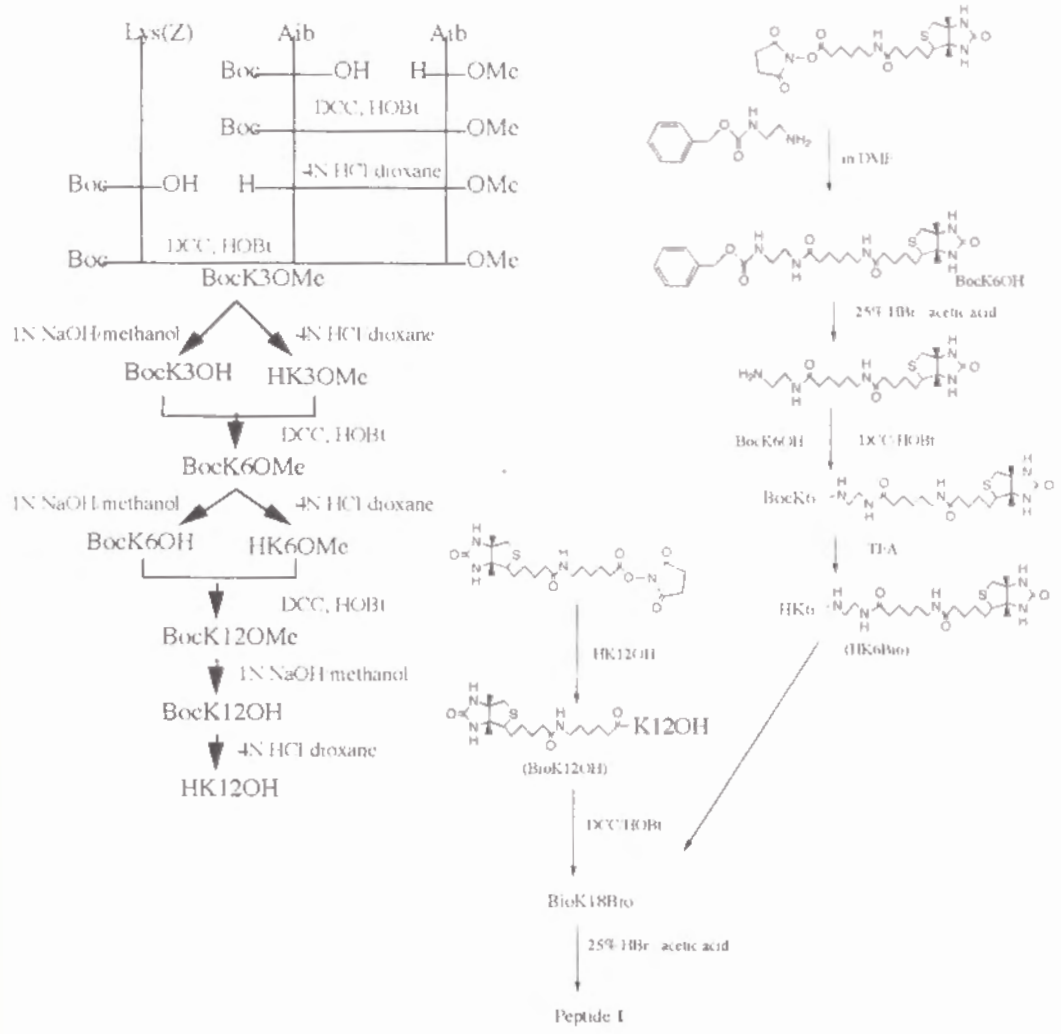

Scheme 1 Synthetic scheme of the peptide **1**.

temperature using an optical cell of 0.5-cm path length. The other experimental conditions were the same as employed in Chapter 1.

Titration of SAv with biotinylated compounds

A 10 mM solution of 2-(*p*-hydroxyphenylazo)benzoic acid in 1 N NaOH (30 μl) was added to SAv solution (3 mg/10 ml of 0.1 M phosphate buffer solution). The mixture was diluted by adding the same volume of 0.1 M phosphate buffer solution and was placed in a UV-VIS cell. The titration curve was obtained from the absorbance at 500 nm of the solution by adding of small amounts of aqueous solution of peptide **1**, biotin or biotinylated suger.[5]

Fluorescence microscopy

The protein bilayer was formed at the air/water interface in a small trough (10 cm^2) by the following procedure: (1) the biotinyl lipid (Figure 2) was spread on the aqueous subphase (0.5 M NaCl) at a concentration of 500 $Å^2$/molecule; (2) an SAv solution was injected into the subphase and the temperature was kept at 30 °C for 30 min, followed by cooling to 20 °C. The subphase was replaced with a new aqueous solution. With procedures (1) and (2), the first SAv layer was formed over the whole area of interface.[4] (3) A 4.2×10^{-8} M aqueous solution of peptide linker **1** was added to the subphase, and was incubated at 20 °C for 120 min. The subphase was replaced with brine. (4) The aqueous solution of FITC-SAv [8] was injected into the subphase.

SPR

A metal surface with a free electron, e.g., gold, is irradiated through a

Kretschmann prism with light. The nonradiative surface is excited electromagnetically (surface plasmon) along the metal-dielectric interface. The mode of excitation depends on the optical properties of the interface. The intensity of the reflected light reached a minimum at the incident angle, at which the energy and momentum of the incident light satisfies conditions for resonantly exciting surface plasmon. When the optical properties of the interface are influenced by adsorption of organic substances etc., the incident angle giving the reflection minimum varies. The thickness of the adsorbed layer can be estimated from the extent of the change of the angle and the refractive index of the layer. The experimental procedure was as follows: (1) adsorption of biotin thiol **2** (Figure 2) and 11-mercaptoundecanol on a gold substrate evaporated onto a slide glass (incubation of the glass with 0.5 mM thiol mixture in 1 : 4 molar ratio for 16 h); (2) substitution of the aqueous phase with 1 μM of SAv solution and incubation for 30 min; (3) substitution with 9.1×10^{-5} M aqueous solution of peptide linker **1** and incubation for 15 min; (4) substitution with 1 μM aqueous SAv solution and incubation for 14 h. Each operation was followed by careful rinsing with water.

Results and Discussion

Conformation of the peptide linker 1

The CD spectrum of the peptide linker, **1**, in pH 7.0 buffer solution at a concentration of 3.0×10^{-6} M showed the double-minimum pattern (Figure 3), indicating a helical conformation.[8] Although the pattern was distorted at the higher concentration than 1.5×10^{-4} M in the buffer solution probably because of the aggregation of the peptide, the CD spectra showed the compatible pattern in water,

0.5 M NaCl, pH 11 and pH 4.5 buffer solution at a concentration of 3.0×10^{-6} M.

Fluorescence microscope

After incubation of an SAv bilayer system (see the experimental procedures for fluorescence microscop) at 20 °C for 15 h, bright domains were observed by fluorescence microscopy (Figure 4).[10] The bright domains were not observed in the control experiment which was carried out without operation (3). This result

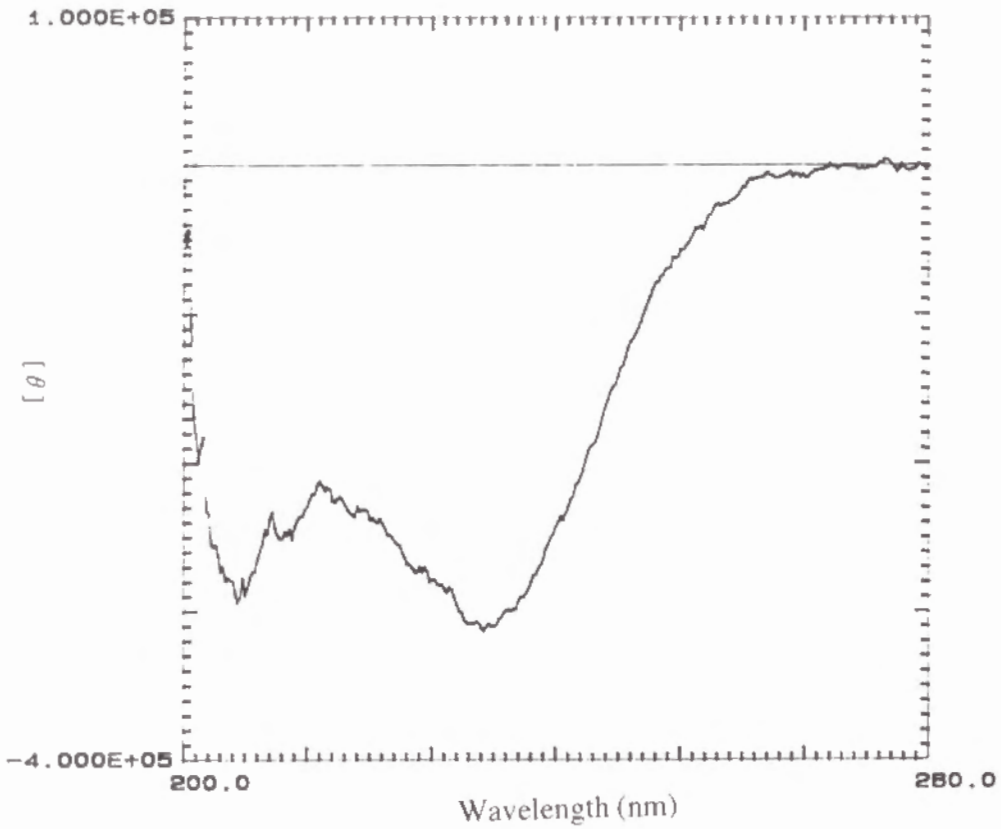

Figure 3 CD spectrum of the peptide linker, **1**, in 50 mM phosphate buffer solution (pH 7.0) at a concentration of 3.0×10^{-6} M.

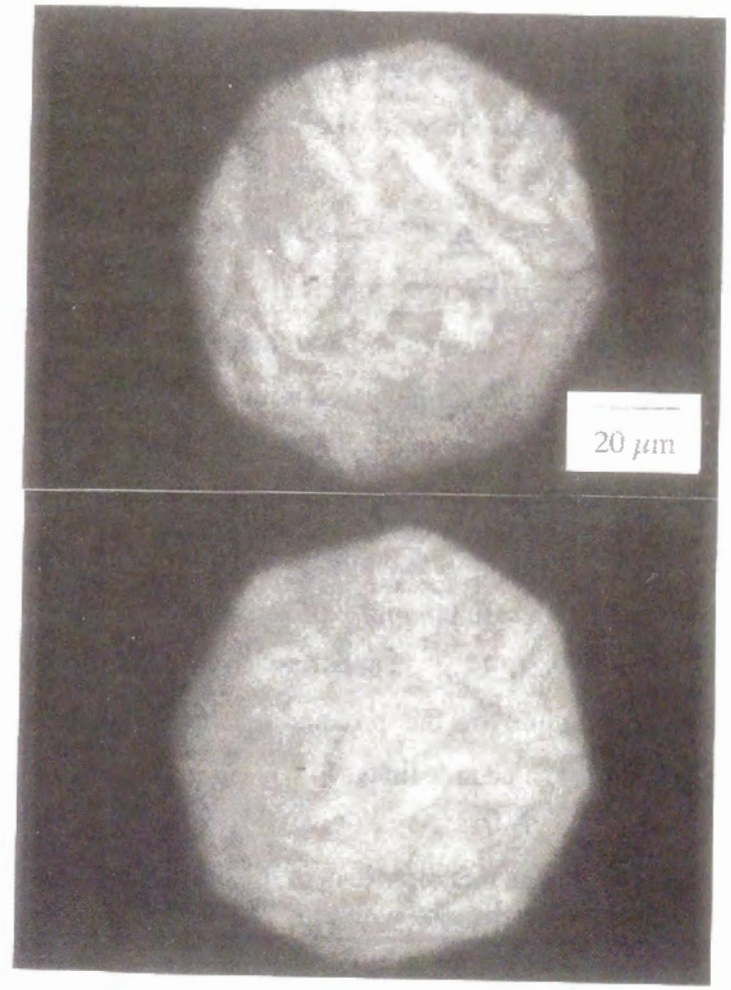

Figure 4 Fluorescence micrograph of SAv bilayer at the air/water interface. The bilayer system; biotinyl lipid, SAv, peptide linker **1** and FITC-SAv, illustrated in Figure 1. The polarization of the incident light was shifted by 90° between two photos.

verifies that the first SAv layer was not substituted with FITC-SAv injected in the procedure (4), and that the bright domains were formed by the second SAv layer formed underneath the first SAv layer with intervention of the linker peptide **1**. It is notable that the bright domains of the second layer showed fluorescence anisotropy, indicating the formation of a two-dimensional crystal of SAv.[2]

Determination of the thickness of adsorbed layers

The protein bilayer was examined by SPR.[11] The thickness of the adsorbed layer after each operation was measured and is summarized in Table I. It is obvious that the thickness of the organic layer increased with SAv or linker adsorption to the surface. The thickness of the first SAv layer was estimated to be 34 Å, which is comparable to the previous results.[12-14] The increase of the thickness of the second layer was not observed in the control experiment when the inactive SAv, which had been saturated with biotin, was used in place of active SAv in procedure (4) (see the exprimental procedure for SPR). Therefore, SPR observation indicates the formation of bilayer structure of the protein, in which one protein layer was connected to the other through peptide linker **1**.

Table I. The thickness data of the SAv bilayer determined with SPR (Å)

+SAv	+**1**	+SAv
34	36	46

The SPR measurement revealed that the thickness of the first SAv layer was 34 A, which is shorter than the protein thickness of 45 Å determined by X-ray analysis of SAv. The effective thickness is underestimated because we calculated the

thickness by using the effective refraction index of n=1.45, which was experimentally determined for a bulk protein. However, it has been indicated by electron microscopy and image processing that the two-dimensional crystal of SAv formed at air/water interface contains much water.[12,14] Therefore, the true refractive index of the SAv layer should be less than 1.45. On the other hand, the effective thickness of 10 Å for the second SAv layer indicates that a partial adsorption of SAv occurs on the first SAv layer. The partial adsorption can be

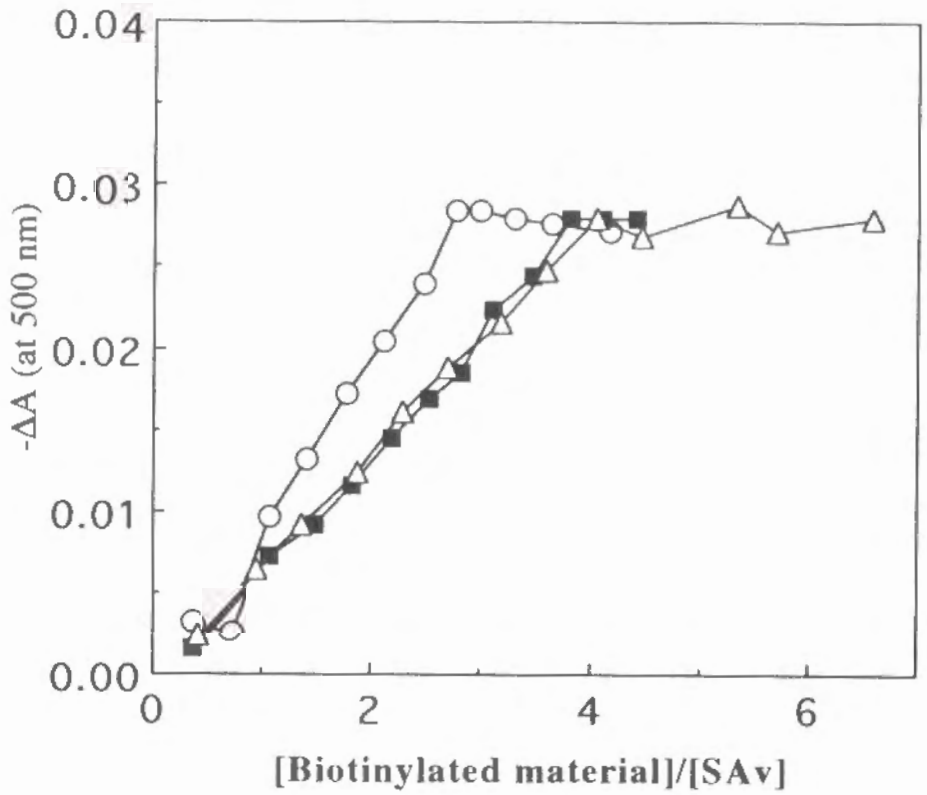

Figure 5 Titration of SAv with peptide **1** (○), biotin (△) or biotinylated suger (■). Biotinylated suger has been reported in ref. 5.

explained by coordination of two terminal biotins of a linker peptide with binding sites of SAv. This explanation is supported by the titration experiment of SAv with peptide **1** (Figure 5), showing that SAv bound only 3-fold molar bisbiotinyl compound, although SAv bound 4-fold molar biotin.

The length of the helix of **1** is 27 Å and the radius of the helix section should be larger than 5 Å, assuming a perfect α-helical structure.[16,17] The distance between the biotin-binding sites of the SAv has been reported to be 20 Å,[15] and that of neighboring SAv molecules in the two-dimensional crystal has been reported to be about 45 Å from two-dimensional projection map of the crystal.[3] Therefore, both biotin moieties of the same peptide linker will not occupy simultaneously the two binding sites of the same SAv molecule nor of the neighboring SAv molecules insofar as the perfect helical conformation of the linker peptide is maintained upon binding to SAv. The backbiting is only possible if the helical structure is disturbed. In order to impose perfectly the second SAv layer underneath the first SAv layer, stabilization of helical structure of the linker peptide should be the key point for further work.

References

(1) Ahlers, M.; Müller, W.; Reichert, A.; Ringsdorf, H.; Venzmer, J. *Angew. Chem., Int. Ed. Engl.* **1990**, *29*, 1269.

(2) Blankenburg, R.; Meller, P.; Ringsdorf, H.; Salesse, C. *Biochemistry* **1989**, *28*, 8214.

(3) Darst, S. A.; Ahlers, M.; Meller, P. H.; Kubalek, E. W.; Blankenburg, R.; Ribi, H. O.; Ringsdorf, H.; Kornberg, R. D. *Biopys. J.* **1991**, *59*, 387.

(4) Herron, J. N.; Muller, W.; Paudler, M.; Riegler, H.; Ringsdorf, H.; Suci, P. A. *Langmuir* **1992**, *8*, 1413.

(5) Knoll, W.; Liley, M.; Muller, W.; Ringsdorf, H.; Rump, E.; Spinke, J.; Wildburg, G.; Zhang, X. *Science* **1993**, *262*, 1706.

(6) (a) Burgess, A. W.; Leach, S. J. *Biopolymers* **1973**, *12*, 2599. (b) Karle, I. L.; Balaram, P. *Biochemistry* **1990**, *29*, 6747.

(7) Häussling, L.; Michel, B.; Ringsdorf, H.; Rohrer, H. *Angew. Chem.* **1991**, *103*, 568.

(8) Holzwarth, G.; Doty, P. *J. Am. Chem. Soc.* **1965**, *87*, 218.

(9) Nargessi, R. D.; Smith, D. S. *Methods Enzymol.* **1986**, *108*, 487.

(10) Meller, P. *Rev. Sci. Instrum.* **1988**, *59*, 2225.

(11) (a) Burstein, E.; Chen, Y. J.; Hartstein, A. *J. Vac. Sci. Thechnol.* **1974**, *11*, 1004. (b) Knoll, W. *MRS Bulletin* **1991**, *XVI(7)*, 29. (c) Terrettaz, S.; Stora, T.; Duschl, C.; Vogel, H. *Langmuir* **1993**, *9*, 1361.

(12) Häussling, L.; Ringsdorf, H.; Schmitt, F. -J.; Knoll, W. *Langmuir* **1991**, *7*, 1837.

(13) Schmitt, F. -J.; Häussling, L.; Ringsdorf, H.; Knoll, W. *Thin Solid Films* **1992**, *210/211*, 815.

(14) Spinke, J.; Liley, M.; Guder, H. -J.; Angermaier, L.; Knoll, W. *Langmuir* **1993**, *9*, 1821.

(15) Hendrickson, W. A.; Pahler, A.; Smith, J. L.; Satow, Y.; Merritt, E. A.; Phizackerley, R. P. *Proc. Natl. Acad. Sci. USA* **1989**, *86*, 2190.

(16) Branden, C.; Tooze, J. *Introduction to Protein Structure*; Garland Publishing: New York & London, 1991.

(17) Lavigne, P.; Tancrede, P.; Lamarche, F.; Max, J.-J. *Langmuir* **1992**, *8*, 1988.

Chapter 6

Self-Assembly of Mastoparan X Derivative Having Fluorescence Probe in Lipid Bilayer Membrane

Introduction

Conformation, orientation and aggregation of biologically active peptides in the phospholipid bilayer membrane are important information for understanding the structure-function relationship of the peptide.[1] For example, helical peptides having a primary amphiphilic structure form ion channel in lipid membrane by aggregation of the peptides spanning across the membrane.[2-4] It is well-known that peptide hormones take a regular conformation in lipid membrane, which is essential for interaction with the receptor in the membrane.[5]

Mastoparans, which are tetradecapeptides isolated from wasp venom, show various biological activities such as degranulation of mast cell,[6] stimulation of G proteins,[7] and facilitation of phospholipase A_2.[8] Ion-channel formation by taking a helix-bundle structure in lipid membrane has also been suggested.[9] CD[10] and NMR[11,12] spectroscopy have shown that mastoparans take partially helical conformation of an amphiphilic structure in lipid membrane. These spectroscopic methods, however, require much higher concentrations of peptide than in biological conditions. For example, mastoparans degranulate mast cell at micromolar concentrations,[13] while approximately 100-fold concentration is required for NMR

measurement. The interaction of peptides with phospholipid bilayer membrane is sensitively influenced by the peptide concentration. For example, the orientation of magainin in a lipid bilayer membrane was changed with varying the concentration.[14] It is, therefore, important to study the interaction of mastoparans with a lipid bilayer membrane by other sensitive spectroscopic method. In this chapter, fluorescence spectroscopy is used to investigate the conformation, orientation and aggregation of the peptide at the biological concentrations.

The anthryl group was connected to the C-terminal residue of mastoparan X (MPX), which has a Trp residue at the third position.[6] MPX-A, therefore, possesses two different fluorescent probes at both ends of a chain (Figure 1). The conformation of MPX-A was estimated by measuring intramolecular excitation energy transfer from the Trp residue to the anthryl group. The orientation of MPX-A in lipid bilayer membrane was assessed by fluorescence quenching of the probes by a water-soluble quencher. Furthermore, the aggregation of MPX in lipid membrane was investigated by measuring intermolecular energy transfer from MPX to F-MPX-A, in which the Trp residue was formylated to be non-fluorescent.[15]

Leu-Asn-Trp-Lys-Gly-Leu-Ala-Ala-Leu-Ala-Lys-Lys-Leu-Ser(Ant)-NH_2

MPX-A

CHO
|
Leu-Asn-Trp-Lys-Gly-Leu-Ala-Ala-Leu-Ala-Lys-Lys-Leu-Ser(Ant)-NH_2

F-MPX-A

Figure 1 Molecular structure of MPX derivatives.

Materials and Methods

Materials

Boc-protected amino acids, 25% HBr/acetic acid, DCC and HOBt were purchased from Kokusan Kagaku, Tokyo, Japan, and BOP reagent, TFA, TFMSA, and 9-hydroxymethylanthracene were purchased from WAKO Pure Chemicals Ind., Osaka, Japan. MPX was obtained from Peninsula Lab., Co., USA. DMPC and 5-, 12- and 16-doxyl stearic acids were purchased from Sigma, St. Louis, USA.

Peptide preparation

The synthetic route of MPX-A and F-MPX-A is shown in Scheme 1. Boc-Ser(Ant)-NH_2 was obtained by the reaction of Boc-Ser-NH_2 with 9-bromomethylanthracene,[16] which was prepared from 9-hydroxymethylanthracene by treating with PBr_3. The first fragment composed of six residues of the N-terminal part of MPX-A and F-MPX-A was synthesized by the conventional liquid phase method using DCC and HOBt as the coupling reagents. The second fragment composed of seven residues of the C-terminal part was synthesized by the solid phase method using oxime resin developed by Kaiser, et al.[17] The protected second fragment was cleaved from the resin by incubation with H-Ser(Ant)-NH_2 for 25 h. Both fragments were purified with a Sephadex LH-20 column using DMF as the elution solvent and recrystallization. The two fragments were coupled by using DCC and HOBt to obtain a fully protected peptide, Z-MPX-A. The product was purified with a Sephadex LH-20 column using DMF as the elution solvent, and was treated with hydrazine monohydrate to remove the formyl group.[18] The Z group was removed by the treatment with TFMSA to obtain crude MPX-A.[19] On the other hand, Z-MPX-A was treated with HBr / acetic acid to obtain crude F-MPX-A.[20]

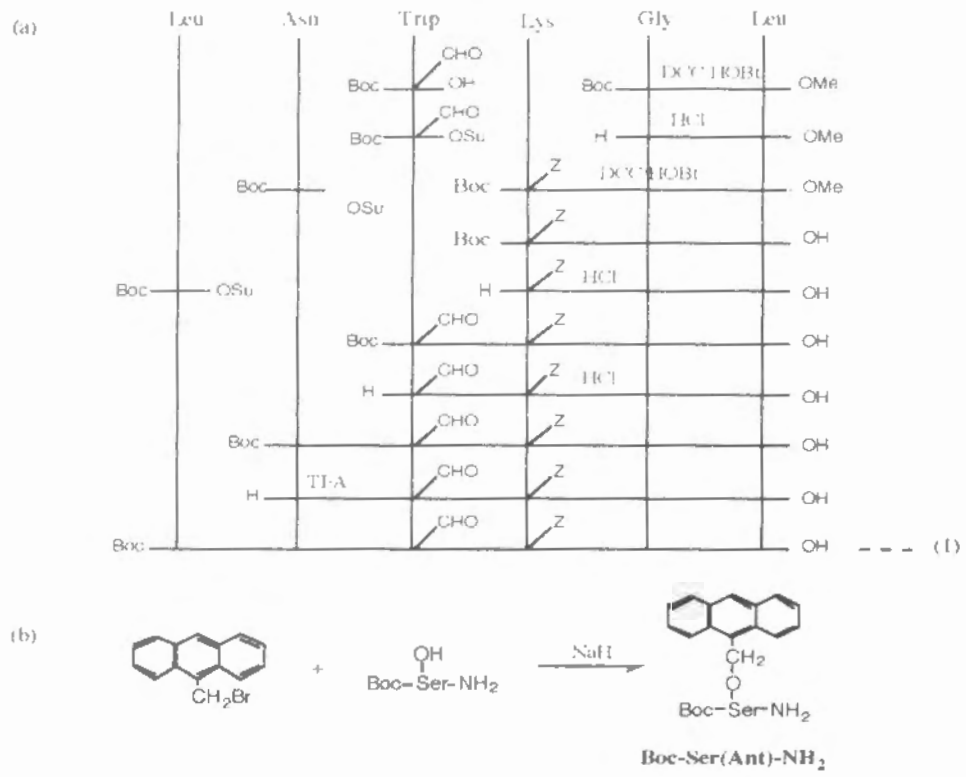

Scheme 1 Synthetic scheme of MPX-A and F-MPX-A: (a) the 1st fragment , (b) Boc-Ser(Ant)-NH_2, (c) the 2nd fragment (d) fragment condensation.

Each crude product was purified by the partition chromatography using a Sephadex G50 column, which was equilibrated with the lower phase of 1-butanol / acetic acid / water (4 : 1 : 5) and eluted with the upper phase. Fractions of the main peak were collected and concentrated by evaporation.[21] The residues were further purified by a reverse-phase HPLC column (Cosmosil 5C18, Nakalai Tesque Inc., Kyoto, Japan) using acetonitrile / water (3/2 v/v) mixture containing 0.1% TFA as the elution solvent.[22] MPX-A and F-MPX-A were identified by NMR spectroscopy and amino acid analysis.

Liposome preparation

Small unilamellar vesicles (SUV) composed of DMPC were prepared by sonication of the lipid dispersion in a phosphate buffer (50 mM, pH 7.0) followed by ultracentrifugation at 100,000 g as reported previously.[23] The lipid concentration was determined by the phospholipid assay kit, Dia Color PL (Ono Yakuhin, Osaka, Japan).[24] All measurements using the SUV were carried out at 30 °C, which is above the phase-transition temperature of DMPC liposome.[25]

Methods

CD, UV and fluorescence spectra were measured on a JASCO J-600 spectropolarimeter using a cell with an optical path length of 2 mm, a JASCO UVIDEC-1 UV/VIS spectrophotometer and a Hitachi MPF-4 fluorophotometer, respectively. Fluorescence depolarization was measured by an equipment installed on the MPF-4 fluorophotometer according to the method as reported previously.[26] The stock solution of peptide (*ca.* 3 mM) in twice distilled TMP was prepared, and the accurate concentration was determined with the absorbance of Trp or the anthryl group.

The dissociation constant of the peptide-containing DMPC vesicles was determined from the increase of the fluorescence intensity of the peptide by the addition of DMPC vesicles according to the method reported previously.[27]

Fluorescence quenching experiments were carried out as follows. A dry film of DMPC containing various doxylstearic acids was dispersed in a phosphate buffer (50 mM, pH 7.0). The dispersion was sonicated for 5 min at 35 °C. The peptide (1.1 μM) was incubated with the liposome ([DMPC] = 0.37 mM) for 15 min, and the fluorescence intensity was measured at 30 °C. The excitation and monitor wavelengths were 280 and 350 nm for the Trp residue and 360 and 415 nm for the anthryl group, respectively.

Fluorescence quantum yield of Trp residue in MPX was determined using quinine sulfate in 1N sulfuric acid as the standard substance.[28] Excitation energy transfer efficiency was determined from the excitation spectra of the energy acceptor, the anthryl group[29]. The distance between the Trp residue and the anthryl group was estimated on the basis of the Förster's theory.[30]

Results and Discussion

Distribution to lipid membrane

Fluorescence spectra of MPX-A were measured with increasing amount of DMPC vesicles (Figure 2). Emission of MPX-A in a buffer solution appeared at 350 and 415 nm upon excitation at 280 nm. The latter is assigned to the fluorescence of the anthryl group due to the excited energy transfer from the Trp residue. The emission of Trp at 350 nm in a buffer solution shifted to a shorter wavelength and strengthened the intensity by the addition of DMPC vesicles, indicating distribution of MPX-A to the phospholipid bilayer membrane. The

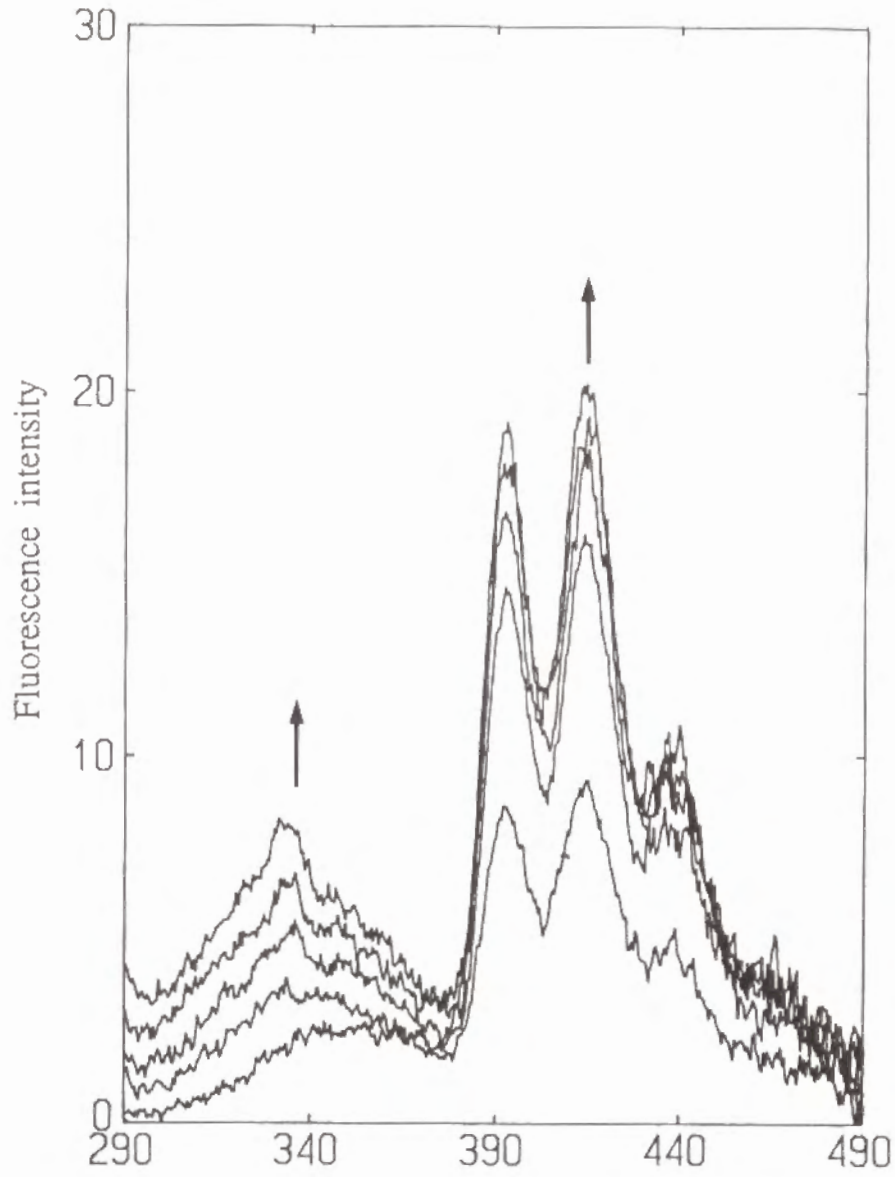

Figure 2 Fluorescence spectra of MPX-A with varying concentrations of DMPC vesicles: 0, 77, 150, 230 and 380 μM from the bottom to the top. Excitation wavelength; 280 nm. [MPX-A] = 1.1 μM.

dissociation constant, K_d , of MPX-A with DMPC membrane was calculated from the intensity change with varying lipid concentrations. K_d (apparent) [27] was 0.18 mM, which is comparable to 0.11 mM for MPX with the DMPC membrane and 0.12 mM for MPX with the egg-yolk lecithin membrane.[31] Therefore, the introduction of the anthryl group to MPX and the replacement of Ile residue of MPX with Leu residue do not strongly influence the affinity of peptide with lipid membrane.

Conformation of MPX-A

Figure 3 shows CD spectra of MPX-A in various media. A negative Cotton effect appearing at 220-230 nm region indicates the occurrence of an α-helical conformation. Although the CD patterns are not of the double-minimum type which is typical for an α-helix, the apparent helix content was estimated from the intensity at 222 nm.[32] It was 22 % in buffer solution, 41 % in SDS micelle, and 70 % in TMP. MPX-A, therefore, is expected to take an α-helical conformation in lipid membrane. However, DMPC vesicles aggregated in the presence of MPX-A of 10 μM, which made the CD measurement difficult due to light-scattering effect.

The conformation of MPX-A in lipid membrane was investigated by fluorescence spectroscopy. The efficiency of excited energy transfer from the Trp residue to the anthryl group of MPX-A was calculated from the excitation spectrum of MPX-A (Figure 4). The molar ratio of MPX-A and DMPC was 1/9800. Under these conditions, intramolecular energy transfer is absolutely predominant over intermolecular process, because at most one peptide molecule is included in one vesicle according to calculation. F-MPX-A, which has a non-fluorescent Trp, was used as the reference compound. The energy-transfer efficiency was calculated

from the intensity at 283 nm to be 34 %. This value corresponds to a distance of 2.49 nm between the Trp residue and the anthryl group of MPX-A according to the Förster's theory.[29] The distance between the indole nitrogen of Trp residue and the center of anthryl group along the molecular axis of MPX-A was calculated to be 2.05 nm on the basis of a fully α-helical conformation and a trans configuration of side

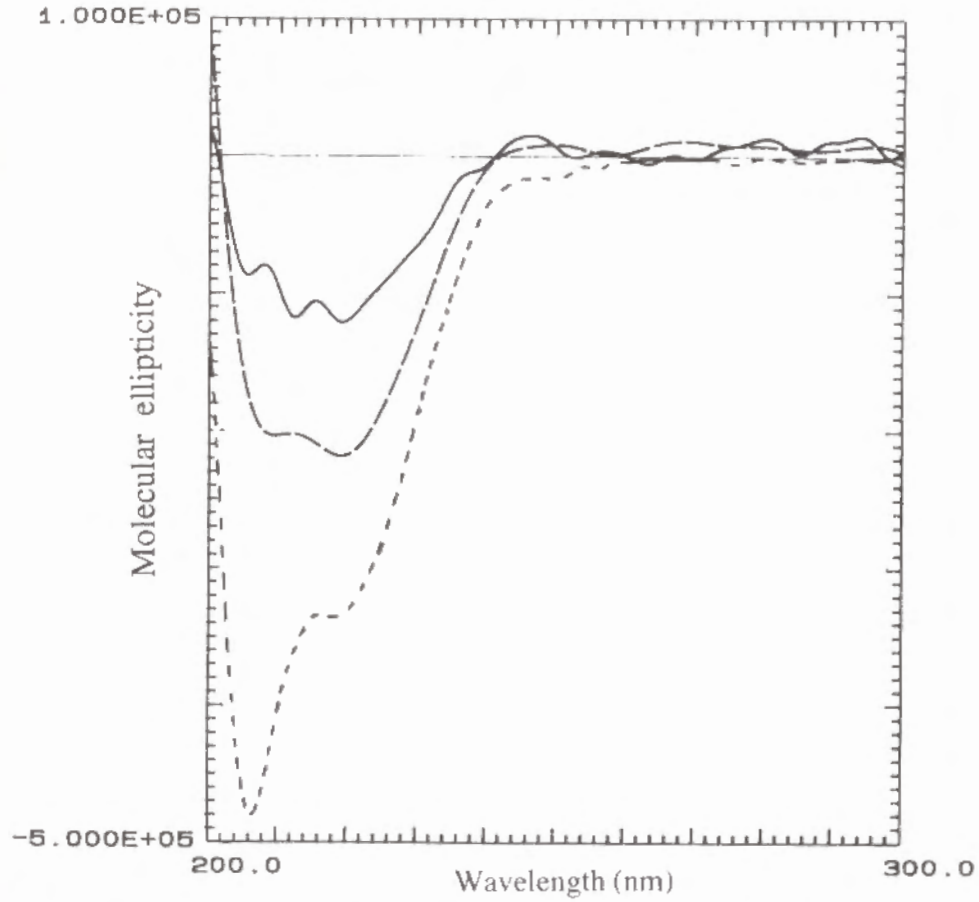

Figure 3 CD spectra of F-MPX-A in 50 mM phosphate buffer, pH 7.0 (——), 10 mM SDS micelle (– – –), and TMP solution (--------). [MPX-A] = 1.8 μM.

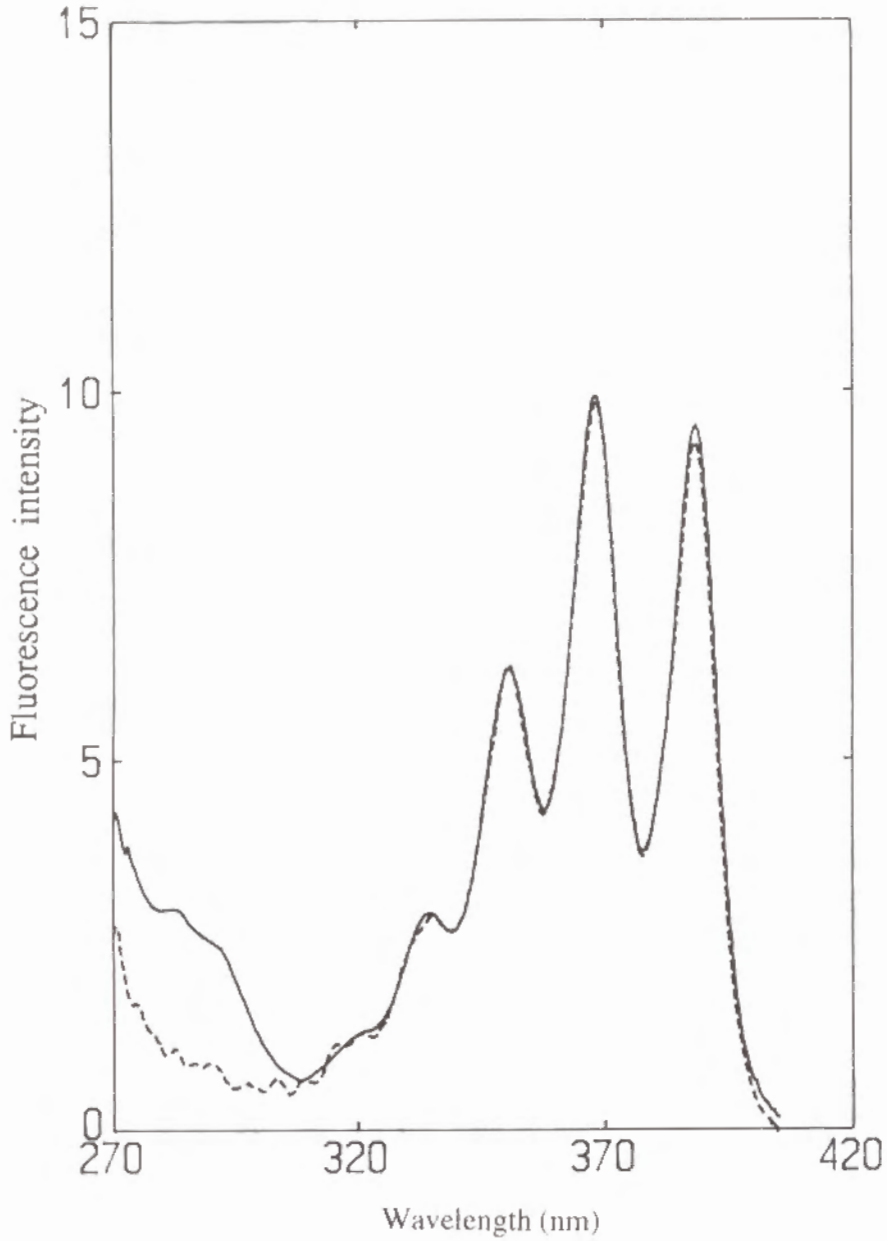

Figure 4 Excitation spectra of MPX-A (——) and F-MPX-A (---------) in the presence of DMPC vesicles. Monitor wavelength; 415 nm. Peptide concentration; 0.43 μM. [DMPC] = 4.2 mM.

chains.[33,34] On the other hand, a distance of 4.0 nm can be obtained for an extended conformation. Therefore, MPX-A is considered to take a highly helical structure in lipid membrane. The result obtained under highly diluted condition appears to be consistent with the previous NMR assignment of the conformation of the vesicle-bound peptide under a concentrated condition.[11,12]

It should be noted, however, that the helix content might not be so high in lipid membrane, if peptide molecules are allowed to undergo an accordion vibration. In this case, the two fluorescent probes should approach within the critical distance for the energy transfer during the fluorescence life time of the Trp residue, and the energy-transfer efficiency increases. This happens to MPX-A in a TMP solution. The energy-transfer efficiency of MPX-A in a TMP solution was calculated to be 65 %, which corresponds to a distance of 2.13 nm between the Trp residue and the

Table I. Fluorescence properties of MPX-A.

Medium	Quantum yield of Trp in MPX	R_0 (Trp→Ant)	Energy-transfer efficiency (%)	R (nm)
SUV suspension	0.32	2.24[a]	34	2.49
TMP solution	0.42[b]	2.32[a,b]	65	2.13

R, The distance between the centers of the donor and the acceptor chromophores determined from the energy-transfer efficiency.

R_0, The distance at which the energy-transfer efficiency is 50 %.

a: The orientation factor, κ^2 was assumed to be 2/3, which is for a random orientation.

b: The refractive indices of 1.336 and 1.369 were adopted for the phosphate buffer and TMP, respectively.

anthryl group, suggesting a fully helical conformation. However, the helix content was 70 % from the CD measurement.

Orientation of MPX-A in lipid membrane

The location and orientation of the helical MPX-A in lipid membrane were investigated by fluorescence quenching of Trp residue and the anthryl group with various doxylstearic acids.[30] The results are shown in Figure 5 in terms of the Stern-Volmer plot. The emission from both probes was most strongly quenched with 5-doxylstearic acid in the presence of DMPC vesicles. Therefore, it is considered that MPX-A is located at the surface of a phospholipid bilayer membrane, and the helix axis of MPX-A is oriented parallel to the membrane surface.

Aggregation of MPX-A in lipid membrane

Aggregation of MPX in lipid membrane was studied by measuring the intermolecular energy transfer from the Trp residue of MPX to the anthryl group of F-MPX-A in the presence of DMPC vesicles. The equimolar mixture of MPX and F-MPX-A was added to DMPC vesicles. The efficiency of intermolecular energy transfer was calculated from the excitation spectra, and the results are summarized in Figure 6. The efficiency increased with increasing peptide concentration in lipid membrane. It is notable that the experimental conditions were limited such that the peptide / lipid molar ratios were lower than 7.5×10^{-4}. Under these conditions, the energy-transfer efficiency has been calculated to be 4 %, assuming a homogeneous dispersion of peptide molecules in the outer leaflet of a lipid bilayer membrane.[35,36] Since much higher efficiency was observed at the peptide / lipid molar ratios lower than 7.5×10^{-4}, the peptide molecules appear to aggregate in these low concentrations.

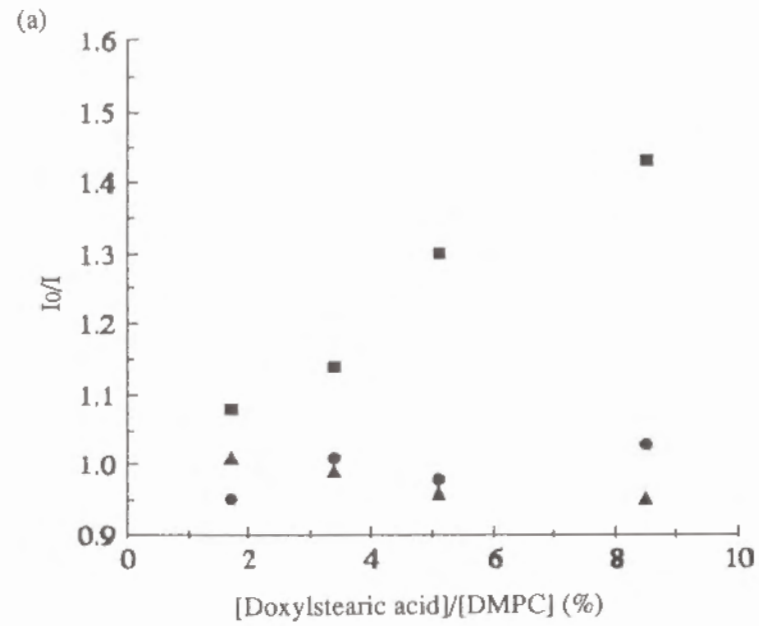

Figure 5 Fluorescence quenching of MPX-A with 5- (■), 12- (●), or 16-doxylstearic acid (▲) in the presence of DMPC vesicles. Fluorescence quenching of (a) Trp and (b) the anthryl group. [DMPC]/[MPX-A] = 337. Other conditions are indicated in the Methods section.

The fluorescence depolarization of the anthryl group of F-MPX-A was also measured under the same conditions, and the results are shown in the same figure (Figure 6). The degree of depolarization value increased with increasing peptide concentrations in the membrane. This trend is similar to the energy-transfer efficiency. The increase of the degree of depolarization can be explained by an energy migration between the anthryl groups due to aggregation of peptide

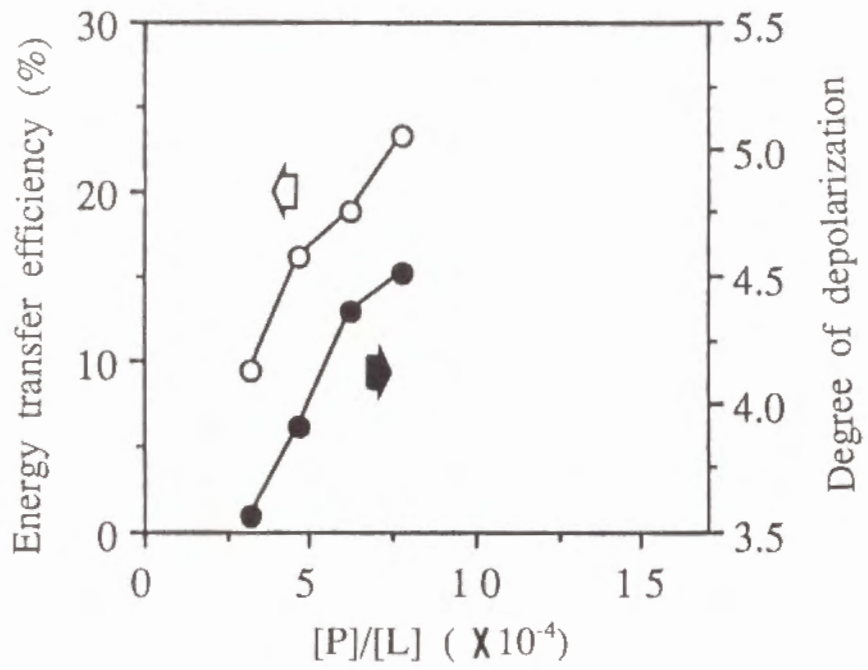

Figure 6 Energy-transfer efficiency (○) and fluorescence depolarization (●) of an equimolar mixture of MPX and F-MPX-A under varying peptide / lipid molar ratios. Excitation wavelength, 280 nm; monitor wavelength, 415 nm. [DMPC] = 2.1 mM. Peptide concentrations varied.

molecules.[2] It is, therefore, considered that MPX and F-MPX-A aggregate in lipid membrane in very low concentrations.

The peptide aggregation in lipid membrane was also indicated by excitation spectra of MPX-A under varying peptide / lipid molar ratios. The energy-transfer efficiency was plotted against the peptide / lipid molar ratio in Figure 7. The efficiency increased with increasing peptide concentrations and reached a plateau

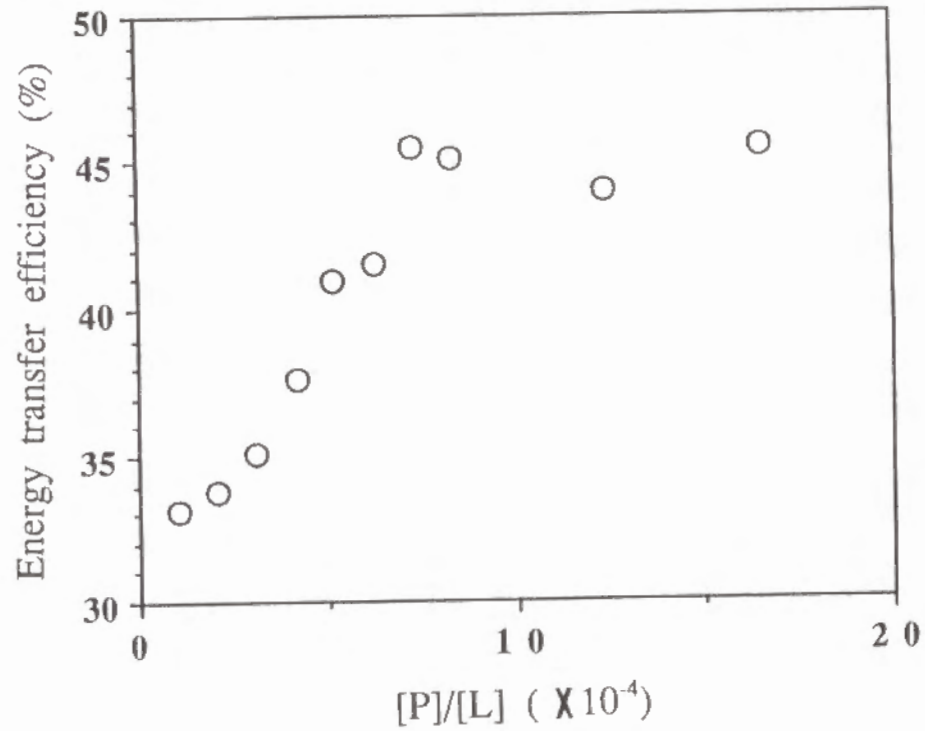

Figure 7 Energy-transfer efficiency of MPX-A under varying peptide / lipid molar ratios. [DMPC] = 4.0 mM, [MPX-A] = 0.43 - 7.0 μM.

beyond a peptide / lipid molar ratio of 7 × 10-4. The increase of the energy-transfer efficiency in these low peptide concentrations can be explained in terms of aggregation of peptide molecules in lipid membrane, accompanying the intermolecular energy transfer. The fluorescence depolarization depended on the peptide / lipid molar ratios in a similar manner to the relation of the energy transfer

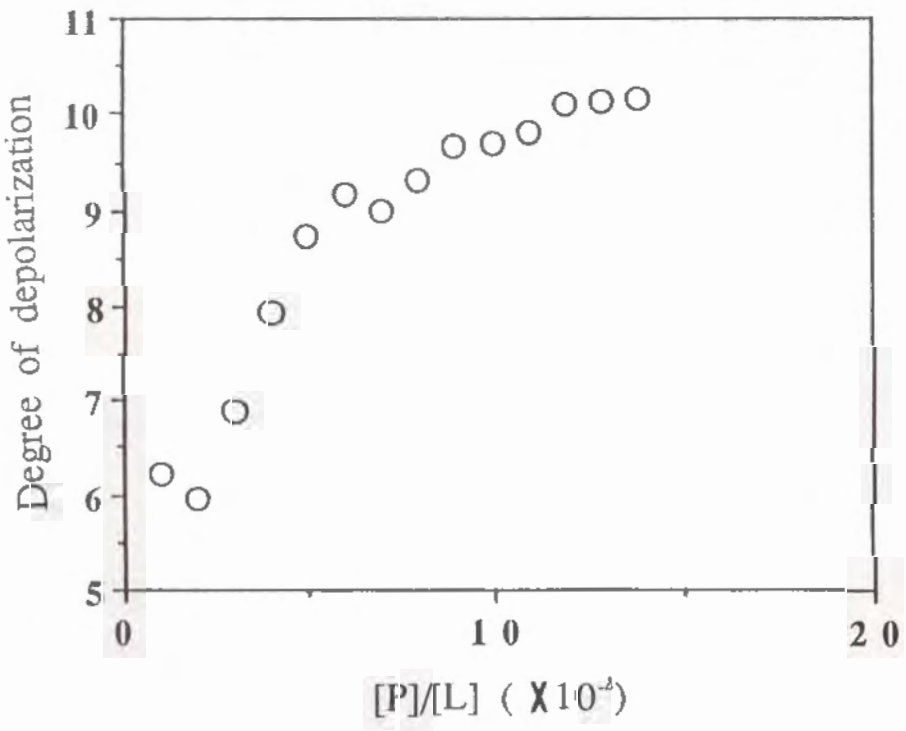

Figure 8 Fluorescence depolarization of MPX-A under varying peptide / lipid molar ratios. Conditions are the same as those in Figure 7.

with the peptide / lipid molar ratios (Figure 8), supporting the aggregation of MPX-A in the lipid membrane.

Interestingly, the energy-transfer efficiency as well as the degree of fluorescence depolarization became constant beyond a peptide / lipid molar ratio of 7 × 10-4. This observation suggests that aggregate of MPX-A having a definite size is formed beyond this molar ratio. Assuming that 5000 lipid molecules form one vesicle having a 30-nm diameter,[35] four MPX-A molecules are included in one DMPC vesicle at this peptide / lipid molar ratio. It is thus considered that the aggregate of MPX-A is an assembly of four molecules on an average. However, this number remains to be investigated further.

It has been reported that several biological activities of mastoparans are elicited by direct interactions with G proteins.[37] Because G proteins exist in the inner surface of a plasma membrane, mastoparans must be translocated across the membrane. It has been proposed that the inside-negative membrane potential may be the driving force for the translocation.[31,38] The assembly formation may facilitate the transmembrane translocation of mastoparans by shielding the hydrophilicity. Furthermore, the aggregation of mastoparans helps concentration of positive charges to activate G proteins as reported for G-protein activating peptides.[39,40]

References

(1) Sargent, D. F.; Schwyzer, R. *Proc. Natl. Acad. Sci. USA* **1986**, *83*, 5774.
(2) Otoda, K.; Kimura, S.; Imanishi, Y. *Biochim. Biophys. Acta* **1993**, *1150*, 1.
(3) Otoda, K.; Kimura, S.; Imanishi, Y. *Biochim. Biophys. Acta* **1992**, *1112*, 1.

(4) Otoda, K.; Kimura, S.; Imanishi, Y. *J. Chem. Soc. Perkin Trans. 1*, **1993**, 3011.

(5) Schwyzer, R. *Biochemistry* **1986**, *25*, 6335.

(6) Nakajima, T.; Uzu, S.; Wakamatsu, K.; Saito, K.; Miyazawa, T.; Yasuhara, T.; Tsukamoto, Y. ; Fujino, M. *Biopolymers* **1986**, *25*, 115.

(7) Higashijma, T., Uzu, S.; Nakajima, T.; Ross, E. M. *J. Biol. Chem.* **1988**, *263*, 6491.

(8) Argiolas, A.; Pisano, J. J. *J. Biol. Chem.* **1983,** *25*, 13697.

(9) Mellor, I. R.; Sanson, M. S. P. *Proc. R. Soc. Lond. B* **1990**, *239*, 383.

(10) Higashijima, T.; Wakamatsu, K.; Takemitsu, M.; Fujino, M.; Nakajima, T.; Miyazawa, T. *FEBS Lett.* **1983**, *152*, 227.

(11) Wakamatsu, K.; Higashijima, T.; Fujino, M.; Nakajima, T.; Miyazawa, T. *FEBS Lett.* **1983**, *162*, 123.

(12) Wakamatsu, K.; Okada, A.; Miyazawa, T.; Ohya, M.; Higashijima, T. *Biochemistry* **1992**, *31*, 5654.

(13) Hirai, Y.; Yasuhara, T.; Yoshida, H.; Nakajima, T.; Fujino, M.; Kitada, C. *Chem. Pharm. Bull.* **1979**, *27*, 1942.

(14) Ludtke, S. J.; He, K.; Wu, Y.; Huang, H. W. *Biochim. Biophys. Acta* **1994**, *1190*, 181.

(15) Kimura, S.; Imanishi, Y. *Helv. Chim. Acta* **1982**, *65*, 2431.

(16) Sugano, H.; Miyoshi, M. *J. Org. Chem.* **1976**, *41*, 2352.

(17) Kaiser, E. T.; Mihara, H.; Laforet, G. A.; Kelly, J. W.; Walters, L.; Findeis, M. A.; Sasaki, T. *Science* **1989**, *243*, 187.

(18) Ohno, M.; Tsukamoto, S.; Makisumi, S.; Izumiya, N. *Bull. Chem. Soc. Jpn.* **1972**, *45*, 2852.

(19) Akaji, K.; Fujii, N.; Yajima, H.; Pearson, D. *Chem. Pharm. Bull.* **1982**, *30*, 349.

(20) Ben-Ishai, D. *J. Org. Chem.* **1954,** *19*, 62.

(21) Yajima, H.; Kanai, J.; Funakoshi, S.; Hirai, Y.; Nakajima, T. *Chem. Pharm. Bull.* **1980**, *28*, 882.

(22) Wakamasu, M.; Kitada, C.; Fujino, M. *Chem. Pharm. Bull.* **1982**, *30*, 7266.

(23) Barenholz, Y.; Gibbes, D.; Litman, B. J.; Goll, J.; Thompson, T. E.; Carlson, F. D. *Biochemistry* **1977**, *16*, 2806.

(24 Nishina, H. *Med. Technol.* **1984**, *12*, 539.

(25) Van Dijck, P. W. M.; de Kruijff, B.; Van Deenen, L. L. M.; de Gier, J.; Demel, R. A.*Biochim. Biophys. Acta* **1976**, *455*, 576.

(26) Ohtoyo, T.; Shimagaki, M.; Otoda, K.; Kimura, S.; Imanishi, Y. *Biochemistry* **1988**, *27*, 6458.

(27) Surewicz, W. K.; Epand, R. M. *Biochemistry* **1984**, *23*, 6072.

(28) Melhuish, W. H. *J. Phys. Chem.* **1960**, *64*, 762.

(29) Stryer, L. *Ann. Rev. Biochem.* **1978**, *47*, 819.

(30) Förster, T. *Modern Quantum Chemistry*, Academic Press, New York, 1965, p.93

(31) de Kroon, A. I. P. M.; de Gier, J.; de Kruijff, B. *Biochim. Biophys. Acta* **1991**, *1068*, 111.

(32) Greenfield, N.; Fasman, G. D. *Biochemistry* **1969**, *8*, 4108.

(33) Momany, F.; McGuire, R. F.; Burgess, A. W.; Sheraga, H. A. *J. Phys. Chem.* **1975**, *79*, 2361.

(34) Sisido, M. private communication.

(35) Fung, B. K.-K.; Stryer, L. *Biochemistry* **1978**, *17*, 5241.

(36) Haung, C.; Mason,J. T. *Pro. Natl. Acad. Sci. USA* **1978**, *75*, 308.

(37) Weigarten, R.; Ransnas, L.; Mueller, H.; Sklar, L. A.; Bokoch, G. M. *J. Biol.*

Chem. **1990**, *265*, 11044.
(38) de Kroon, A. I. P. M.; Vogt, B.; van't Hof, R.; de Kruijff, B.; de Gier, J. *Biophys. J.* **1991**, *60*, 525.
(39) Higashijima, T.; Burnier, J.; Ross, E. M. *J. Biol. Chem.* **1990,** *265*, 14176.
(40) Tomita, U.; Inanobe, A.; Kobayashi, I.; Takahashi, K., Ui, M.; Katada, T. *J. Biochem.* **1991**, *109*, 184.

CONCLUDING REMARKS

This thesis summarizes the results of investigation on the construction of higher-order structure of α-helical peptides at the air/water interface and in the lipid membrane. The experimental results clearly showed the properties of the peptides to form "supramolecular assembly systems", which are briefly summarized below.

In Part I of this thesis, the monolayer formation of α-helical peptides at the air/water interface was investigated.

In Chapter 1, a hydrophobic peptide, BA16M, and its end-modified derivatives were synthesized and π-A isotherms of the peptides spread at the air/water interface were investigated from the viewpoint of interactions between helices. All π-A isotherms of the synthetic peptides showed an inflection and weak irregular bumping at a surface area of *ca.* 240 and 230 Å^2/molecule, respectively, indicating that the helix axis of the peptide is oriented parallel to the interface. A small mound was observed at around 300 Å^2/molecule in the π-A isotherm of BA16M, which was ascribed to the phase transition from a liquid state to a solid state. The monolayer of an equimolar mixture of the peptides having opposite charges in the end group underwent the phase transition in the π-A isotherm, which was not observed with the individual peptide. The electrostatic interaction between the end groups should have stabilized the molecular packing at the interface.

In Chapter 2, monolayer formation of hydrophobic α-helical peptides, X-(Ala-Aib)$_8$-Y (X = Boc-, $HOOCCH_2CH_2CO$-, biotinyl, biotinyl-(Sar)$_3$-; Y = OMe, OBzl, OH), at the air/water interface was investigated by the fluorescence

microscopic method. Some peptides showed a mound in the π-A isotherm. When the monolayer containing a small amount of FITC-labelled peptide was held at the surface pressure corresponding to the top of the mound, bright and dark domains were observed by the fluorescence microscopy. The domain formation was also observed by the addition of a cationic dye ($DiIC_1$) into the subphase underneath the peptide monolayer. The mound in the π-A isotherm is, therefore, ascribed to the phase transition from a liquid state to a solid state. Two different shapes (leaflet and needle) of solid domains were observed and discussed in terms of different orientations of the peptides in the monolayer.

In Chapter 3, ten kinds of helical peptides were synthesized to study interaction between helices in the peptide monolayer formed at the air/water interface. Five of those have a repeating sequence of Ala-Aib and different end groups, other two a repeating sequence of Lys(Z)-Aib, and the rest three a repeating sequence of Leu-Aib. All the peptides take a helical conformation in ethanol as confirmed by CD spectroscopy. The π-A isotherms of the peptide monolayers showed an inflection at the surface area corresponding to the cross section along the helix axis, where the monolayers are considered to collapse. The monolayers were transferred onto various substrates and subjected to IR transmission and reflection absorption spectroscopy. By comparing the amide I and II absorbance, the peptides seemed to lie on the substrates. It was concluded that the peptides in the monolayer orient their helical axis parallel to the air/water interface.

In Part II, two-dimensional crystallization of a protein at the air/water interface by using an assembly of α-helical peptides was investigated. The conformation, orientation and assembly formation of a naturally occurring, biologically active

peptide was investigated, too.

In Chapter 4, two kinds of biotinyl peptides, BioS3A16M and BioA16M, were synthesized. Biotin, which is a specific ligand for SAv, was connected to the N terminus of the hydrophobic helical peptides. The former possesses a longer spacer chain between the biotinyl group and the N terminus of the helical peptide than the latter. The biotinyl peptides were spread at the air/water interface, and the interaction with SAv injected in the subphase was investigated. The π-A isotherm of the biotinyl peptides spread at the air/water interface was measured in the presence of SAv, and was compared with that in the presence of inactive SAv, in which the binding sites were occupied by biotin. It was shown that SAv was specifically bound to the biotinyl peptides and the complex formed a stable monolayer at the interface. The monolayer carrying SAv labeled with rhodamine or fluorescein was investigated with a fluorescence microscope. The fluorescence from SAv bound to the monolayer of BioS3A16M was anisotropic when excited by polarized light. This observation indicates that SAv formed a well-ordered structure, *i. e.*, a two-dimensional crystalline domain underneath the monolayer. On the other hand, such domain was not formed in the case of the monolayer of BioA16M. A long spacer chain between the biotin unit and the helical peptide is necessary for the molecular packing of the biotinyl peptide and the two-dimensional crystallization of SAv.

In Chapter 5, the formation of protein double-layer at the air/water interface was investigated. It has been revealed that SAv interacts with a biotinyl lipid specifically at the air/water interface and the complex forms an interfacial two-dimensional crystal. The two-dimensional crystal is regarded as an ordered template for biotinylated compounds because two of the four binding sites for biotin are left free and exposed to aqueous subphase. Hydrophilic helical peptides having two biotin moieties at both ends of a helix chain were synthesized to connect a second

SAv layer to the first SAv layer at the air/water interface. The formation of the second SAv layer underneath the first SAv layer was shown by fluorescence microscopy. It is notable that the bright domains of the second SAv layer showed fluorescence anisotropy. The thickness of the second SAv layer was determined by surface plasmon resonance.

In Chapter 6, a mastoparan X (MPX) derivative having an anthryl group at the C-terminal residue was synthesized (MPX-A) and its conformation, orientation, and aggregation in phospholipid bilayer membrane were studied. The efficiency of intramolecular energy transfer from the Trp residue to the anthryl group under a highly diluted condition suggested an α-helical conformation in the lipid membrane, which is consistent with the previous investigation by NMR of MPX concentrated in lipid membrane. Emission either from the Trp residue or from the anthryl group of MPX-A in the lipid membrane was quenched with 5-doxylstearic acid, suggesting that MPX-A is located at the membrane surface with the helix axis oriented parallel to the surface. The dependence of the excited energy transfer and the fluorescence depolarization of MPX-A on the peptide concentration revealed that a self-assembly of MPX-A having a definite structure is formed in the lipid membrane.

The present thesis revealed that peptide molecules form regular assemblies at the air/water interface or in lipid bilayer membrane, and some of them can be regarded as a crystal. Since peptides take a secondary structure, the assembly structure should be highly ordered. The two-dimensional crystal of peptides formed at the air/water interface can be regarded as "supersecondary structure". A two-dimensional crystal of protein was also constructed by using an array of α-helical peptides. To conclude, the peptides can be utilized not only for construction of a self-organized structure but also for organization of a supramolecular assembly

of protein. The supersecondary structure constructed in the present investigation can be the basis for the design of biologically functional materials such as molecular sensing device.

LIST OF PUBLICATIONS

Chapter 1 "Monolayer Properties of Hydrophobic α-Helical Peptides Having Various End Groups at Air/Water Interface";
K. Fujita, S. Kimura, Y. Imanishi, E. Rump and H. Ringsdorf;
Langmuir **1994**, *10*, 2731-2735.

Chapter 2 "Two Dimensional Assembly Formation of Hydrophobic Helical Peptides at the Air/Water Interface: Fluorescence Microscopic Study";
K. Fujita, S. Kimura, Y. Imanishi, E. Rump and H. Ringsdorf;
Langmuir accepted.

Chapter 3 "Monolayer Formation and Molecular Orientation of Various Helical Peptides at the Air/Water Interface";
K. Fujita, S. Kimura, Y. Imanishi, E. Okamura and J. Umemura;
Langmuir, submitted.

Chapter 4 "The Molecular Recognition of Biotinyl Hydrophobic Helical Peptides with Streptavidin at the Air/Water Interface";
K. Fujita, S. Kimura, Y. Imanishi, E. Rump and H. Ringsdorf;
J. Am. Chem. Soc. **1994**, *116*, 2185-2186.

Chapter 5 "Bilayer Formation of Streptavidin Bridged by Bis(biotinyl) Peptide at the Air/Water Interface";
K. Fujita, S. Kimura, Y. Imanishi, E. Rump , J. van Esch and H. Ringsdorf;
J. Am. Chem. Soc. **1994**, *116*, 5479-5480.

Chapter 6 "Self-Assembly of Mastoparan X Derivative Having Fluorescence Probe in Lipid Bilayer Membrane";
K. Fujita, S. Kimura, Y. Imanishi
Biochim. Biophys. Acta **1994**, 1195, 157-163.

ACKNOWLEDGEMENT

This research was carried out from 1989 to 1994 at the Department of Polymer Chemistry, Faculty of Engineering, Kyoto University.

The author would like to express his deepest gratitude to Professor Yukio Imanishi, Division of Material Chemistry, Kyoto University, for his continuous guidance and encouragement throughout the course of this work, and for detailed criticisms on the manuscript.

Grateful acknowledge is due to Dr. Shunsaku Kimura, Division of Material Chemistry, Kyoto University, for his constant guidance and encouragement.

The author wishes to express his sincere thanks to Dr. Yoshihiro Ito, Division of Material Chemistry, Kyoto University, for his valuable suggestions and discussions.

The author wishes to express his thanks to Professor Helmut Ringsdorf and Drs. Elmar Rump and Jan van Esch, Institute of Organic Chemistry, University of Mainz, and Drs. Emiko Okamura and Junzo Umemura, Institute for Chemical Research, Kyoto University, for their valuable suggestions and discussions.

Finally, the author wishes to express his thanks to his colleagues in the Imanishi Laboratory for their encouragement during the course of the investigation.

November, 1994.

Katsuhiko Fujita